THE ROLE OF ATF5 IN MITOCHONDRIAL MAINTENANCE, BIOGENESIS AND UPR^{MT} SIGNALING FOLLOWING ACUTE EXERCISE IN SKELETAL MUSCLE

MIKHAELA B. SLAVIN

A THESIS SUBMITTED TO THE FACULTY OF GRADUATE STUDIES IN PARTIAL FULFILLMENT OF THE REQUIREMENTS FOR THE DEGREE OF

MASTER OF SCIENCE

GRADUATE PROGRAM IN KINESIOLOGY AND HEALTH SCIENCE

YORK UNIVERSITY
TORONTO, ONTARIO

NOVEMBER 2021

ABSTRACT

Maintenance of the mitochondrial protein folding environment is essential for organellar and cellular homeostasis. The Mitochondrial Unfolded Protein Response (UPR^{mt}) is a protein quality control mechanism that relieves intraorganellar proteotoxic stress in a manner dependent on activating transcription factor 5 (ATF5) during mitochondrial dysfunction. Protein homeostasis can temporarily be disrupted by acute exercise, inducing the UPR^{mt}. Using WT and whole-body ATF5 KO animals, we sought to determine the role of ATF5 in regulating basal mitochondrial content and function, in addition to acute exercise-induced changes in UPR^{mt} signaling. Our data reveal that ATF5 is required in the maintenance of a high-quality mitochondrial pool and mediating the transcription of UPR^{mt} genes during exercise. However, the specific mechanisms by which ATF5 and the UPR^{mt} coordinate the preservation of mitochondrial homeostasis and whether they are required in mediating mitochondrial adaptations to chronic exercise are avenues of future work.

ACKNOWLEDGEMENTS

"The mind is not a vessel to be filled, but a fire to be kindled."

-Plutarch

I would first and foremost like to thank my parents. Thank you for stoking the fire of my inquisitive mind since I was a child, listening to me talk about my various passions and patiently receiving my incessant questioning. You both taught me that I can accomplish anything I set my mind to and have supported me in all my endeavours. For that, I am forever grateful. Thank you to my sister, Nakisha, for being there when I need you, and most of all, for keeping me fed during my science marathons.

I would like to thank my mentor, Dave. You have taught me to be an ambitious, curious, realistic, and persevering scientist. Thank you for your time, effort, and guidance, and pointing me in the right direction while patiently listening to my questions and ideas. I am grateful for my development and all that I have learned throughout the past 2+ years under your supervision, and am eager to see what we accomplish in my PhD studies.

To my lab vets, Ashley, Matt, and Jon. I am extremely lucky to have entered a lab with such intelligent and respectable scientists. You all truly paved the way for me and are tremendous examples of the patience, curiosity and ambition that are required to succeed in research. Thank you for being such great scientists and individuals, and for the support you have shown me throughout my degree.

To Neushaw, our late-night lab sessions (and laughing sessions) are some of the memories I cherish the most in my Master's. Thank you for your support and for being a great friend. I would also like to thank our postdoctoral fellow Rita, for your assistance and guidance throughout my project.

Lastly, thank you to the world of science, for keeping me curious, humble and passionate. I believe the trials and tribulations of research have made me a better person, teaching me patience and perseverance. I have grown to find beauty in the mysterious nature of the unknown, and although intimidating, it is twice as compelling.

TABLE OF CONTENTS

ABSTRACT ii

ACKNOWLEDGEMENTS iii

TABLE OF CONTENTS iv

LIST OF FIGURES vii

LIST OF TABLES viii

LIST OF ABBREVIATIONS xi

CHAPTER 1 - REVIEW OF LITERATURE 1

1.0. SKELETAL MUSCLE 2

1.1. INTRODUCTION: THE IMPORTANCE OF SKELETAL MUSCLE IN HUMAN HEALTH 2

1.2. SKELETAL MUSCLE PHYSIOLOGY

1.2.1. STRUCTURAL PHYSIOLOGY OF SKELETAL MUSCLE 3

1.2.2. FIBER TYPES 4

1.2.3. CELLULAR PHYSIOLOGY OF SKELETAL MUSCLE 5

1.2.3.A. MITOCHONDRIAL STRUCTURE: MULTIPLE MEMBRANES ARE BETTER THAN ONE 5

1.2.3.B. MITOCHONDRIAL FUNCTION: LIFE IN THE RETICULUM 6

1.2.3.C. MITOCHONDRIAL POPULATIONS IN SKELETAL MUSCLE 8

1.2.3.D. ELECTRON TRANSPORT CHAIN 9

2.0. SKELETAL MUSCLE ADAPTATIONS TO EXERCISE 12

2.1. MITOCHONDRIAL BIOGENESIS 12

2.1.1. ACUTE EXERCISE AND TRAINING 15

2.1.2. PGC-1A 16

2.1.3. SIGNALING 17

2.2. MITOCHONDRIAL PROTEIN HANDLING AND IMPORT 19

2.3. MITOCHONDRIAL TURNOVER (MITOPHAGY) 20

3.0. THE MITOCHONDRIAL UNFOLDED PROTEIN RESPONSE (UPR^{MT}) 22

3.1. THE UPR^{MT} IN *CAENORHABDITIS ELEGANS (C. ELEGANS)* 23

3.2. The Mammalian UPR^{MT} 24
3.2.1. Transcriptional Regulation 24
3.2.2. ATF5: A Mediator of Retrograde Signaling in the UPR^{MT} 26
3.2.3. Translational Regulation: The UPR^{MT} and the ISR 29
3.2.4. The UPR^{MT} and Exercise in Skeletal Muscle 30
Research Objectives 34
Hypotheses 34
References 35
Chapter 2: Manuscript 57
Manuscript Author Contributions 58
The Role of ATF5 in Mitochondrial Maintenance, Biogenesis and UPR^{MT} Signaling Following Acute Exercise in Skeletal Muscle 59
Abstract 60
Introduction 61
Methods 63
Results 70
Discussion 85
Acknowledgements 89
References 90
Future Directions 97
Appendix A: Data and Statistical Analyses 100
Appendix B: Additional Data 119
Appendix C: Laboratory Methods and Protocols 123
Cytochrome c oxidase (COX) enzyme assay 124
Gel Electrophoresis 128
Western blotting and immunodetection 131
RNA isolation 133
Reverse transcription: first strand cDNA synthesis 135
Mitochondrial Isolations from Skeletal Muscle 136
Mitochondrial Respiration 139

ROS EMISSION 140

APPENDIX D: OTHER CONTRIBUTIONS TO THE LITERATURE 143

PEER-REVIEWED PUBLICATIONS 143

PUBLISHED ABSTRACTS AND CONFERENCE PROCEEDINGS 143

ORAL PRESENTATIONS 144

LIST OF FIGURES

CHAPTER 1: REVIEW OF LITERATURE

Fig. 1 – The Electron Transport Chain 11

Fig 2. – The UPR^{mt} in Relation to the Mitochondrial Life Cycle 13

CHAPTER 2: MANUSCRIPT

Fig. 1 – Genotyping of ATF5 KO animals and mRNA levels 71

Fig. 2 – Animal characteristics and response to exercise 72

Fig. 3 – Effects of acute continuous and exhaustive exercise on upstream signaling, represented by eIF2α and JNK phosphorylation in WT and KO muscle 74

Fig. 4 – Subcellular localization of ATF5 following acute continuous and exhaustive exercise in WT animals 76

Fig. 5 – Subcellular localization of PGC-1α following acute continuous and exhaustive exercise in WT and KO animals 77

Fig. 6 – Subcellular localization of ATF4 following acute continuous and exhaustive exercise in WT and KO animals 78

Fig. 7 – Basal protein expression in WT and KO muscle 79

Fig. 8 – ATF5 KO muscle exhibits a greater mitochondrial pool 80

Fig. 9 – Diminished function in mitochondria from ATF5 KO muscle 83

Fig. 10 – Changes in mRNA levels in response to acute continuous exercise in WT and KO animals 84

APPENDIX B: ADDITIONAL DATA

Fig. S1 – Changes in gene expression in WT muscle immediately after continuous exercise and following three hours of recovery 120

Fig. S2 – Basal mRNA levels in WT, HET and ATF5 KO mice 121

Fig. S3 – Basal mRNA levels in WT and PGC-1α KO mice 122

LIST OF TABLES

CHAPTER 2: MANUSCRIPT

Table 1 – List of primer sequences used in genotyping and qPCR 69

Table 2 – List of antibodies used in Western Blotting 69

APPENDIX A: DATA AND STATISTICAL ANALYSIS

Table 1 – Phenotypic characteristics of WT and KO animals

A – Animal body weights 101

B – TA weights/Body weights 101

C – Distance to exhaustion during the exhaustive exercise test 102

D – Blood lactate levels before and immediately after exhaustive exercise 102

Table 2 – Protein levels of upstream signaling regulators with acute exercise

A – Phosphorylated eIF2α 103

B – Phosphorylated JNK 104

Table 3 – Protein levels of PGC-1α in nuclear and cytosolic fractions with acute exercise

A – PGC-1α: protein levels in WT and KO animals 105

B – PGC-1α: % nuclear protein basally and after exhaustive exercise in WT and KO animals 105

C – PGC-1α: % nuclear protein basally and after both exercise protocols in WT mice 106

Table 4 – Protein levels of ATF4 in nuclear and cytosolic fractions with acute exercise

A – ATF4: protein levels in WT and KO animals 106

B – ATF4: % nuclear protein basally and after exhaustive exercise in WT and KO animals 106

C – ATF4: % nuclear protein basally and after both exercise protocols in WT mice 107

Table 5 – Protein levels of ATF5 in nuclear and cytosolic fractions with acute exercise

A – ATF5: protein levels basally and after both exercise protocols in WT animals 107

B – ATF5: % nuclear protein basally and after both exercise protocols in WT animals 107

Table 6 – Basal protein expression in WT and KO muscle

A – VDAC 108

B – ATF4 108

C – HSP60 109

D – mtHSP70 109

E – LONP 110

F – Fold changes (KO/WT) 110

Table 7 – Mitochondrial content in WT and KO muscle

A – COX Activity 111

B – Mitochondrial Yields 111

Table 8 – Respiration of mitochondria isolated from WT and KO muscle

A – SS mitochondria 112

B – IMF mitochondria 112

C – RCRs 113

Table 9 – ROS emissions of mitochondria isolated from WT and KO muscle

A – SS mitochondria 114

B – IMF mitochondria 114

Table 10 – mRNA levels basally and following continuous exercise in WT and KO muscle

A – PGC-1α 115

B – COX-IV 115

C – ATF5 116

D – ATF4 116

E – CHOP 116

F – HSP60 117

G – LONP 117
H – mtHSP70 117
I – ClpP 118
J – UPR^{mt} downstream targets 118

LIST OF ABBREVIATIONS

AARE	Amino acid response element
Ach	Acetylcholine
AchR	Acetylcholine Receptor
ADP	Adenosine diphosphate
Akt	Serine/threonine protein kinase Akt
AMP	Adenosine monophosphate
AMPK	AMP-activated protein kinase
ANOVA	Analysis of variance
ANT	Adenine nucleotide translocase
AP-1	Activator protein-1
ARE	ATF5-specific response element
ATF	Activating transcription factor
ATFS-1	Activating transcription factor associated with stress-1
ATG	Autophagy-related protein
ATP	Adenosine triphosphate
bZIP	Basic leucine zipper
C/EBP	CCAAT-enhancer binding protein
Ca^{2+}	Calcium ion
CaMK	Ca^{2+}/calmodulin-dependent protein kinase
cAMP	Cyclic AMP
CCA	Chronic contractile activity
cDNA	Complimentary DNA
C/EBPβ	CCAAT/enhancer binding protein
CHOP	C/EBP homologous protein
ClpP	Caseinolytic mitochondrial matrix peptidase proteolytic subunit
COX	Cytochrome c oxidase
CRE	cAMP response element
CREB	cAMP response element-binding protein
DNA	Deoxyribonucleic acid
Drp1	Dynamin-related protein 1
eIF2α	Eukaryotic translation-initiation factor-2 alpha
ER	Endoplasmic reticulum
ERR	Estrogen related receptor
ETC	Electron transport chain
FA	Fatty acids
FAD^+	Flavin adenine dinucleotide
$FADH_2$	Flavin adenine dinucleotide (reduced)
Fis1	Mitochondrial fission 1
Foxo	Forkhead box O
FTR	Fast-twitch red

FTW	Fast-twitch white
FUNDC1	FUN14 domain containing 1
GCN2	General control nonderepressible 2 (serine/threonine protein kinase)
G-CSF	Granulocyte colony-stimulating factor
GPE1	C/EBP gamma
GPE1-BP	C/EBP gamma binding protein
H^+	Hydrogen ion
HAF-1	ABC (ATP Binding Cassette) transporter
HDAC	Histone deacetylase
H_2DCF-DA	2',7' dichlorodihydrofluorescein diacetate
HIIT	High intensity interval training
HRI	Heme-regulated inhibitor
HRP	Horseradish peroxidase
HSF-1	Heat shock factor-1
HSP	Heat shock protein
HSP60	60 kDa heat shock protein
HSP10	10 kDa heat shock protein
HSP70	70 kDa heat shock protein
HSP90	90 kDa heat shock protein
IMF	Intermyofibrillar
IMM	Inner mitochondrial membrane
IMS	Intermembrane space
ISR	Integrated Stress Response
JNK	c-jun N-terminal kinase
K^+	Potassium ion
KO	Knockout
kDa	Kilodaltons
LC3	Microtubule-associated proteins 1A/1B light chain 3A
LDH-H	Heart-specific lactate dehydrogenase
LDH-M	Muscle-specific lactate dehydrogenase
LONP	Lon protease
LPS	Lipopolysaccharide
MAPK	Mitogen-activated protein kinase
MEF2	Myocyte enhancer factor 2
Mfn2	Mitofusin-2
MHC	Myosin heavy chain
MICT	Moderate intensity continuous training
mRNA	Messenger RNA
mtDNA	Mitochondrial DNA
mtHSP70	75 kDA mitochondrial heat shock protein
mTORC1	Mammalian/mechanistic target of rapamycin complex 1
mPTP	Mitochondrial permeability transition pore
MTS	Mitochondrial targeting sequence

MURE	UPR^{mt} response element
MuSC	Muscle stem cell
Na^+	Sodium ion
NAD^+	Nicotinamide adenine dinucleotide
NADH	Nicotinamide adenine dinucleotide (reduced)
NF-κB	Nuclear factor kappa-light-chain-enhancer of activated B cells
NLS	Nuclear localization sequence
NR	Nicotinamide riboside
NRF-1/-2	Nuclear respiratory factor-1 and -2
Nrf2	Nuclear factor (erythroid-derived 2)-like 2
NUGEMPs	Nuclear genes encoding mitochondrial proteins
OMM	Outer mitochondrial membrane
OPA1	Optic atrophy 1
ΔOTC	Ornithine transcarbamylase (mutant)
OXPHOS	Oxidative phosphorylation
p62	Sequestosome-1 (SQSTM1)
PARP	Poly-ADP ribose polymerase
PCR	Polymerase chain reaction
PERK	PKR-like ER kinase
PGC-1α	Peroxisome proliferator activator receptor (PPAR) γ coactivator 1 alpha
PIM	Protein import machinery
PINK1	PTEN-induced putative kinase 1
PKR	Protein kinase RNA-activated
PMF	Proton motive force
PQC	Protein quality control genes
RNA	Ribonucleic acid
ROS	Reactive oxygen species
rRNA	Ribosomal RNA
SDS-PAGE	Sodium dodecyl sulfate polyacrylamide gel electrophoresis
SirT3	Sirtuin-3
SirtT1	Sirtuin-1
SIT	Sprint interval training
SR	Sarcoplasmic reticulum
SS	Subsarcolemmal
STR	Slow-twitch red
TA	Tibialis anterior
TCA	Tricarboxylic acid cycle
TFAM	Mitochondrial transcription factor A
TFEB	Transcription factor EB
TIM	Translocase of the inner mitochondrial membrane
TOM	Translocase of the outer mitochondrial membrane
tRNA	Transfer RNA

UCP3	Uncoupling protein 3
ULK1	Serine/threonine protein kinase ULK1
uORF	Upstream open reading frame
UPR	Unfolded protein response
UPR^{er}	Endoplasmic reticulum UPR
UPR^{mt}	Mitochondrial UPR
USF-1	Upstream stimulatory factor 1
UQ	Ubiquinone
VDAC1	Voltage-dependent anion channel 1
YME1L1	YME1 like 1 ATPase (protease)

CHAPTER 1:

REVIEW OF LITERATURE

1.0. SKELETAL MUSCLE

1.1. Introduction: The Importance of Skeletal Muscle in Human Health

Superb locomotive ability and adaptation of metabolism to the external environment were once essential for human survival, and fundamental reasons why *Homo Sapiens* prospered and evolved [1]. The evolutionary theory describes natural selection as "survival of the fittest", as those who had superior endurance capacity and the ability to thermoregulate could obtain nutrient-rich food, essential for the development and evolution of humanity that thrives today. Optimal muscular fitness was, and still is, a pinnacle of whole-body health, and a plethora of research is dedicated to unravelling its functions in mediating systemic homeostasis and preventing metabolic diseases [2].

Skeletal muscle is one of three muscle types within the body, alongside cardiac and smooth muscle, and comprises approximately ~40% of total human body weight. Uniquely, skeletal muscle is of a malleable and 'plastic' nature, having the capacity to alter its structural, physiological and molecular phenotypes to match the tissue's energy demands in response to external stressors [3]. The main function of skeletal muscle is utilizing cellular energy in the form of ATP and converting it into mechanical energy to facilitate locomotion and maintenance of posture. This organ accomplishes this whilst being a regulatory hub in the coordination of whole-body energy metabolism, regulating substrate utilization, energy expenditure, glucose homeostasis and heat production [4–6]. These beneficial qualities of muscle identified from both mechanical and metabolic perspectives reveal this organ to be crucial in the acquisition of functional independence and a positive quality of life [6,7].

1.2. Skeletal Muscle Physiology

1.2.1. Structural Physiology of Skeletal Muscle

In order to be able to interpret the adaptive features of skeletal muscle that make it such an integral component of the body's physiology, it is important to appreciate its distinct architecture and morphological features. This tissue consists of cylindrical, elongated muscle fibers referred to as 'myofibers' that are organized in parallel to eachother and enveloped in a sheath of connective tissue, giving rise to its 'striated' description. Myofibers are composed of bundles of myofibrils, housing muscle's basic contractile units called sarcomeres, made up of actin and myosin proteins repeated in units. Muscle tissue is additionally laden with capillaries for oxygenation and motor neurons for innervation. The physiology of muscle activation is referred to as excitation-contraction coupling, describing the coordination of neural transmission and the mechanical action of the actin-myosin cross-bridges to generate force. At the neuromuscular junction, the α-motor neuron releases the neurotransmitter Ach into the synaptic cleft, which binds to AchRs at the post-synaptic terminal. Depolarization of the muscle cell triggers calcium release from the sarcoplasmic reticulum, promoting actin-myosin interaction and subsequently, a muscle contraction via the power stroke, in a manner that is dependent on ATP hydrolysis [7]. Muscle is composed of 20% protein, and contains approximately 50-75% of the body's proteins, justifying its requirement to be multinucleated, providing regulation of gene programs for protein synthesis along the length of the myofiber [8]. Myonuclei reside beneath the sarcolemma of myofibers and regulate the transcription of gene programs to control protein expression in a localized manner, dependent on external stimuli and myogenic factors. Muscle satellite cells localized under the basal lamina additionally control protein synthesis, contributing to muscle growth, repair and regeneration [7,9].

1.2.2. Fiber Types

Alongside the structural and cellular characteristics of mammalian skeletal muscle that deem it a unique organ, this tissue is also extremely heterogenous in nature, in that it possesses four different types of muscle fibers. Fiber types are typically classified based on their contractile speed, ranging from fast to slow-twitch. They additionally differ in their contractile, metabolic and oxidative phenotypes, and have different adaptive capacities to respond to altered functional demands [10]. The common classified fiber types in humans are: Type I, STR; Type IIa, FTR; IIx, FTW, with type II fibers being more glycolytic, and type I fibers being oxidative [11]. Rodents also express Type IIb, which is more fast-twitch and glycolytic than IIx fibers. STR and FTR fiber types are recruited primarily during endurance exercise and are the most fatigue-resistant, due to their enhanced levels of oxidative enzymes to facilitate aerobic metabolism. In contrast, FTW fibers are typically recruited during high-intensity, phasic exercise, as they are composed of larger motor units and produce more force. However, they are more fatigable, as they rely on glycolytic metabolism. Although fiber types are typically delineated based on the expression of the myosin heavy chain (MHC) isoform, the following criteria also contribute to their classification: 1) twitch kinetics (Myosin ATPase activity), 2) calcium handling in the cytosol, 3) calcium release/uptake from/into the SR, 4) mitochondrial content, 5) expression of oxidative and glycolytic enzymes, 6) capillarization, 7) isoforms of muscle proteins, and 8) properties of motor unit recruitment [12–14]. Fiber type conversions are observed following periods of exercise and disuse, represented by the following paradigm describing changes in MHC isoform expression: MHC IIx ⇄ MHC IIa ⇄ MHC I. Mechanical overload and endurance exercise typically elicit increases in the proportion of IIa fibers with reductions in IIx and IIb fibers, while detraining and immobilization induce fiber type switches to those of a more glycolytic nature, due to changes in the biochemical characteristics

of fibers outlined above. Interestingly, mitochondrial content among fiber types may differ between humans and animals [15]. Type II fibers undergo more hypertrophy and signaling toward protein synthesis, following electrical stimulation and resistance exercise [16,17], and are also more susceptible to atrophy during sarcopenia [18,19]. From a metabolic perspective, an increased amount of type IIx fibers is associated with obesity and type 2 diabetes [11,20], most likely as a result of smaller mitochondrial pools, altered insulin sensitivity and lipid metabolism [21,22]. The general physiology and phenotypic characteristics of fiber types are important to consider as they influence their adaptations to exercise and their susceptibility to pathologies, revealing implications not just in muscle performance, but also in overall health.

1.2.3. Cellular Physiology of Skeletal Muscle

1.2.3.a. Mitochondrial Structure: Multiple Membranes are Better than One

Mitochondria are derived from a common ancestral organelle, that originated from the integration of a proteobacterium into a eukaryotic cell via endocytosis [23]. The genesis of the mitochondrion in this manner explains its double-membraned structure, and the presence of its own genome, a double-stranded plasmid referred to as mtDNA, encoding 13 proteins, 22 tRNAs and 2 rRNAs [24]. The basic understanding of mitochondrial structure and its internal organization was tremendously enhanced by the development of electron microscopy techniques performed on rat liver mitochondria in the 1990s [25,26]. This revealed the presence of two distinct organellar compartments 1) the mitochondrial matrix, encompassing the space created by the extensive folds of the IMM (cristae), and 2) the IMS, located between the OMM and the IMM. Determination of protein composition of the matrix is a tightly regulated process, as transport across the IMM is extremely selective, occurring through specialized protein import machinery [27]. The mitochondrial proteome consists of ~1200 proteins, and since mtDNA only encodes for 37, the

rest are transcribed in the nucleus [28]. Once translated in the cytosol, they are linearized by chaperones, including HSP70 and HSP90, and are imported into the matrix in a manner dependent on membrane potential. Subsequently, they are refolded by mitochondrial chaperones HSP60 and HSP10 and transported to their destined locations within the organelle [29]. Once folded into functional proteins, both nuclear and mitochondrially-encoded proteins are utilized in the assembly of holoenzymes, a critical event in the production of new mitochondria (mitochondrial biogenesis).

1.2.3.b. Mitochondrial Function: Life in the Reticulum

The classical depiction of mitochondria are singular, bean-shaped structures that are the 'powerhouses' of the cell, with the sole function of generating ATP to fuel cellular and metabolic functions. This simple view of mitochondria is an underrepresentation of not only its morphological architecture in the cell, but also of its variety of roles that this organelle has within the cell. It is now known that these organelles exist within many cell types as a reticulum, a continuous membranous network in which mitochondria are both electrically coupled and physically bound. Branching in both longitudinal and transverse directions, mitochondria are linked via nanotunnels, facilitating the sharing of substrates, and the maintenance of ion and electrical homeostasis [30]. Their morphological connectivity in the cell establishes them as critical regulators of general cellular homeostasis, being involved in cell signaling, stress responses, calcium-ion control, redox homeostasis and mediating programmed cell death (apoptosis) [31–34]. The dynamic and multifaceted qualities of the mitochondria have remarkable implications for skeletal muscle, establishing them as critical regulators of muscle mass, fitness, and substrate metabolism, contributing to whole-body vitality in health and disease.

It is not only their extensive distribution that allows them to exert tremendous influence on the cellular milieu, but also their extremely labile nature. The mitochondria and the cells in which

they inhabit form a beautiful, reciprocal relationship. A product of its environment, the mitochondrial network responds to altered functional demands on the muscle to either expand or become fragmented [35]. Furthermore, the extent of mitochondrial connectivity influences organellar bioenergetic and metabolic function, and the efficiency of numerous mitochondrial quality control pathways. Upon increased contractile and energetic demands, the mitochondrial network can expand via biogenesis and fusion processes to increase the capacity of muscle for ATP synthesis, oxygen consumption, and oxidation of carbohydrates and lipids. Fusion of the outer and inner mitochondrial membranes, orchestrated by OPA1 and MFN2, permits expansion of the reticulum. Conversely, proteins Drp1 and Fis1 regulate mitochondrial fission – the division of mitochondria into smaller pieces, or fragments. When mitochondria are dysfunctional, they undergo fission and degradation (mitophagy) processes to re-establish metabolic homeostasis and promote mitochondrial recovery. Upon local dysfunction, the defective mitochondrion is separated from the reticulum to be subsequently retracted and degraded through mitophagy [36,37], preventing the spread of regional deficiency to the entire organelle network. More recent work has revealed the existence of two distinct types of fission, either in the periphery or midzone of mitochondria, that predicates either organellar degradation or proliferation, respectively [36]. Thus, the distribution, volume and shape of the mitochondrial network reflects the balance of these processes, determined by the energy demands and metabolic status of the cell [38]. Elongated and reticular mitochondria, a product of biogenesis and fusion processes, is associated with healthy skeletal muscle, being identified as a beneficial adaptation to exercise [35,39]. Conversely, impaired fusion and excess fission yields more fragmented and ‘simple’ muscle mitochondria, observed in conditions of disuse-induced atrophy, aging, metabolic diseases and mitochondrial myopathies [30,35,40–42]. The remarkable plasticity of the mitochondrial pool in skeletal muscle,

and the physiological significance of their function establishes them as important mediators of muscle homeostasis, lying at the crossroads of health and disease.

1.2.3.c. Mitochondrial Populations in Skeletal Muscle

As a total population, mitochondria make up approximately 2-7% of skeletal muscle volume [43]. Exclusive to the organ, mitochondria are present as two distinct populations, with one group located beneath the sarcolemma (SS mitochondria), and the other positioned between myofibrils (IMF mitochondria). In addition to their differing subcellular localizations, these two subpopulations are morphologically, functionally and biochemically divergent. Differential centrifugation has been routinely employed to physically separate mitochondrial fractions and delineate their enzymatic and proteomic differences [44,45]. More recently, quantitative mapping of muscle has allowed for the computational visualization of the mitochondrial network, characterizing the biological significance of transitions in SS and IMF mitochondrial morphology in cellular function [30]. As such, SS mitochondria tend to be more punctate and globular in their shape, while IMF organelles, in contrast, form more complex and interconnected structures [30], making up the majority of total mitochondrial volume. The SS pool resides close to the surface of the muscle fiber, proximal to myonuclei, providing ATP for ion and substrate transporters, and for nuclear gene transcription. The proximity of this subpopulation to nuclei makes them quite labile and vulnerable to intracellular signaling, as mitochondrial turnover is more pronounced in SS mitochondria during conditions of use and disuse in comparison to IMF [46,47]. However, IMF mitochondria possess higher rates of respiration, protein import and synthesis, and located adjacent to sarcomeres, provide ATP for muscle contractions [44,45,48,49]. The contrasting bioenergetic contributions and adaptive plasticities of SS and IMF mitochondria in muscle cells represent the unique and dedicated nature of the organ to maintain its own homeostasis and optimal physiology.

These characteristics reveal the existence of diverse regulatory mechanisms coordinating the constant provision of ATP to meet the organ's ever-changing metabolic requirements, supporting the human body's need for locomotion and functional efficiency.

1.2.3.d. Electron Transport Chain

Living up to their popularized name as the powerhouses of the cell, the mitochondria produce the cellular energetic currency, ATP, in a process called oxidative phosphorylation. The energetic and metabolic potentials of the cell (its ability to produce ATP and metabolize substrates) are dependent on ADP availability, and cytosolic concentrations of NADH and NAD^+. Located within the cristae of the mitochondria, five multi-protein complexes and two mobile electron carriers make up the electron transport chain, wherein the transport of electrons via iron-sulfur clusters is coupled with ATP synthesis (Fig.1). This mechanism is based on the chemiosmotic hypothesis, a theory proposed by Peter Mitchell in 1961 [50]. The presence of a mitochondrial membrane potential and the establishment of an electrochemical gradient, created by the pumping of protons from the matrix into the IMS, provides the energy necessary to produce ATP. The positive charges of the hydrogen ions create an electrical gradient, while the discrepancy in ion concentration between either side of the IMM forms a chemical gradient, facilitating the flow of protons through ATP Synthase and subsequently, ADP phosphorylation to yield ATP. In conditions of low ADP availability, electron flow can be uncoupled from ATP production by protons passing through UCP3 to be dissipated as heat (thermogenesis), also known as State IV respiration (passive) [51]. This relieves the PMF and prevents the leaking of electrons from the ETC that could form free radicals and cause mitochondrial damage. State III respiration (active), however, occurs when ADP availability is high, such as during exercise, where hydrogens can pass freely through ATP Synthase, diminishing the PMF and generating less ROS [51].

To begin, oxidizable substrates, NADH and $FADH_2$, are produced in Krebs' Cycle as by-products during the metabolizing of ingested carbohydrates and lipids (Fig. 1). NADH is oxidized into NAD^+ at Complex I (NADH dehydrogenase), upon which 2 electrons are released, creating energy to pump hydrogen ions into the IMS. In a similar fashion, $FADH_2$ is oxidized into FAD^+ at Complex II (succinate dehydrogenase), and catalyzes the conversion of succinate to fumarate, acting as an additional entry point for electrons. Both Complex I and II transfer electrons to UQ, however, the release of electrons at Complex II is not accompanied by proton translocation. Complex III (cytochrome bc_1 complex) receives electrons from UQ and transfers them to the electron carrier cytochrome c, thereby reducing it, while translocating hydrogens into the IMS. Complex IV (COX) also acts as proton pump, upon its oxidation of cytochrome c. COX is also a unique complex in that it "holds" oxygen until it receives four electrons to become stable, acting as the final electron acceptor. With the addition of four hydrogens, one oxygen molecule is reduced to yield two water molecules, terminating electron flow. Subsequently, the electrochemical gradient generated by the PMF provokes hydrogen ions to pass through ATP Synthase into the relatively negatively charged matrix, creating energy necessary to phosphorylate ADP to produce ATP. Free ADP is provided by ATP hydrolysis at Myosin ATPase during muscle contractions, where ADP is transported into the matrix via ANT, and acts as the rate-limiting step. Under conditions of low ADP availability, more hydrogens are dissipated through UCP3 and passed off as heat, and there is an increase in electrons that "leak" from the respiratory chain, generating ROS. Of note, heat and ROS molecules are known to be potent signaling initiators, influencing downstream molecular mechanisms [52].

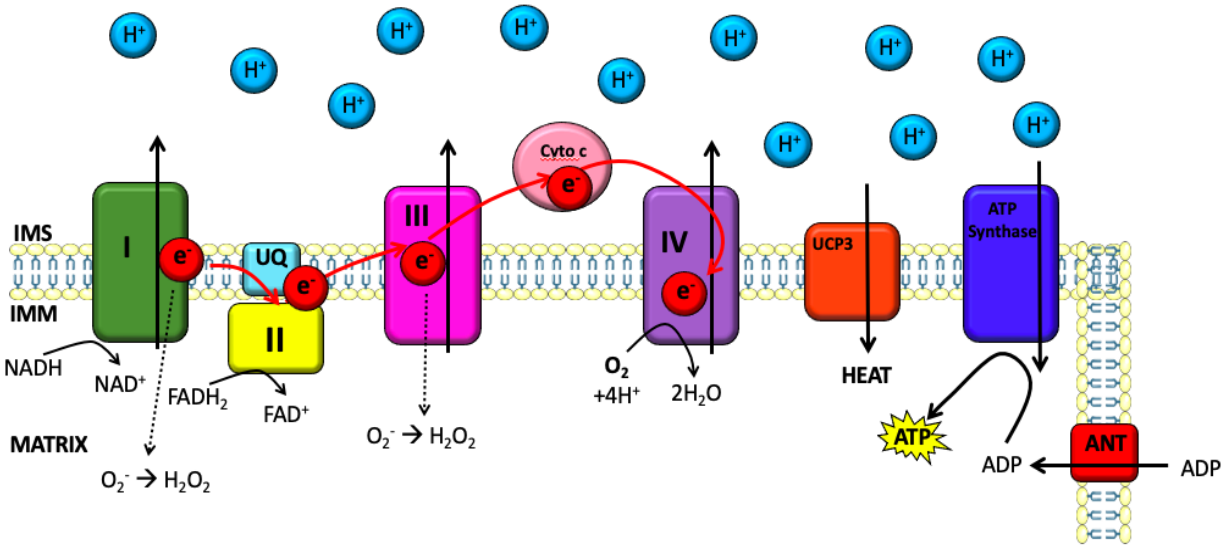

Figure 1. The Electron Transport Chain. The electron transport chain (ETC) in the mitochondria is comprised of multi-protein complexes with the purpose of producing cellular ATP to fulfill the organelle's bioenergetic function. Electrons derived from oxidizable substrates (NADH and $FADH_2$), produced in the Krebs' Cycle, are oxidized by Complex I and Complex II, respectively, driving the pumping of H^+ into the IMS at Complex I, III and IV. As electrons are passed from complex to complex, some may leak out into the matrix and bind to oxygen, forming superoxide anions (O_2^-) that can be converted into hydrogen peroxide (H_2O_2), also known as ROS, damaging proteins, lipids and DNA, causing mitochondrial dysfunction. At Complex IV, oxygen (O_2) acts as the final electron acceptor, and is reduced into water (H_2O). The energy of the proton gradient in the IMS (PMF) provokes the passing of H^+ through ATP Synthase and creating energy for the phosphorylation of ADP to generate ATP. For this to occur, ADP, produced by ATP hydrolysis at Myosin ATPase, passes through ANT within the IMM into the matrix. In conditions of low ADP availability, H^+ passes through UCP3 to dissipate the PMF, generating heat and uncoupling electron flow from ATP synthesis.

2.0. Skeletal Muscle Adaptations to Exercise

2.1. Mitochondrial Biogenesis

Exercise presents a challenge to whole-body homeostasis and elicits a complex adaptive response. This includes supplying working muscles with substrates and oxygen to account for the energy and oxygen deficits that arise in muscle cells from their enhanced metabolic activity during contractions. As previously discussed, the lability and plastic nature of muscle is extremely important in mediating the muscular adaptation to exercise, adapting to stressful stimuli that exert a functional and metabolic challenge. Accordingly, these insufficiencies act as potent intracellular signals, stimulating molecular pathways to favour the production of new mitochondria (mitochondrial biogenesis), and improvements in function (Fig. 2) [53–55]. This process requires the coordination of multiple cellular events, including transcription from both nuclear and mitochondrial genomes, synthesis of lipids and proteins, integration into the reticulum, and the stoichiometric assembly of multi-protein complexes to form the respiratory chain [56]. During exercise, the activation of cytosolic kinases influence the activity of transcription factors involved in the transcription of mitochondrial genes [57]. Over time, as a consequence of repetitive bouts of exercise, the cumulative, transient increases in mitochondrial gene expression results in net increases in mitochondrial proteins and subsequently, increases in mitochondrial content [58–62]. Physiologically, this improves the metabolic and oxidative phenotype of muscle, with the functional consequences of enhanced endurance capacity and resistance to fatigue [59,60]. The transduction of exercise-induced physiological stress into transcriptional reprogramming has been extensively investigated in muscle using human, animal, and cell models, revealing a plethora of intricate molecular pathways coordinating mitochondrial biogenesis and establishing exercise as "muscle mitochondrial medicine" [63].

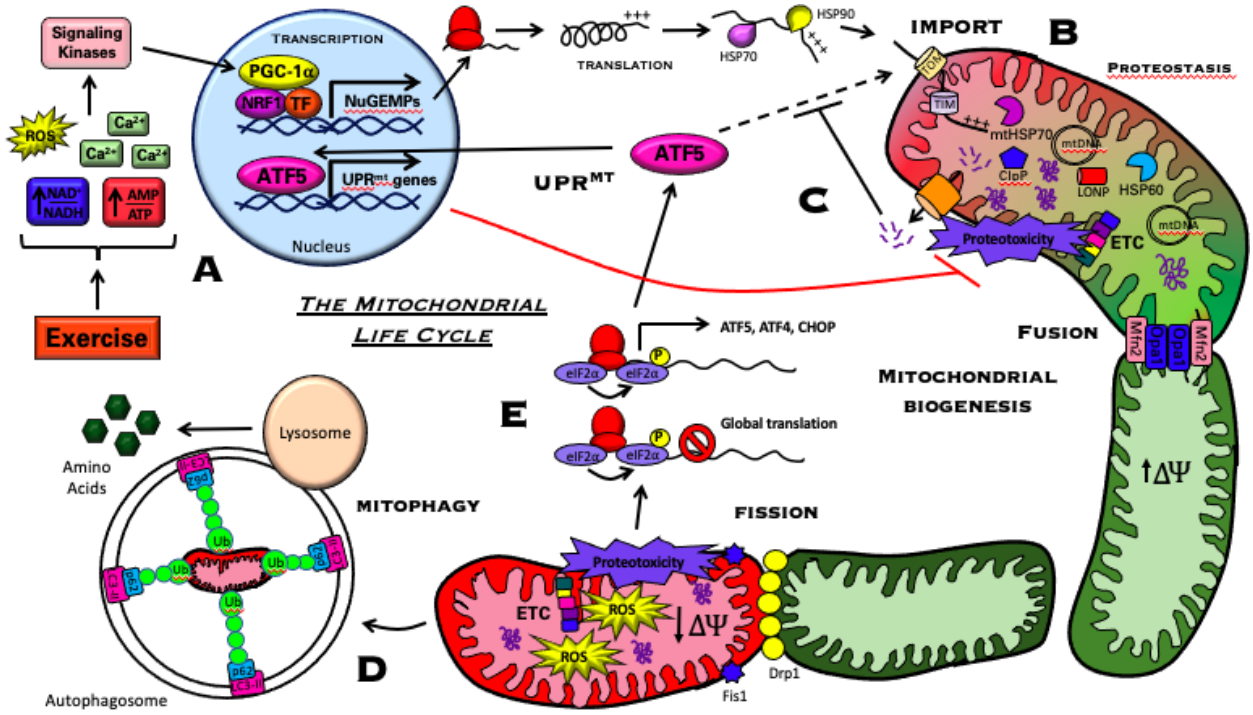

Figure 2. The UPR^{mt} in relation to the mitochondrial life cycle - mitochondrial biogenesis and mitophagy. A) Contractile activity of muscle during exercise generates various intracellular signals, including increases in ROS production, cytosolic Ca^{2+} concentrations, NAD^{+}/NADH, and AMP/ATP. These alterations in the cellular milieu activate signaling kinases, which activate and induce the nuclear localization of the master regulator of mitochondrial biogenesis, PGC-1α. Acting as a transcriptional co-activator, PGC-1α binds to NRF1 and other transcription factors to induce the transcription of NUGEMPs. Upon their export from the nucleus, mitochondrial mRNAs are translated on cytosolic ribosomes, linearized and shuttled to the mitochondria by cytosolic chaperones HSP70 and HSP90. These proteins (termed pre-proteins) possess a positively-charged cleavable presequence on their N-terminals that is removed upon its import into the matrix. **B)** The maintenance of protein homeostasis (proteostasis) is integral in the maintenance of mitochondrial function. As such, mitochondria are equipped with specific enzymes to maintain optimal proteostasis within the matrix, including chaperones HSP60, mtHSP70 and proteases ClpP

and LONP. However, the import of NUGEMPs into the matrix via TOMs and TIMs (PIM) may temporarily disrupt proteostasis, as the amount of imported pre-proteins may exceed the number of chaperones and proteases that work to refold and degrade these proteins, respectively. This causes an accumulation of misfolded proteins, causing temporary mitochondrial proteotoxicity. **C)** These proteins are broken down into peptides by ClpP and exported into the cytosol, inhibiting the mitochondrial import of ATF5. As it additionally harbours a NLS, this prompts the translocation of ATF5, where it binds to UPR^{mt} response elements on the promoters of its downstream targets, upregulating the expression of UPR^{mt} genes, including HSP60, LONP and mtHSP70. The increased expression of these enzymes mitigates proteotoxicity and rescues proteostasis, allowing for mitochondrial biogenesis to occur, which also includes the fusing of the growing organelle to the reticulum by fusion proteins OPA1 and MFN2**. D)** Alternatively a dysfunctional organelle that cannot recover from stress is characterized by excessive ROS production, proteotoxicity and a dissipated membrane potential ($\Delta\Psi$). In this case, the dysfunctional organelle is removed from the reticulum via fission by proteins FIS1 and DRP1. The organelle is subsequently engulfed by an autophagosome, mediated by Ubiquitin chains and proteins p62 and LC3-II, and degraded at the lysosomes, generating amino acids. **E)** As part of the translational attenuation mechanism of the UPR^{mt}, also involving the ISR, mitochondrial ROS and proteotoxicity cause the phosphorylation of eIF2α. This induces the preferential translation of ATF5, CHOP, and ATF4 to enhance their protein expression, while reducing global translation.

2.1.1. Acute Exercise and Training

The stimulus of acute endurance exercise carries a molecular signature that imposes significant effects on muscle. This encompasses the physiological signals generated and the state of the tissue, being in an untrained or trained state. An acute bout of exercise stimulates the nuclear localization of transcription factors and the subsequent expression of mitochondrial genes, observed approximately 2-8 hours post-exercise, with kinase activation, and transcriptional activity occurring immediately after the exercise bout [55,64–68]. Although currently up for debate, the intensity-dependent degree of metabolic perturbation during acute exercise seemingly modulates the mitochondrial biogenesis mRNA response in muscle [54,69]. The surges in various metabolites, including intracellular lactate, AMP and ADP, indicative of cellular stress, occur proportional to exercise intensity and initiate mitochondrial signaling cascades [70]. Similar to MICT, HIIT and SIT stimulate this [69], however, PGC-1α mRNA abundance has been found to increase in an intensity-dependent manner, associated with greater activation of kinases [54,71]. Thus, the strength of the metabolic signal is important to consider as different exercise intensities may have divergent influences on mitochondrial stress responses, affecting mitochondrial biogenesis.

In line with evidence illustrating the importance of exercise intensity on mitochondrial biogenesis, pioneering work by John O. Holloszy revealed that a progressive increase in workload throughout a training protocol is fundamental in eliciting adaptive increases in mitochondrial content [58]. His work also suggested improvements in mitochondrial function can be achieved with the "right" exercise conditions described above, although smaller than observed in comparison to changes in density, which is supported by more recent work in the field [72]. The notion that "surprising" the muscle with unaccustomed intensities enhances the metabolic response

and subsequent adaptive signaling is something researchers have known for some time [73,74]. High mitochondrial content in muscle achieved with training is associated with attenuated metabolic disturbance and associated kinase phosphorylation [75,76], yielding smaller changes in intracellular metabolites and PGC-1α mRNA in response to the same absolute workload when compared with untrained muscle [72,75,77]. Interestingly, only a few exercise bouts are required for attenuations in the exercise-induced increases in PGC-1α, COX-IV and cytochrome c mRNA to manifest, emphasizing the extreme responsiveness and adaptive capacity of muscle to acute exercise [62,78]. The exercise-induced mRNA response of UPR markers, indicative of cellular protein folding stress, is also blunted with training [79], further defining the reduced transcriptional sensitivity of trained muscle to exercise. This novel finding also characterizes contractile activity as a beneficial stressor, exerting protective effects against further homeostatic disruption and mitigating the requirement for the activation of acute stress responses.

2.1.2. PGC-1α

PGC-1α is a transcriptional coactivator that stimulates the transcription of mitochondrial genes, with its prominent influence being in highly metabolic organs, such as the heart, liver, brain, adipose tissue and skeletal muscle. It was first discovered to provoke adaptive thermogenesis in brown adipose tissue [80], and is now identified as the "master regulator" of exercise-induced mitochondrial biogenesis in skeletal muscle [81]. Intracellular signals invoked during contractile activity induce the activation and nuclear translocation of PGC-1α [66,67,82,83], where it interacts with the nuclear receptors NRFs, PPARs and ERRα to increase the transcription of NUGEMPs [84–86]. Of note, PGC-1α stimulates the transcription of TFAM through its interaction with NRF-1, where although transcribed in the nucleus, is imported into the mitochondria and regulates transcription of genes encoded by mtDNA [87,88]. Furthermore, PGC-1α controls the expression

of a plethora of genes that regulate muscle metabolism and physiology, including those involved in angiogenesis and fatty acid and glucose metabolism [86], significantly contributing to the remodeling of the muscle phenotype [89]. Its muscle-specific overexpression promotes fiber type switching to more slow-twitch, type I oxidative fibers characterized by increased mitochondrial content [81], and functional improvements in oxygen uptake and exercise performance [90]. In contrast, the ablated expression of PGC-1α reveals its regulatory role in the coordination of basal mitochondrial homeostasis in muscle, as prominent reductions are observed in mitochondrial content and function [68,91,92], confirmed in animal models and myotubes. In the acute response to exercise, PGC-1α KO muscle displays attenuated mitochondrial biogenesis and mitophagy signaling, in conjunction with enhanced metabolic stress and reduced endurance capacity versus WT animals [68,92,93]. However, PGC-1α is not required for training-induced mitochondrial adaptations in young muscle, revealing the existence of pathway redundancies in the molecular response to exercise to improve mitochondrial health [91,94].

2.1.3. Signaling

Muscle contractile activity alters levels of intracellular metabolites and molecules to initiate signaling toward mitochondrial biogenesis (Fig. 2). The most commonly considered pathways are stimulated by contraction-induced rises in calcium due to release from the SR, activating CaMKs; increases in AMP derived from ATP hydrolysis and myokinase acting on AMPK; increases in mitochondrial ROS production stimulating action of p38 MAPK; and a rising NAD^+/NADH ratio triggering SIRT-1 function [95,96]. Cytosolic calcium is robustly increased during muscle contractions, as its release from the SR through voltage-gated channels is triggered by the depolarization of the cell during neuromuscular stimulation. Its activation of the CaMKs (CaMKIV, CaMKII) phosphorylates CREB [97,98], which binds to the CRE element on the PGC-

1α promoter, while activation of CAMKKβ directly phosphorylates and activates AMPK [99]. Furthermore, calcium activates the phosphatase Calcineurin, which dephosphorylates and induces the nuclear localization of MEF2, stimulating transcription of PGC-1α [100]. Next, AMPK activity is known to coordinate PGC-1α transcription and mitochondrial biogenesis [101]. AMPK binds to the E-box on the PGC-1α promoter and interacts with transcription factor USF-1 to drive its transcription [102], while also directly phosphorylating it post-translationally to enhance its activity [103]. Increases in ROS production during exercise also activate AMPK [101], JNK [104–106], and p38 MAPK, which phosphorylates ATF2 and MEF2, coinciding with enhanced PGC-1α mRNA [107]. AMPK and CAMKII also phosphorylate HDACs, leading to their nuclear exclusion and relieving their inhibitory effects on MEF2 transcriptional activity on the PGC-1α promoter [71]. The dynamic fluctuations in the cytosolic NAD^+/NADH ratio, indicative of cellular redox potential, are also a critical node in exercise-induced signal transduction. An increase in the ratio, established by increasing NAD^+ levels from NADH oxidation at complex I during exercise, activates the SIRT-1 deacetylase, provoking the activating deacetylation of PGC-1α [108,109]. Based on what was just described, the multitude of molecular pathways that converge on PGC-1α to induce the transcription of mitochondrial genes are extremely interrelated, forming complex networks [110]. This exquisite quality of muscle cell signaling allows for compensatory alterations to occur in the absence of specific proteins, and for beneficial adaptations to occur, highly dependent on the nature of the exercise stimulus and the cellular environment, awarding skeletal muscle its infamous and impressive plasticity.

2.2. Mitochondrial Protein Handling and Import

Mitochondrial biogenesis is a product of multiple coordinated molecular events, with the aims of increasing the expression of mitochondrial proteins, and expanding the surface area of the reticulum. In response to exercise, increases in mitochondrial gene expression are also accompanied by cardiolipin synthesis, expression of PIM, import kinetics, and mitochondrial fusion [111–113]. A unique characteristic of mitochondria is their protein composition, being made up of proteins that originate from both nuclear and mitochondrial genomes. Proteins translated from mRNAs transcribed in the nucleus require import into the mitochondria, in a manner dependent on membrane potential, via specialized import machinery (PIM) (Fig. 2). Upon recognition of a mitochondrial presequence on the protein's N-terminus, the protein is imported through both membranes, and the presequence is finally cleaved in the matrix. The protein can subsequently be incorporated into the organelle and carry out its functions. Protein import also plays a pivotal role in the maintenance of cellular homeostasis, acting as a sensor of mitochondrial dysfunction and triggering adaptive stress responses, including the UPR^{mt} [114,115] and mitophagy [116]. Characterized as crucial in exercise-induced mitochondrial biogenesis [117], chronic stimulation and voluntary exercise yield improved import of precursor proteins and TOM and TIM protein expression [118–120]. The expression of mitochondrial chaperones HSP60 and mtHSP70 and the cytosolic chaperone HSP70 is also increased with CCA, which are crucial components of the protein import process [121,122]. These molecular changes with exercise are important for the assembly of holoenzymes, including those in the ETC, which are made up of specific stoichiometric proportions of nuclear and mitochondrially-encoded proteins [123]. As the necessary proteins encoded by the nucleus are being incorporated into mitochondria, the

machinery responsible for network fusion are also being upregulated during exercise [35], resulting in expansion of the reticulum.

2.3. Mitochondrial Turnover (Mitophagy)

The degradation of organelles and long-lived proteins in the cell is referred to as autophagy, and although seemingly counter-intuitive, autophagy is required in the maintenance of muscle mass and function, with deficiencies in this process leading to diminished strength, muscle wasting, reduced endurance capacity and metabolic defects [124–127]. When discussing the specific degradation of mitochondria, the term mitophagy is used. In addition to exercise-induced biogenesis to improve the mitochondrial content of muscle, it is also vital to remove/degrade any dysfunctional mitochondrial segments via mitophagy, in order to improve and maintain the quality of the mitochondrial pool (Fig. 2) [128,129]. Defective basal mitophagy results in the accumulation of abnormal and dysfunctional mitochondria that consume less oxygen and produce more ROS [124,130,131], significantly contributing to the physiological and metabolic perturbations of muscle that occur in the absence of proper mitochondrial clearance. Mitophagy occurs as such: organelles with a dissipated membrane potential and/or excessive ROS production are cleaved from the reticulum via fission and tagged for degradation through the attachment of a ubiquitin chain by Parkin, an E3 ubiquitin ligase [132]. The mitochondrial recruitment of Parkin is mediated by the accumulation of PINK1 on the OMM due to its failed import into the defective mitochondrion, resulting in its activating phosphorylation of Parkin and OMM proteins [133]. Induction of autophagic machinery is induced by multiple intracellular signals initiated during exercise, resulting in the lipidation of LC3-I into its active form, LC3-II, mediating nucleation and growth of the phagophore [133]. Next, the phagophore selects its cargo destined for degradation and encapsulates the damaged mitochondria. The adaptor protein Sqstm1/p62 binds to ubiquitin

chains attached to the organelle, in addition to LC3-II on the phagophore, and the growing membrane develops into a double-membraned autophagosome [116,134]. After travelling down microtubule tracks in the cell, the autophagosome fuses with lysosomes where its contents are degraded by proteolytic enzymes resident within the lysosomal lumen, generating amino acids to be utilized in protein synthesis [116].

Muscle activity is a potent stimulus for mitophagy signaling, as the intracellular energetic imbalance that is sensed by AMPK, in addition to biogenesis, also initiates mitophagy through its phosphorylation of ULK1 and induction of the appropriate molecular machinery [135]. Acute exercise stimulates increases in mitophagic gene expression and mitophagy flux [68,132], an effect that is attenuated with training [132], most likely as a result of a more functional and abundant mitochondrial pool, reducing the requirement for exercise-induced signaling to clear dysfunctional organelles [76]. Exercise training in rodents and humans increases basal autophagy and mitophagy gene and protein expression in muscle [129,136,137], although, CCA models elicit reduced mitophagy flux, suggesting that an improvement in mitochondrial quality reduces the need for mitochondrial turnover [138,139]. In addition to its influential role in basal muscle homeostasis, autophagy is also required for exercise training and CCA-induced mitochondrial adaptations in muscle, and improved muscle performance [129,131,140]. Unsurprisingly, within the myriad of genes regulated by PGC-1α are those involved in mitophagy, establishing the master regulator of mitochondrial biogenesis to also coordinate mitochondrial turnover. During exercise, PGC-1α contributes to the upregulated expression of mitophagy genes [68,129,141], in addition to the transcription and nuclear localization of TFEB [93,142], a transcription factor involved in lysosomal biogenesis [143].

3.0. The Mitochondrial Unfolded Protein Response (UPR^{mt})

Encompassing all the topics outlined above, the genesis and maintenance of a mitochondrial pool in skeletal muscle is a complex compilation of events, vulnerable to enhanced physiological demands. In these contexts, it is imperative for the cell to monitor the integrity of the mitochondrial network and initiate an appropriate response for beneficial adaptations to occur. Of the many facets of mitochondrial maintenance, the regulation of the mitochondrial proteome is of particular interest. Its mosaic composition, being largely comprised of nuclear-encoded proteins and some mitochondrially-encoded proteins, establishes the organelle to be quite vulnerable to dysregulations in proteostasis, occurring in response to a multitude of mitochondrial stressors [144–146]. Proteins originating from the nuclear genome require import into the mitochondrion and subsequent refolding, to then be incorporated into holoenzymes in the process of mitochondrial biogenesis. The import of pre-proteins and their handling by MQC enzymes (chaperones and proteases) is a finely orchestrated process, and conflicts with the synchronisation of these events can lead to the accumulation of mis-folded preproteins. Their accretion may exceed the number of chaperones and proteases, reflective of the organelle's folding capacity, causing proteotoxic stress. Speaking to the complex and versatile nature of the mitochondria, these organelles have developed an intricate protein quality control mechanism to monitor protein homeostasis and trigger compensatory and adaptive responses, via the UPR^{mt} [147]. Through retrograde signaling mechanisms, the mitochondria communicates to the nucleus, promoting the expression of various chaperones and proteases in an attempt to restore intramitochondrial homeostasis and maintain organellar function [148–153].

3.1. The UPR^{mt} in *Caenorhabditis elegans* (*C. elegans*)

This pathway was originally discovered in mammalian cells [154], but in the recent decade, research performed in the nematode *C. elegans* has been monumental in expanding the molecular characterization of this pathway [114,115,155–157]. Dysregulated UPR^{mt} signaling is observed in neurodegeneration, cancer, and congenital disorders [158–162], illustrating the importance of this signaling mechanism in the maintenance of cellular homeostasis. During various forms of mitochondrial stress, the import efficiency of ATFS-1 into mitochondria was found to be a key point of regulation within the UPR^{mt}, as it possesses both a NLS and MTS [115]. Unfolded proteins within the mitochondrial matrix can be proteolytically processed by the ATP-dependent protease, ClpP, and the subsequently-derived peptides are exported into the cytosol via HAF-1, an ATP-binding cassette transporter that resides in the IMM [163,164]. In healthy cellular conditions, ATFS-1 is mitochondrially-imported and subsequently degraded by LONP1 [149]. However, during conditions of mitochondrial dysfunction, in a mechanism that is seemingly dependent on peptide efflux, the import of ATFS-1 into the mitochondria is perturbed, prompting its subsequent translocation to the nucleus where it activates the UPR^{mt} by inducing the transcription of stress-responsive genes [114,149,164]. ATFS-1 also positively regulates the transcription of import components, antioxidant enzymes, and autophagy markers, while negatively regulating the expression of OXPHOS transcripts, and shifting metabolism toward glycolysis [156]. In parallel to the transcriptional regulation of the UPR^{mt}, alterations in protein translation and synthesis also occur in the cell. During excessive ROS production, the kinase GCN2 phosphorylates ribosomal eIF2α and attenuates global protein synthesis, revealing mitochondrial function and translational capacity to be coupled in order to maintain cell viability [155,165]. These unique signaling mechanisms channel the cell's transcriptional and translational energy toward the synthesis of

protective markers during initial repair, thus matching biogenesis and protein folding load with its proteostatic capacity. In doing so, mitochondria can overcome the acute homeostatic threat, and become equipped with an abundance of protein handling machinery to deal with future challenges.

3.2. The Mammalian UPR^{mt}

3.2.1. Transcriptional Regulation

In mammals, similar to retrograde pathways discovered in lower-level organisms [166,167], the UPR^{mt} was discovered to expand mitochondrial protein quality control under conditions of stress and mitochondrial deficiency [168–170], named after the classic UPR that senses disruptions in proteostasis in the ER [171–174]. Evidence describing the mammalian UPR^{mt} is rudimentary, thus, pathways described below are characterized from studies in mammalian cells, as very little work has been dedicated to the UPR^{mt} in muscle. In early work, depleting cells of mtDNA and inducing heat shock induced the expression of the stress-responsive chaperones HSP60/10 and proteases ClpP and YME1L1 [175]. Later, the same effects were achieved upon the overexpression of a terminally-misfolded matrix protein (ΔOTC) to induce mitochondrial proteotoxicity, in a manner dependent on transcription factors CHOP and C/EBPβ [148,151,154,176,177]. These two transcription factors heterodimerize and bind to CHOP elements present in the promoters of downstream targets in the UPR^{mt}, flanked by two UPR^{mt} response elements [177]. Of note, although CHOP regulates genes involved in the UPR^{er}, ΔOTC overexpression did not induce ER chaperones, suggesting a compartment-specific response that is exclusive to the initiation of mitochondrial-protective genes during mitochondrial proteotoxicity [32,177], a phenomenon that was also revealed in *C.elegans* [157]. Great progress in the investigation of the UPR^{mt} has been made using other pharmacological and genetic interventions to trigger this pathway. These include the knockdown of protein import components and

proteostatic machinery [146,178], treatment with pesticides to impair OXPHOS [146,179], the inhibition of mitochondrial transcription and translation [145,146,180–182], and NAD^+ repletion [144,183–185]. UPR^{mt} activation also occurs naturally in contexts of disease and tissue injury, including during cardiac injury [185,186], mitochondrial diseases [181,187] and in cancers [188], generating possibilities of exploiting UPR^{mt} genes as potential therapeutic targets.

The UPR^{mt} is suggested to be the first line of defence against mitochondrial stress. If the stress cannot be alleviated, in instances of chronic dysfunction, mitophagy is activated to eliminate the dysfunctional organelles, and if it persists, the activation of apoptosis/cell death occurs [168]. Although, recent novel work suggests that the UPR^{mt} is downstream of the mitophagy pathway, as it is activated upon the inhibition of mitophagy, preserving mitochondrial homeostasis and cardiac function [189]. Nevertheless, the UPR^{mt} signaling pathway is fairly acute in its activation, and is conserved between organisms. Misfolded proteins that accumulate in the mitochondrial matrix are broken down into peptides by ClpP and transported into the cytosol by a mechanism unknown in mammals (Fig. 2) [190]. This peptide efflux inhibits mitochondrial protein import [178], particularly that of ATF5 [146], which is discussed below. Consequently, this activates PKR, which in turn phosphorylates JNK2, resulting in the activation of the transcription factor c-Jun [191–194]. Via AP-1 sites in their promoters, upon its nuclear localization, c-Jun stimulates the transcription of CHOP and C/EBPβ, inducing the expression of UPR^{mt} genes [176] with the aim of restoring mitochondrial proteostasis. The further accumulation of protein aggregates is also prevented by blocking protein import via degradation of TIM17A by the protease YME1L1 [195] and the ISR-mediated phosphorylation of eIF2a [179,194], which is described below in Translational Regulation.

3.2.2. ATF5: A Mediator of Retrograde Signaling in the UPR^{mt}

Exceptional advances in the characterization of the mammalian UPR^{mt} were achieved upon the identification of ATF5, a stress-responsive bZIP protein of the CREB/ATF family, that mediates mitochondrial-nuclear communication during mitochondrial stress. The ~31 kDa ATF5 protein is made up of 283 amino acids and possesses a DNA-binding domain, facilitating binding to CRE, ARE, AARE and MURE sites, in addition to a C-terminal bZIP region facilitating its interaction with other proteins of its family [196,197]. Intriguingly, ATF5 mRNA retains two uORFs, influencing its translation in diverse cellular conditions, which is described in greater detail in the subsequent section. It was first described by Nishizawa and Nagata in 1992, as they found it to interact with the GPE1-BP on the GPE1 gene, an LPS-inducible regulatory element within the G-CSF promoter, a protein produced in macrophages [198]. Since then, the characterization of ATF5 has greatly expanded. Highly abundant in the liver, a great amount of literature is dedicated to describing its role in the cellular response to starvation and amino acid limitation as it mediates the transcription of the asparagine synthetase gene [199,200], in addition to its requirement in neuronal differentiation and maturation [201,202]. Its steadfast role in cell survival [160,203] has coined ATF5 to be a critical therapeutic target in neurodegeneration [204] and particularly cancer, as a wealth of research proves its depletion to prevent tumour growth and disease progression [159,161]. Although ATF5 is emerging as an influential mediator of the cellular stress response, it remains in the shadow of ATF4, a prominent transcription factor regulating both cell survival and cell death [192,205], of which ATF5 has been suggested to be a member of its subfamily [206]. However, in 2016, ATF5 became novel in its own right, as it was revealed to be a potent transcription factor in the UPR^{mt}, participating in mitochondrial and nuclear localization [146]. A Mitoprot screen identified ATF5 to have a NLS and an N-terminal MTS

similar to ATFS-1, revealing it to be its mammalian homologue [146]. Importantly, the overexpression of ATF5 restores UPR^{mt} function in nematodes lacking ATFS-1 [146], prompting further investigation into the function of this transcription factor in mediating the cellular stress response.

The function of ATF5 in the UPR^{mt} has been primarily investigated in mammalian cell models, revealing it to be upregulated in response to a plethora of cellular stressors [207]. This work has motivated the investigation of ATF5 in the context of mitochondrial-specific stressors. The ATF5 transcript is upregulated during mitochondrial dysfunction stimulated by excessive ROS production, mitochondrial proteotoxicity [146], and mitophagy inhibition [189]. Furthermore, the import efficiency of ATF5 into mitochondria seems to regulate its nuclear translocation to induce the transcription of its downstream UPR^{mt} targets, including HSP60, mtHSP70 and LONP1 during various mitochondrial stressors in cells, while also being required in the maintenance of basal mitochondrial function (Fig. 2) [146]. However, in the absence of stress, ATF5 localizes to mitochondria, revealing its cellular localization and organelle-partitioning activity to be dependent on cellular conditions, comparable to events in worms. The involvement of ATF5 in this mitochondrial stress response is somewhat illustrated in muscle, as ATF5 transcripts are upregulated in skeletal muscle during mitochondrial myopathy [181], β-adrenergic stimulation [208], and in myoblasts during impaired protein translation [209]. Currently, more evidence of ATF5 regulating a UPR^{mt} exists in cardiac muscle in the context of cardiac injury. ATF5 is upregulated during mechanical and pharmacological cardiac insult, and is required for activation of the UPR^{mt} and its rescuing of mitochondrial and cardiac function in animals and cultured cardiomyocytes [185,186,202]. Very recent work has identified increases in ATF5 mRNA and that of its downstream targets involved in the UPR^{mt} in heart muscle of FUNDC1-KO

animals, lacking mitophagy processes [189]. This proves exciting, as this establishes a tentative connection between the ATF5-mediated UPR^{mt} and mitophagy in mammalian tissue, two mitochondrial quality control mechanisms whose molecular relationship is ill-defined. However, the nuclear translocation of ATF5 requires further investigation and observation in different cellular stress conditions, particular in response to exercise stress in muscle, to definitively identify this transcription factor as a critical mediator of the stress-induced adaptive transcriptional response. Despite this, one can gather that ATF5 retains a beneficial role in improving organ function upon mitochondrial dysfunction and injury, creating a foundation for the pursuit in investigating its action in muscle.

The regulation of ATF5 expression in the UPR^{mt} is multifaceted, in that in addition to its cellular localization, its transcription and translation is also controlled to enhance its expression under stressful conditions. ATF5 transcription is suggested to lie downstream of the PKR/JNK2/c-Jun/CHOP pathway during mitochondrial dysfunction as described in the previous section, and is also regulated by ATF4 in various cellular stress conditions [207]. However, once the ATF5 gene is transcribed, it is subject to regulation by an additional regulatory mechanism to modulate its translation and subsequent expression of its protein. The ATF5 transcript possesses two uORFs, with the 5' leading ORF (uORF1) promoting its expression, and the downstream ORF (uORF2) being inhibitory. The "choice" of which uORF is subject to ribosomal scanning is controlled by cellular stimuli, influencing the phosphorylation state of eIF2α [207], providing the UPR^{mt} with an additional layer of homeostatic control. This is discussed in further detail in the following section.

3.2.3. Translational Regulation: The UPR^{mt} and the ISR

In addition to alterations in transcriptional signaling that occur, cellular translation and protein synthesis are also subject to changes in response to elevated mitochondrial stress, resulting in the selective translation of ATF5, CHOP and ATF4 [210]. Activation of the ISR, an adaptive program complementary to the UPR^{mt}, is required for this translational shift [211,212]. The ISR has been coined as a crucial rheostat in the cellular response to disruptions in homeostasis by inducing a protective translational program to reduce the protein folding load of the cell, stimulate the transcription of cytoprotective genes, and rescue organellar dysfunction [169]. Comprised of four distinct kinases, the ISR receives input signals during stress from different subcellular compartments, including the mitochondria and the ER, to converge on the phosphorylation of eIF2α [169,213]. Notably, in *C. elegans*, ROS production activates GCN2, while in mammals, mitochondrial dysfunction during ETC inhibition activates kinases GCN2 and HRI, while mitochondrial proteotoxicity is observed to activate PKR [179,194,195,205,214–216], upregulating CHOP and ATF4 expression. In a translational triaging mechanism, the phosphorylation of eIF2α causes ribosomal stalling, attenuating global protein translation and favouring the selective translation of mRNAs harbouring inhibitory uORFs in their 5' UTRs [217]. Delayed re-initiation of the ribosome allows the complex to bypass the inhibitory uORF and translate the coding sequence, culminating in the increased protein expression of ATF5, CHOP and ATF4 (Fig. 2) [207]. During a plethora of cellular stressors, including thapsigargin treatment (ER stress), arsenite exposure, and proteasome inhibition, all three transcription factors are upregulated, and notably, ATF5 translation and protein expression is increased, in a manner dependent on GCN2 and eIF2α phosphorylation [218]. This novel work is mostly performed in

mammalian cell models of stress, requiring further investigation into the regulation of this pathway during mitochondrial-specific stress in skeletal muscle.

The coordination and function of the ISR and the UPR^{mt} have been tentatively characterized in skeletal muscle. CHOP is known to influence basal mitochondrial content [219] and subsequently, exercise metabolism and performance [79]. Furthermore, ATF4 has been recently established as the main effector of the ISR responding to mitochondrial stress [205], and is required in mediating a collection of cellular adaptations during mitochondrial myopathy in muscle, including amino acid synthesis, autophagy and metabolic remodeling [181]. Both transcription factors can transcriptionally regulate ATF5 [218,220], although, their activation does not always elicit ATF5 expression and UPR^{mt} activation downstream [172,178,205,214]. It is interesting to note that although the signaling pathways of the ISR and the UPR^{mt} overlap, there is significant independence between the transcriptional and translational responses that occur during mitochondrial stress [191,195], with the activation of one not necessarily inducing, or requiring the other. In future investigations, it is worthwhile to question the exact mitochondrial perturbations that induce the UPR^{mt} and the ISR, and whether they occur simultaneously, or at different time points following the induction of the stressor. With the mitochondria existing at the centrum of intersecting signaling axes of stress responses, further knowledge on the various ways in which these pathways are connected, or distinct, could greatly improve the field's understanding of how mitochondria adapt to physiological challenge.

3.2.4. The UPR^{mt} and Exercise in Skeletal Muscle

More evidence is beginning to emerge concerning the role of the UPR^{mt} in mediating adaptations to exercise in muscle, in addition to the relationship between the expression of UPR^{mt} markers and muscle development. Increases in ATF4 and ATF5 expression have been observed

during myoblast differentiation [219,221], and interestingly, CHOP and ATF4 are only upregulated in response to mitochondrial dysfunction in myoblasts and not myotubes, suggesting a role for the cellular metabolic status in activation of stress responses [179]. Furthermore, the expression of UPR^{mt} markers are downregulated in aged muscle [222], and in MuSCs from aged mice [183], coinciding with declines in mitochondrial and muscle function that occur with advancing age [42,223]. Exercise rescued the expression of UPR^{mt} markers in aged muscle [222], while NR treatment, a known inducer of the UPR^{mt} by enhancing NAD^+ pools [144,185], improved UPR^{mt} activation, mitochondrial function, and rescued MuSCs from senescence [183]. Furthermore, eliciting the UPR^{mt} with PARP inhibitors boosts energy expenditure in mouse skeletal muscle [184,224], and improves mitochondrial function and fatty acid oxidation in myotubes of obese humans [224]. Together, these results indicate a potential link between mitochondrial quality and UPR^{mt} signaling in the maintenance of skeletal muscle homeostasis throughout the lifespan and in the presence of metabolic defects.

It has been established to great lengths in this review that skeletal muscle is an extremely malleable tissue, able to alter its intracellular signaling to match the increased physiological demands placed upon it. It is no surprise then, that attention is being shifted toward the regulation of the UPR^{mt} and the UPR^{er} during exercise, and how signaling within these pathways is linked to mitochondrial biogenesis in muscle. Acute treadmill exercise upregulates the gene expression of ISR/UPR^{er} markers, namely CHOP and ATF4 in mouse muscle [79], two transcription factors that have the potential of inducing UPR^{mt} signaling. Increases in the phosphorylation of eIF2α are also observed [79], suggesting the potential regulation of ATF5 protein expression with acute exercise. Resistance exercise and endurance exercise differ in their stress stimuli on muscle, creating a divergence in the molecular pathways that they stimulate. As such, their influence on

mitochondrial adaptations also differ, producing different cellular outcomes and phenotypic alterations [225]. Thus, it is of interest to observe discrepancies in UPR^{mt} signaling between resistance and endurance-type exercise. One bout of unaccustomed resistance exercise induces increases in UPR^{er} proteins [226,227], but not those of the UPR^{mt} or the ISR, suggesting a limited stress response in mitochondria during muscle overload. CCA, a model commonly used in animals and cells to mimick the effects of exercise, is also capable of eliciting acute unfolded protein response signaling [121,122,219]. UPR^{mt} markers are upregulated at the onset of CCA in rodents, and is attenuated with subsequent bouts [122], coinciding with data illustrating the blunted response of mitochondrial gene expression with multiple exercise bouts [62]. In line with this, exercise training is suggested to improve the basal expression of UPR^{mt} proteins [222], as well as blunt the UPR^{mt} response to acute exercise [79], supporting the wealth of evidence outlined previously, that muscle with greater mitochondrial content experiences attenuated signaling to exercise stress [72,76,77]. Furthermore, over the course of a 7-day CCA protocol, changes in UPR^{mt} gene expression precede signaling toward mitochondrial biogenesis, indicating a potential requirement of the UPR^{mt} in skeletal muscle remodeling following contractile activity [122]. Collectively, these studies reveal potential putative roles of the UPR^{mt} and the UPR^{er} in regulating the molecular response to acute exercise, equipping muscle cells with proteostatic machinery to afford protection against future stressors, enabling the maintenance of muscle homeostasis. However, the regulation of ATF5 during exercise, and its role in mediating UPR^{mt} and mitochondrial biogenesis signaling during acute exercise remains to be elucidated.

The importance of PGC-1α in mediating mitochondrial adaptations to exercise in muscle is extensively characterized [228–230], and recent work suggests a role for this transcriptional co-activator in UPR^{mt} signaling. Interestingly, PGC-1α KO mice display deficient UPR activation in

skeletal muscle, coinciding with exercise intolerance [79]. Furthermore, evidence from mammalian cardiac muscle and cardiomyocytes reveals a regulatory function of PGC-1α in coordinating ATF5 expression and thus, UPR^{mt} activation in the rescuing of cardiac dysfunction during injury [186]. The discovery of this novel PGC-1α/ATF5 regulatory axis in the heart creates a possible avenue worth exploring, raising the question of whether this molecular coordination holds true in skeletal muscle in the adaptation to exercise stress.

RESEARCH OBJECTIVES:

Based on the literature cited above, the objectives of my thesis were to:

1. Assess basal mitochondrial content and function in the absence of the UPR^{mt} transcription factor ATF5;
2. Examine the effects of two different acute exercise protocols, one continuous at a moderate intensity, and the other exhaustive, on UPR^{mt} signaling in skeletal muscle;
3. Determine whether ATF5 plays a role in mediating changes in UPR^{mt} gene expression and mitochondrial biogenesis signaling in response to acute exercise;
4. Identify whether ATF5 translocates to the nucleus upon acute exercise stress.

HYPOTHESES

We hypothesized that:

1. Basally, ATF5 KO mice will display reduced mitochondrial content and function;
2. Both exercise protocols will stimulate UPR^{mt} signaling, including upregulations in mRNA of ATF5, in addition to that of its downstream targets;
3. ATF5 KO mice will display attenuated UPR^{mt} signaling in response to acute exercise;
4. Exercise will stimulate the nuclear translocation of ATF5.

REFERENCES

[1] D.M. Bramble, D.E. Lieberman, Endurance running and the evolution of Homo, Nature. 432 (2004) 345–352. https://doi.org/10.1038/nature03052.

[2] D.A. Hood, G. Uguccioni, A. Vainshtein, D. D'souza, Mechanisms of exercise-induced mitochondrial biogenesis in skeletal muscle: implications for health and disease, Compr. Physiol. 1 (2011) 1119–1134. https://doi.org/10.1002/cphy.c100074.

[3] B. Blaauw, S. Schiaffino, C. Reggiani, Mechanisms Modulating Skeletal Muscle Phenotype, in: Compr. Physiol., American Cancer Society, 2013: pp. 1645–1687. https://doi.org/10.1002/cphy.c130009.

[4] D.P. Blondin, F. Haman, Shivering and nonshivering thermogenesis in skeletal muscles, Handb. Clin. Neurol. 156 (2018) 153–173. https://doi.org/10.1016/B978-0-444-63912-7.00010-2.

[5] R.M. Murphy, M.J. Watt, M.A. Febbraio, Metabolic communication during exercise, Nat. Metab. 2 (2020) 805–816. https://doi.org/10.1038/s42255-020-0258-x.

[6] B. Egan, J.R. Zierath, Exercise Metabolism and the Molecular Regulation of Skeletal Muscle Adaptation, Cell Metab. 17 (2013) 162–184. https://doi.org/10.1016/j.cmet.2012.12.012.

[7] W.R. Frontera, J. Ochala, Skeletal Muscle: A Brief Review of Structure and Function, Calcif. Tissue Int. 96 (2015) 183–195. https://doi.org/10.1007/s00223-014-9915-y.

[8] D.L. Allen, S.R. Monke, R.J. Talmadge, R.R. Roy, V.R. Edgerton, Plasticity of myonuclear number in hypertrophied and atrophied mammalian skeletal muscle fibers, J. Appl. Physiol. Bethesda Md 1985. 78 (1995) 1969–1976. https://doi.org/10.1152/jappl.1995.78.5.1969.

[9] J.E. Morgan, T.A. Partridge, Muscle satellite cells, Int. J. Biochem. Cell Biol. 35 (2003) 1151–1156. https://doi.org/10.1016/s1357-2725(03)00042-6.

[10] D. Pette, R.S. Staron, Myosin isoforms, muscle fiber types, and transitions, Microsc. Res. Tech. 50 (2000) 500–509. https://doi.org/10.1002/1097-0029(20000915)50:6<500::AID-JEMT7>3.0.CO;2-7.

[11] J. Talbot, L. Maves, Skeletal muscle fiber type: using insights from muscle developmental biology to dissect targets for susceptibility and resistance to muscle disease, Wiley Interdiscip. Rev. Dev. Biol. 5 (2016) 518–534. https://doi.org/10.1002/wdev.230.

[12] J.R. Zierath, J.A. Hawley, Skeletal Muscle Fiber Type: Influence on Contractile and Metabolic Properties, PLoS Biol. 2 (2004) e348. https://doi.org/10.1371/journal.pbio.0020348.

[13] R. Bottinelli, C. Reggiani, Human skeletal muscle fibres: molecular and functional diversity, Prog. Biophys. Mol. Biol. 73 (2000) 195–262. https://doi.org/10.1016/s0079-6107(00)00006-7.

[14] C.R. Lamboley, R.M. Murphy, M.J. McKenna, G.D. Lamb, Sarcoplasmic reticulum Ca2+ uptake and leak properties, and SERCA isoform expression, in type I and type II fibres of human skeletal muscle, J. Physiol. 592 (2014) 1381–1395. https://doi.org/10.1113/jphysiol.2013.269373.

[15] D. D'souza, R.Y.J. Lai, M. Shuen, D.A. Hood, mRNA stability as a function of striated muscle oxidative capacity, Am. J. Physiol. Regul. Integr. Comp. Physiol. 303 (2012) R408-417. https://doi.org/10.1152/ajpregu.00085.2012.

[16] L.B. Verdijk, B.G. Gleeson, R.A.M. Jonkers, K. Meijer, H.H.C.M. Savelberg, P. Dendale, L.J.C. van Loon, Skeletal muscle hypertrophy following resistance training is accompanied by a fiber type-specific increase in satellite cell content in elderly men, J. Gerontol. A. Biol. Sci. Med. Sci. 64 (2009) 332–339. https://doi.org/10.1093/gerona/gln050.

[17] K. Baar, K. Esser, Phosphorylation of p70(S6k) correlates with increased skeletal muscle mass following resistance exercise, Am. J. Physiol. 276 (1999) C120-127. https://doi.org/10.1152/ajpcell.1999.276.1.C120.

[18] R. Nilwik, T. Snijders, M. Leenders, B.B.L. Groen, J. van Kranenburg, L.B. Verdijk, L.J.C. van Loon, The decline in skeletal muscle mass with aging is mainly attributed to a reduction in type II muscle fiber size, Exp. Gerontol. 48 (2013) 492–498. https://doi.org/10.1016/j.exger.2013.02.012.

[19] L.B. Verdijk, R. Koopman, G. Schaart, K. Meijer, H.H.C.M. Savelberg, L.J.C. van Loon, Satellite cell content is specifically reduced in type II skeletal muscle fibers in the elderly, Am. J. Physiol. Endocrinol. Metab. 292 (2007) E151-157. https://doi.org/10.1152/ajpendo.00278.2006.

[20] A. Oberbach, Y. Bossenz, S. Lehmann, J. Niebauer, V. Adams, R. Paschke, M.R. Schön, M. Blüher, K. Punkt, Altered fiber distribution and fiber-specific glycolytic and oxidative enzyme activity in skeletal muscle of patients with type 2 diabetes, Diabetes Care. 29 (2006) 895–900. https://doi.org/10.2337/diacare.29.04.06.dc05-1854.

[21] G.D. Cartee, E.B. Arias, C.S. Yu, M.W. Pataky, Novel single skeletal muscle fiber analysis reveals a fiber type-selective effect of acute exercise on glucose uptake, Am. J. Physiol. Endocrinol. Metab. 311 (2016) E818–E824. https://doi.org/10.1152/ajpendo.00289.2016.

[22] N. Hua, H. Takahashi, G.M. Yee, Y. Kitajima, S. Katagiri, M. Kojima, K. Anzai, Y. Eguchi, J.A. Hamilton, Influence of muscle fiber type composition on early fat accumulation under high-fat diet challenge, PloS One. 12 (2017) e0182430. https://doi.org/10.1371/journal.pone.0182430.

[23] A.J. Roger, S.A. Muñoz-Gómez, R. Kamikawa, The Origin and Diversification of Mitochondria, Curr. Biol. CB. 27 (2017) R1177–R1192. https://doi.org/10.1016/j.cub.2017.09.015.

[24] I. Garcia, E. Jones, M. Ramos, W. Innis-Whitehouse, R. Gilkerson, The little big genome: the organization of mitochondrial DNA, Front. Biosci. Landmark Ed. 22 (2017) 710–721.

[25] T.G. Frey, C.A. Mannella, The internal structure of mitochondria, Trends Biochem. Sci. 25 (2000) 319–324. https://doi.org/10.1016/s0968-0004(00)01609-1.

[26] C.A. Mannella, M. Marko, P. Penczek, D. Barnard, J. Frank, The internal compartmentation of rat-liver mitochondria: tomographic study using the high-voltage transmission electron microscope, Microsc. Res. Tech. 27 (1994) 278–283. https://doi.org/10.1002/jemt.1070270403.

[27] A.T. Erlich, L.D. Tryon, M.J. Crilly, J.M. Memme, Z.S.M. Moosavi, A.N. Oliveira, K. Beyfuss, D.A. Hood, Function of specialized regulatory proteins and signaling pathways in exercise-induced muscle mitochondrial biogenesis, Integr. Med. Res. 5 (2016) 187–197. https://doi.org/10.1016/j.imr.2016.05.003.

[28] S.E. Calvo, V.K. Mootha, The Mitochondrial Proteome and Human Disease, Annu. Rev. Genomics Hum. Genet. 11 (2010) 25–44. https://doi.org/10.1146/annurev-genom-082509-141720.

[29] R.D. Martinus, M.T. Ryan, D.J. Naylor, S.M. Herd, N.J. Hoogenraad, P.B. Høj, Role of chaperones in the biogenesis and maintenance of the mitochondrion, FASEB J. Off. Publ. Fed. Am. Soc. Exp. Biol. 9 (1995) 371–378. https://doi.org/10.1096/fasebj.9.5.7896006.

[30] A. Vincent, K. White, J. Phillips, T. Ogden, C. Lawless, C. Warren, M. Hall, Y.S. Ng, G. Falkous, D. Deehan, D. Turnbull, M. Picard, Quantitative 3D Mapping of the Human Skeletal Muscle Mitochondrial Network, Cell Rep. 26 (2019). https://doi.org/10.1016/j.celrep.2019.01.010.

[31] N. Pfanner, B. Warscheid, N. Wiedemann, Mitochondrial protein organization: from biogenesis to networks and function, Nat. Rev. Mol. Cell Biol. 20 (2019) 267–284. https://doi.org/10.1038/s41580-018-0092-0.

[32] Q. Zhao, J. Wang, I.V. Levichkin, S. Stasinopoulos, M.T. Ryan, N.J. Hoogenraad, A mitochondrial specific stress response in mammalian cells, EMBO J. 21 (2002) 4411–4419. https://doi.org/10.1093/emboj/cdf445.

[33] P.J. Adhihetty, M.F.N. O'Leary, D.A. Hood, Mitochondria in skeletal muscle: adaptable rheostats of apoptotic susceptibility, Exerc. Sport Sci. Rev. 36 (2008) 116–121. https://doi.org/10.1097/JES.0b013e31817be7b7.

[34] P.H.G.M. Willems, R. Rossignol, C.E.J. Dieteren, M.P. Murphy, W.J.H. Koopman, Redox Homeostasis and Mitochondrial Dynamics, Cell Metab. 22 (2015) 207–218. https://doi.org/10.1016/j.cmet.2015.06.006.

[35] S. Iqbal, O. Ostojic, K. Singh, A.-M. Joseph, D.A. Hood, Expression of mitochondrial fission and fusion regulatory proteins in skeletal muscle during chronic use and disuse, Muscle Nerve. 48 (2013) 963–970. https://doi.org/10.1002/mus.23838.

[36] T. Kleele, T. Rey, J. Winter, S. Zaganelli, D. Mahecic, H. Perreten Lambert, F.P. Ruberto, M. Nemir, T. Wai, T. Pedrazzini, S. Manley, Distinct fission signatures predict mitochondrial degradation or biogenesis, Nature. 593 (2021) 435–439. https://doi.org/10.1038/s41586-021-03510-6.

[37] B. Glancy, L.M. Hartnell, C.A. Combs, A. Femnou, J. Sun, E. Murphy, S. Subramaniam, R.S. Balaban, Power Grid Protection of the Muscle Mitochondrial Reticulum, Cell Rep. 19 (2017) 487–496. https://doi.org/10.1016/j.celrep.2017.03.063.

[38] S.P. Kirkwood, E.A. Munn, G.A. Brooks, Mitochondrial reticulum in limb skeletal muscle, Am. J. Physiol. 251 (1986) C395-402. https://doi.org/10.1152/ajpcell.1986.251.3.C395.

[39] S.P. Kirkwood, L. Packer, G.A. Brooks, Effects of endurance training on a mitochondrial reticulum in limb skeletal muscle, Arch. Biochem. Biophys. 255 (1987) 80–88. https://doi.org/10.1016/0003-9861(87)90296-7.

[40] A.E. Vincent, Y.S. Ng, K. White, T. Davey, C. Mannella, G. Falkous, C. Feeney, A.M. Schaefer, R. McFarland, G.S. Gorman, R.W. Taylor, D.M. Turnbull, M. Picard, The Spectrum of Mitochondrial Ultrastructural Defects in Mitochondrial Myopathy, Sci. Rep. 6 (2016) 30610. https://doi.org/10.1038/srep30610.

[41] A. Zorzano, M. Liesa, M. Palacín, Mitochondrial dynamics as a bridge between mitochondrial dysfunction and insulin resistance, Arch. Physiol. Biochem. 115 (2009) 1–12. https://doi.org/10.1080/13813450802676335.

[42] V. Ljubicic, A.-M. Joseph, P.J. Adhihetty, J.H. Huang, A. Saleem, G. Uguccioni, D.A. Hood, Molecular basis for an attenuated mitochondrial adaptive plasticity in aged skeletal muscle, Aging. 1 (2009) 818–830.

[43] H. Hoppeler, Exercise-induced ultrastructural changes in skeletal muscle, Int. J. Sports Med. 7 (1986) 187–204. https://doi.org/10.1055/s-2008-1025758.

[44] A.M. Cogswell, R.J. Stevens, D.A. Hood, Properties of skeletal muscle mitochondria isolated from subsarcolemmal and intermyofibrillar regions, Am. J. Physiol.-Cell Physiol. 264 (1993) C383–C389. https://doi.org/10.1152/ajpcell.1993.264.2.C383.

[45] M.K. Connor, O. Bezborodova, C.P. Escobar, D.A. Hood, Effect of contractile activity on protein turnover in skeletal muscle mitochondrial subfractions, J. Appl. Physiol. Bethesda Md 1985. 88 (2000) 1601–1606. https://doi.org/10.1152/jappl.2000.88.5.1601.

[46] V.B. Ritov, E.V. Menshikova, J. He, R.E. Ferrell, B.H. Goodpaster, D.E. Kelley, Deficiency of subsarcolemmal mitochondria in obesity and type 2 diabetes, Diabetes. 54 (2005) 8–14. https://doi.org/10.2337/diabetes.54.1.8.

[47] D.A. Krieger, C.A. Tate, J. McMillin-Wood, F.W. Booth, Populations of rat skeletal muscle mitochondria after exercise and immobilization, J. Appl. Physiol. 48 (1980) 23–28. https://doi.org/10.1152/jappl.1980.48.1.23.

[48] R. Ferreira, R. Vitorino, R.M.P. Alves, H.J. Appell, S.K. Powers, J.A. Duarte, F. Amado, Subsarcolemmal and intermyofibrillar mitochondria proteome differences disclose functional specializations in skeletal muscle, Proteomics. 10 (2010) 3142–3154. https://doi.org/10.1002/pmic.201000173.

[49] M. Takahashi, D.A. Hood, Protein Import into Subsarcolemmal and Intermyofibrillar Skeletal Muscle Mitochondria, J. Biol. Chem. 271 (1996) 27285–27291. https://doi.org/10.1074/jbc.271.44.27285.

[50] P. Mitchell, Coupling of phosphorylation to electron and hydrogen transfer by a chemi-osmotic type of mechanism, Nature. 191 (1961) 144–148. https://doi.org/10.1038/191144a0.

[51] B. Chance, G.R. Williams, The respiratory chain and oxidative phosphorylation, Adv. Enzymol. Relat. Subj. Biochem. 17 (1956) 65–134. https://doi.org/10.1002/9780470122624.ch2.

[52] R.-Z. Zhao, S. Jiang, L. Zhang, Z.-B. Yu, Mitochondrial electron transport chain, ROS generation and uncoupling (Review), Int. J. Mol. Med. 44 (2019) 3–15. https://doi.org/10.3892/ijmm.2019.4188.

[53] J. Bangsbo, P.D. Gollnick, T.E. Graham, C. Juel, B. Kiens, M. Mizuno, B. Saltin, Anaerobic energy production and O2 deficit-debt relationship during exhaustive exercise in humans, J. Physiol. 422 (1990) 539–559. https://doi.org/10.1113/jphysiol.1990.sp018000.

[54] M. Fiorenza, T.P. Gunnarsson, M. Hostrup, F.M. Iaia, F. Schena, H. Pilegaard, J. Bangsbo, Metabolic stress-dependent regulation of the mitochondrial biogenic molecular response to high-intensity exercise in human skeletal muscle, J. Physiol. 596 (2018) 2823–2840. https://doi.org/10.1113/JP275972.

[55] J.P. Little, A. Safdar, D. Bishop, M.A. Tarnopolsky, M.J. Gibala, An acute bout of high-intensity interval training increases the nuclear abundance of PGC-1α and activates mitochondrial biogenesis in human skeletal muscle, Am. J. Physiol. Regul. Integr. Comp. Physiol. 300 (2011) R1303-1310. https://doi.org/10.1152/ajpregu.00538.2010.

[56] D.A. Hood, I. Irrcher, V. Ljubicic, A.-M. Joseph, Coordination of metabolic plasticity in skeletal muscle, J. Exp. Biol. 209 (2006) 2265–2275. https://doi.org/10.1242/jeb.02182.

[57] H. Hoppeler, S. Klossner, M. Flück, Gene expression in working skeletal muscle, Adv. Exp. Med. Biol. 618 (2007) 245–254. https://doi.org/10.1007/978-0-387-75434-5_19.

[58] J.O. Holloszy, Biochemical Adaptations in Muscle, J. Biol. Chem. 242 (1967) 2278–2282. https://doi.org/10.1016/S0021-9258(18)96046-1.

[59] H. Howald, H. Hoppeler, H. Claassen, O. Mathieu, R. Straub, Influences of endurance training on the ultrastructural composition of the different muscle fiber types in humans, Pflugers Arch. 403 (1985) 369–376. https://doi.org/10.1007/BF00589248.

[60] R.A. Jacobs, D. Flück, T.C. Bonne, S. Bürgi, P.M. Christensen, M. Toigo, C. Lundby, Improvements in exercise performance with high-intensity interval training coincide with an increase in skeletal muscle mitochondrial content and function, J. Appl. Physiol. Bethesda Md 1985. 115 (2013) 785–793. https://doi.org/10.1152/japplphysiol.00445.2013.

[61] P.D. Gollnick, B. Saltin, Significance of skeletal muscle oxidative enzyme enhancement with endurance training, Clin. Physiol. Oxf. Engl. 2 (1982) 1–12. https://doi.org/10.1111/j.1475-097x.1982.tb00001.x.

[62] C.G.R. Perry, J. Lally, G.P. Holloway, G.J.F. Heigenhauser, A. Bonen, L.L. Spriet, Repeated transient mRNA bursts precede increases in transcriptional and mitochondrial proteins during training in human skeletal muscle, J. Physiol. 588 (2010) 4795–4810. https://doi.org/10.1113/jphysiol.2010.199448.

[63] A.N. Oliveira, B.J. Richards, M. Slavin, D.A. Hood, Exercise Is Muscle Mitochondrial Medicine, Exerc. Sport Sci. Rev. 49 (2021) 67–76. https://doi.org/10.1249/JES.0000000000000250.

[64] B. Egan, B.P. Carson, P.M. Garcia-Roves, A.V. Chibalin, F.M. Sarsfield, N. Barron, N. McCaffrey, N.M. Moyna, J.R. Zierath, D.J. O'Gorman, Exercise intensity-dependent regulation of peroxisome proliferator-activated receptor coactivator-1 mRNA abundance is associated with differential activation of upstream signalling kinases in human skeletal muscle, J. Physiol. 588 (2010) 1779–1790. https://doi.org/10.1113/jphysiol.2010.188011.

[65] N. Brandt, T.P. Gunnarsson, M. Hostrup, J. Tybirk, L. Nybo, H. Pilegaard, J. Bangsbo, Impact of adrenaline and metabolic stress on exercise-induced intracellular signaling and PGC-1α mRNA response in human skeletal muscle, Physiol. Rep. 4 (2016) e12844. https://doi.org/10.14814/phy2.12844.

[66] A. Saleem, H.N. Carter, D.A. Hood, p53 is necessary for the adaptive changes in cellular milieu subsequent to an acute bout of endurance exercise, Am. J. Physiol. - Cell Physiol. 306 (2014) C241–C249. https://doi.org/10.1152/ajpcell.00270.2013.

[67] H. Pilegaard, P.D. Neufer, Transcriptional regulation of pyruvate dehydrogenase kinase 4 in skeletal muscle during and after exercise, Proc. Nutr. Soc. 63 (2004) 221–226. https://doi.org/10.1079/pns2004345.

[68] A. Vainshtein, L.D. Tryon, M. Pauly, D.A. Hood, Role of PGC-1α during acute exercise-induced autophagy and mitophagy in skeletal muscle, Am. J. Physiol. Cell Physiol. 308 (2015) C710-719. https://doi.org/10.1152/ajpcell.00380.2014.

[69] M.J. MacInnis, M.J. Gibala, Physiological adaptations to interval training and the role of exercise intensity, J. Physiol. 595 (2017) 2915–2930. https://doi.org/10.1113/JP273196.

[70] R.A. Howlett, M.L. Parolin, D.J. Dyck, E. Hultman, N.L. Jones, G.J. Heigenhauser, L.L. Spriet, Regulation of skeletal muscle glycogen phosphorylase and PDH at varying exercise power outputs, Am. J. Physiol. 275 (1998) R418-425. https://doi.org/10.1152/ajpregu.1998.275.2.R418.

[71] B. Egan, B.P. Carson, P.M. Garcia-Roves, A.V. Chibalin, F.M. Sarsfield, N. Barron, N. McCaffrey, N.M. Moyna, J.R. Zierath, D.J. O'Gorman, Exercise intensity-dependent regulation of peroxisome proliferator-activated receptor γ coactivator-1α mRNA abundance is associated with differential activation of upstream signalling kinases in human skeletal muscle, J. Physiol. 588 (2010) 1779–1790. https://doi.org/10.1113/jphysiol.2010.188011.

[72] G.A. Dudley, P.C. Tullson, R.L. Terjung, Influence of mitochondrial content on the sensitivity of respiratory control, J. Biol. Chem. 262 (1987) 9109–9114.

[73] J. Henriksson, J.S. Reitman, Time Course of Changes in Human Skeletal Muscle Succinate Dehydrogenase and Cytochrome Oxidase Activities and Maximal Oxygen Uptake with Physical Activity and Inactivity, Acta Physiol. Scand. 99 (1977) 91–97. https://doi.org/10.1111/j.1748-1716.1977.tb10356.x.

[74] G. Benzi, P. Panceri, M. de Bernardi, R. Villa, E. Arcelli, L. D'Angelo, E. Arrigoni, F. Bertè, Mitochondrial enzymatic adaptation of skeletal muscle to endurance training, J. Appl. Physiol. 38 (1975) 565–569. https://doi.org/10.1152/jappl.1975.38.4.565.

[75] S.H. Constable, R.J. Favier, J.A. McLane, R.D. Fell, M. Chen, J.O. Holloszy, Energy metabolism in contracting rat skeletal muscle: adaptation to exercise training, Am. J. Physiol. 253 (1987) C316-322. https://doi.org/10.1152/ajpcell.1987.253.2.C316.

[76] V. Ljubicic, D.A. Hood, Specific attenuation of protein kinase phosphorylation in muscle with a high mitochondrial content, Am. J. Physiol. Endocrinol. Metab. 297 (2009) E749-758. https://doi.org/10.1152/ajpendo.00130.2009.

[77] N.B. Nordsborg, C. Lundby, L. Leick, H. Pilegaard, Relative Workload Determines Exercise-Induced Increases in PGC-1α mRNA, Med. Sci. Sports Exerc. 42 (2010) 1477–1484. https://doi.org/10.1249/MSS.0b013e3181d2d21c.

[78] B. Egan, P.L. O'Connor, J.R. Zierath, D.J. O'Gorman, Time course analysis reveals gene-specific transcript and protein kinetics of adaptation to short-term aerobic exercise training in human skeletal muscle, PloS One. 8 (2013) e74098. https://doi.org/10.1371/journal.pone.0074098.

[79] J. Wu, J.L. Ruas, J.L. Estall, K.A. Rasbach, J.H. Choi, L. Ye, P. Boström, H.M. Tyra, R.W. Crawford, K.P. Campbell, D.T. Rutkowski, R.J. Kaufman, B.M. Spiegelman, The unfolded protein

response mediates adaptation to exercise in skeletal muscle through a PGC-1α /ATF6α complex, Cell Metab. 13 (2011) 160–169. https://doi.org/10.1016/j.cmet.2011.01.003.

[80] P. Puigserver, Z. Wu, C.W. Park, R. Graves, M. Wright, B.M. Spiegelman, A cold-inducible coactivator of nuclear receptors linked to adaptive thermogenesis, Cell. 92 (1998) 829–839. https://doi.org/10.1016/s0092-8674(00)81410-5.

[81] J. Lin, H. Wu, P.T. Tarr, C.-Y. Zhang, Z. Wu, O. Boss, L.F. Michael, P. Puigserver, E. Isotani, E.N. Olson, B.B. Lowell, R. Bassel-Duby, B.M. Spiegelman, Transcriptional co-activator PGC-1 alpha drives the formation of slow-twitch muscle fibres, Nature. 418 (2002) 797–801. https://doi.org/10.1038/nature00904.

[82] K. Baar, A.R. Wende, T.E. Jones, M. Marison, L.A. Nolte, M. Chen, D.P. Kelly, J.O. Holloszy, Adaptations of skeletal muscle to exercise: rapid increase in the transcriptional coactivator PGC-1, FASEB J. Off. Publ. Fed. Am. Soc. Exp. Biol. 16 (2002) 1879–1886. https://doi.org/10.1096/fj.02-0367com.

[83] J.P. Little, A. Safdar, N. Cermak, M.A. Tarnopolsky, M.J. Gibala, Acute endurance exercise increases the nuclear abundance of PGC-1alpha in trained human skeletal muscle, Am. J. Physiol. Regul. Integr. Comp. Physiol. 298 (2010) R912-917. https://doi.org/10.1152/ajpregu.00409.2009.

[84] Mechanisms controlling mitochondrial biogenesis and respiration through the thermogenic coactivator PGC-1 - PubMed, (n.d.). https://pubmed.ncbi.nlm.nih.gov/10412986/ (accessed August 16, 2021).

[85] R.B. Vega, J.M. Huss, D.P. Kelly, The coactivator PGC-1 cooperates with peroxisome proliferator-activated receptor alpha in transcriptional control of nuclear genes encoding mitochondrial fatty acid oxidation enzymes, Mol. Cell. Biol. 20 (2000) 1868–1876. https://doi.org/10.1128/MCB.20.5.1868-1876.2000.

[86] P.M. Quirós, A. Mottis, J. Auwerx, Mitonuclear communication in homeostasis and stress, Nat. Rev. Mol. Cell Biol. 17 (2016) 213–226. https://doi.org/10.1038/nrm.2016.23.

[87] A. Saleem, D.A. Hood, Acute exercise induces tumour suppressor protein p53 translocation to the mitochondria and promotes a p53-Tfam-mitochondrial DNA complex in skeletal muscle, J. Physiol. 591 (2013) 3625–3636. https://doi.org/10.1113/jphysiol.2013.252791.

[88] J.W. Gordon, A.A. Rungi, H. Inagaki, D.A. Hood, Effects of contractile activity on mitochondrial transcription factor A expression in skeletal muscle, J. Appl. Physiol. Bethesda Md 1985. 90 (2001) 389–396. https://doi.org/10.1152/jappl.2001.90.1.389.

[89] B. Egan, J.R. Zierath, Exercise Metabolism and the Molecular Regulation of Skeletal Muscle Adaptation, Cell Metab. 17 (2013) 162–184. https://doi.org/10.1016/j.cmet.2012.12.012.

[90] J.A. Calvo, T.G. Daniels, X. Wang, A. Paul, J. Lin, B.M. Spiegelman, S.C. Stevenson, S.M. Rangwala, Muscle-specific expression of PPARgamma coactivator-1alpha improves exercise performance and increases peak oxygen uptake, J. Appl. Physiol. Bethesda Md 1985. 104 (2008) 1304–1312. https://doi.org/10.1152/japplphysiol.01231.2007.

[91] P.J. Adhihetty, G. Uguccioni, L. Leick, J. Hidalgo, H. Pilegaard, D.A. Hood, The role of PGC-1alpha on mitochondrial function and apoptotic susceptibility in muscle, Am. J. Physiol. Cell Physiol. 297 (2009) C217-225. https://doi.org/10.1152/ajpcell.00070.2009.

[92] G. Uguccioni, D.A. Hood, The importance of PGC-1α in contractile activity-induced mitochondrial adaptations, Am. J. Physiol.-Endocrinol. Metab. 300 (2011) E361–E371. https://doi.org/10.1152/ajpendo.00292.2010.

[93] A.T. Erlich, D.M. Brownlee, K. Beyfuss, D.A. Hood, Exercise induces TFEB expression and activity in skeletal muscle in a PGC-1α-dependent manner, Am. J. Physiol. Cell Physiol. 314 (2018) C62–C72. https://doi.org/10.1152/ajpcell.00162.2017.

[94] L. Leick, J.F.P. Wojtaszewski, S.T. Johansen, K. Kiilerich, G. Comes, Y. Hellsten, J. Hidalgo, H. Pilegaard, PGC-1alpha is not mandatory for exercise- and training-induced adaptive gene responses in mouse skeletal muscle, Am. J. Physiol. Endocrinol. Metab. 294 (2008) E463-474. https://doi.org/10.1152/ajpendo.00666.2007.

[95] D.A. Hood, L.D. Tryon, H.N. Carter, Y. Kim, C.C.W. Chen, Unravelling the mechanisms regulating muscle mitochondrial biogenesis, Biochem. J. 473 (2016) 2295–2314. https://doi.org/10.1042/BCJ20160009.

[96] Y. Zhang, G. Uguccioni, V. Ljubicic, I. Irrcher, S. Iqbal, K. Singh, S. Ding, D.A. Hood, Multiple signaling pathways regulate contractile activity-mediated PGC-1α gene expression and activity in skeletal muscle cells, Physiol. Rep. 2 (2014) e12008. https://doi.org/10.14814/phy2.12008.

[97] H. Wu, S.B. Kanatous, F.A. Thurmond, T. Gallardo, E. Isotani, R. Bassel-Duby, R.S. Williams, Regulation of mitochondrial biogenesis in skeletal muscle by CaMK, Science. 296 (2002) 349–352. https://doi.org/10.1126/science.1071163.

[98] A.J. Rose, M. Hargreaves, Exercise Increases Ca2+–Calmodulin-Dependent Protein Kinase II Activity in Human Skeletal Muscle, J. Physiol. 553 (2003) 303–309. https://doi.org/10.1113/jphysiol.2003.054171.

[99] T.E. Jensen, A.J. Rose, S.B. Jørgensen, N. Brandt, P. Schjerling, J.F.P. Wojtaszewski, E.A. Richter, Possible CaMKK-dependent regulation of AMPK phosphorylation and glucose uptake at the onset of mild tetanic skeletal muscle contraction, Am. J. Physiol. Endocrinol. Metab. 292 (2007) E1308-1317. https://doi.org/10.1152/ajpendo.00456.2006.

[100] S.L. McGee, M. Hargreaves, Exercise and myocyte enhancer factor 2 regulation in human skeletal muscle, Diabetes. 53 (2004) 1208–1214. https://doi.org/10.2337/diabetes.53.5.1208.

[101] I. Irrcher, V. Ljubicic, D.A. Hood, Interactions between ROS and AMP kinase activity in the regulation of PGC-1alpha transcription in skeletal muscle cells, Am. J. Physiol. Cell Physiol. 296 (2009) C116-123. https://doi.org/10.1152/ajpcell.00267.2007.

[102] I. Irrcher, V. Ljubicic, A.F. Kirwan, D.A. Hood, AMP-activated protein kinase-regulated activation of the PGC-1alpha promoter in skeletal muscle cells, PloS One. 3 (2008) e3614. https://doi.org/10.1371/journal.pone.0003614.

[103] S. Jäger, C. Handschin, J. St-Pierre, B.M. Spiegelman, AMP-activated protein kinase (AMPK) action in skeletal muscle via direct phosphorylation of PGC-1alpha, Proc. Natl. Acad. Sci. U. S. A. 104 (2007) 12017–12022. https://doi.org/10.1073/pnas.0705070104.

[104] A.C. Petersen, M.J. McKenna, I. Medved, K.T. Murphy, M.J. Brown, P. Della Gatta, D. Cameron-Smith, Infusion with the antioxidant N-acetylcysteine attenuates early adaptive responses to exercise in human skeletal muscle, Acta Physiol. Oxf. Engl. 204 (2012) 382–392. https://doi.org/10.1111/j.1748-1716.2011.02344.x.

[105] M. Whitham, M.H.S. Chan, M. Pal, V.B. Matthews, O. Prelovsek, S. Lunke, A. El-Osta, H. Broenneke, J. Alber, J.C. Brüning, F.T. Wunderlich, G.I. Lancaster, M.A. Febbraio, Contraction-induced interleukin-6 gene transcription in skeletal muscle is regulated by c-Jun terminal kinase/activator protein-1, J. Biol. Chem. 287 (2012) 10771–10779. https://doi.org/10.1074/jbc.M111.310581.

[106] A. Vainshtein, L. Kazak, D.A. Hood, Effects of endurance training on apoptotic susceptibility in striated muscle, J. Appl. Physiol. Bethesda Md 1985. 110 (2011) 1638–1645. https://doi.org/10.1152/japplphysiol.00020.2011.

[107] T. Akimoto, S.C. Pohnert, P. Li, M. Zhang, C. Gumbs, P.B. Rosenberg, R.S. Williams, Z. Yan, Exercise stimulates Pgc-1alpha transcription in skeletal muscle through activation of the p38 MAPK pathway, J. Biol. Chem. 280 (2005) 19587–19593. https://doi.org/10.1074/jbc.M408862200.

[108] K.J. Menzies, K. Singh, A. Saleem, D.A. Hood, Sirtuin 1-mediated effects of exercise and resveratrol on mitochondrial biogenesis, J. Biol. Chem. 288 (2013) 6968–6979. https://doi.org/10.1074/jbc.M112.431155.

[109] C. Cantó, Z. Gerhart-Hines, J.N. Feige, M. Lagouge, L. Noriega, J.C. Milne, P.J. Elliott, P. Puigserver, J. Auwerx, AMPK regulates energy expenditure by modulating NAD+ metabolism and SIRT1 activity, Nature. 458 (2009) 1056–1060. https://doi.org/10.1038/nature07813.

[110] H. Hoppeler, Molecular networks in skeletal muscle plasticity, J. Exp. Biol. 219 (2016) 205–213. https://doi.org/10.1242/jeb.128207.

[111] A.-M. Joseph, H. Pilegaard, A. Litvintsev, L. Leick, D.A. Hood, Control of gene expression and mitochondrial biogenesis in the muscular adaptation to endurance exercise, Essays Biochem. 42 (2006) 13–29. https://doi.org/10.1042/bse0420013.

[112] O. Ostojic, M.F.N. O'Leary, K. Singh, K.J. Menzies, A. Vainshtein, D.A. Hood, The effects of chronic muscle use and disuse on cardiolipin metabolism, J. Appl. Physiol. Bethesda Md 1985. 114 (2013) 444–452. https://doi.org/10.1152/japplphysiol.01312.2012.

[113] M. Takahashi, D.A. Hood, Chronic stimulation-induced changes in mitochondria and performance in rat skeletal muscle, J. Appl. Physiol. Bethesda Md 1985. 74 (1993) 934–941. https://doi.org/10.1152/jappl.1993.74.2.934.

[114] S.G. Rolland, S. Schneid, M. Schwarz, E. Rackles, C. Fischer, S. Haeussler, S.G. Regmi, A. Yeroslaviz, B. Habermann, D. Mokranjac, E. Lambie, B. Conradt, Compromised Mitochondrial Protein Import Acts as a Signal for UPRmt, Cell Rep. 28 (2019) 1659-1669.e5. https://doi.org/10.1016/j.celrep.2019.07.049.

[115] A.M. Nargund, M.W. Pellegrino, C.J. Fiorese, B.M. Baker, C.M. Haynes, Mitochondrial import efficiency of ATFS-1 regulates mitochondrial UPR activation, Science. 337 (2012) 587–590. https://doi.org/10.1126/science.1223560.

[116] Y. Kim, M. Triolo, D.A. Hood, Impact of Aging and Exercise on Mitochondrial Quality Control in Skeletal Muscle, Oxid. Med. Cell. Longev. 2017 (2017) 3165396. https://doi.org/10.1155/2017/3165396.

[117] D.A. Hood, A.-M. Joseph, Mitochondrial assembly: protein import, Proc. Nutr. Soc. 63 (2004) 293–300. https://doi.org/10.1079/PNS2004342.

[118] A.-M. Joseph, D.A. Hood, Plasticity of TOM complex assembly in skeletal muscle mitochondria in response to chronic contractile activity, Mitochondrion. 12 (2012) 305–312. https://doi.org/10.1016/j.mito.2011.11.005.

[119] M. Takahashi, A. Chesley, D. Freyssenet, D.A. Hood, Contractile activity-induced adaptations in the mitochondrial protein import system, Am. J. Physiol. 274 (1998) C1380-1387. https://doi.org/10.1152/ajpcell.1998.274.5.C1380.

[120] Y. Zhang, S. Iqbal, M.F.N. O'Leary, K.J. Menzies, A. Saleem, S. Ding, D.A. Hood, Altered mitochondrial morphology and defective protein import reveal novel roles for Bax and/or Bak in skeletal muscle, Am. J. Physiol. Cell Physiol. 305 (2013) C502-511. https://doi.org/10.1152/ajpcell.00058.2013.

[121] O.I. Ornatsky, M.K. Connor, D.A. Hood, Expression of stress proteins and mitochondrial chaperonins in chronically stimulated skeletal muscle, Biochem. J. 311 (Pt 1) (1995) 119–123. https://doi.org/10.1042/bj3110119.

[122] J.M. Memme, A.N. Oliveira, D.A. Hood, Chronology of UPR activation in skeletal muscle adaptations to chronic contractile activity, Am. J. Physiol. - Cell Physiol. 310 (2016) C1024–C1036. https://doi.org/10.1152/ajpcell.00009.2016.

[123] C. Greggio, P. Jha, S.S. Kulkarni, S. Lagarrigue, N.T. Broskey, M. Boutant, X. Wang, S. Conde Alonso, E. Ofori, J. Auwerx, C. Cantó, F. Amati, Enhanced Respiratory Chain Supercomplex Formation in Response to Exercise in Human Skeletal Muscle, Cell Metab. 25 (2017) 301–311. https://doi.org/10.1016/j.cmet.2016.11.004.

[124] E. Masiero, L. Agatea, C. Mammucari, B. Blaauw, E. Loro, M. Komatsu, D. Metzger, C. Reggiani, S. Schiaffino, M. Sandri, Autophagy is required to maintain muscle mass, Cell Metab. 10 (2009) 507–515. https://doi.org/10.1016/j.cmet.2009.10.008.

[125] K.H. Kim, Y.T. Jeong, H. Oh, S.H. Kim, J.M. Cho, Y.-N. Kim, S.S. Kim, D.H. Kim, K.Y. Hur, H.K. Kim, T. Ko, J. Han, H.L. Kim, J. Kim, S.H. Back, M. Komatsu, H. Chen, D.C. Chan, M. Konishi, N. Itoh, C.S. Choi, M.-S. Lee, Autophagy deficiency leads to protection from obesity and insulin resistance by inducing Fgf21 as a mitokine, Nat. Med. 19 (2013) 83–92. https://doi.org/10.1038/nm.3014.

[126] C. He, M.C. Bassik, V. Moresi, K. Sun, Y. Wei, Z. Zou, Z. An, J. Loh, J. Fisher, Q. Sun, S. Korsmeyer, M. Packer, H.I. May, J.A. Hill, H.W. Virgin, C. Gilpin, G. Xiao, R. Bassel-Duby, P.E. Scherer, B. Levine, Exercise-induced BCL2-regulated autophagy is required for muscle glucose homeostasis, Nature. 481 (2012) 511–515. https://doi.org/10.1038/nature10758.

[127] M.F. Paré, B.L. Baechler, V.A. Fajardo, E. Earl, E. Wong, T.L. Campbell, A.R. Tupling, J. Quadrilatero, Effect of acute and chronic autophagy deficiency on skeletal muscle apoptotic signaling, morphology, and function, Biochim. Biophys. Acta Mol. Cell Res. 1864 (2017) 708–718. https://doi.org/10.1016/j.bbamcr.2016.12.015.

[128] J.M. Memme, A.T. Erlich, G. Phukan, D.A. Hood, Exercise and mitochondrial health, J. Physiol. 599 (2021) 803–817. https://doi.org/10.1113/JP278853.

[129] V.A. Lira, M. Okutsu, M. Zhang, N.P. Greene, R.C. Laker, D.S. Breen, K.L. Hoehn, Z. Yan, Autophagy is required for exercise training-induced skeletal muscle adaptation and improvement of physical performance, FASEB J. Off. Publ. Fed. Am. Soc. Exp. Biol. 27 (2013) 4184–4193. https://doi.org/10.1096/fj.13-228486.

[130] A.S. Nichenko, J.R. Sorensen, W.M. Southern, A.E. Qualls, A.G. Schifino, J. McFaline-Figueroa, J.E. Blum, K.F. Tehrani, H. Yin, L.J. Mortensen, A.E. Thalacker-Mercer, S.M. Greising, J.A. Call,

Lifelong Ulk1-Mediated Autophagy Deficiency in Muscle Induces Mitochondrial Dysfunction and Contractile Weakness, Int. J. Mol. Sci. 22 (2021) 1937. https://doi.org/10.3390/ijms22041937.

[131] A. Parousis, H.N. Carter, C. Tran, A.T. Erlich, Z.S. Mesbah Moosavi, M. Pauly, D.A. Hood, Contractile activity attenuates autophagy suppression and reverses mitochondrial defects in skeletal muscle cells, Autophagy. 14 (2018) 1886–1897. https://doi.org/10.1080/15548627.2018.1491488.

[132] C.C.W. Chen, A.T. Erlich, D.A. Hood, Role of Parkin and endurance training on mitochondrial turnover in skeletal muscle, Skelet. Muscle. 8 (2018) 10. https://doi.org/10.1186/s13395-018-0157-y.

[133] A. Vainshtein, D.A. Hood, The regulation of autophagy during exercise in skeletal muscle, J. Appl. Physiol. 120 (2016) 664–673. https://doi.org/10.1152/japplphysiol.00550.2015.

[134] M. Triolo, D.A. Hood, Mitochondrial breakdown in skeletal muscle and the emerging role of the lysosomes, Arch. Biochem. Biophys. 661 (2019) 66–73. https://doi.org/10.1016/j.abb.2018.11.004.

[135] R.C. Laker, J.C. Drake, R.J. Wilson, V.A. Lira, B.M. Lewellen, K.A. Ryall, C.C. Fisher, M. Zhang, J.J. Saucerman, L.J. Goodyear, M. Kundu, Z. Yan, Ampk phosphorylation of Ulk1 is required for targeting of mitochondria to lysosomes in exercise-induced mitophagy, Nat. Commun. 8 (2017) 548. https://doi.org/10.1038/s41467-017-00520-9.

[136] N. Brandt, T.P. Gunnarsson, J. Bangsbo, H. Pilegaard, Exercise and exercise training-induced increase in autophagy markers in human skeletal muscle, Physiol. Rep. 6 (2018) e13651. https://doi.org/10.14814/phy2.13651.

[137] Y. Dun, S. Liu, W. Zhang, M. Xie, L. Qiu, Exercise Combined with Rhodiola sacra Supplementation Improves Exercise Capacity and Ameliorates Exhaustive Exercise-Induced Muscle Damage through Enhancement of Mitochondrial Quality Control, Oxid. Med. Cell. Longev. 2017 (2017) e8024857. https://doi.org/10.1155/2017/8024857.

[138] H.N. Carter, Y. Kim, A.T. Erlich, D. Zarrin-Khat, D.A. Hood, Autophagy and mitophagy flux in young and aged skeletal muscle following chronic contractile activity, J. Physiol. 596 (2018) 3567–3584. https://doi.org/10.1113/JP275998.

[139] Y. Kim, M. Triolo, A.T. Erlich, D.A. Hood, Regulation of autophagic and mitophagic flux during chronic contractile activity-induced muscle adaptations, Pflüg. Arch. - Eur. J. Physiol. 471 (2019) 431–440. https://doi.org/10.1007/s00424-018-2225-x.

[140] J.-S. Ju, S.-I. Jeon, J.-Y. Park, J.-Y. Lee, S.-C. Lee, K.-J. Cho, J.-M. Jeong, Autophagy plays a role in skeletal muscle mitochondrial biogenesis in an endurance exercise-trained condition, J. Physiol. Sci. JPS. 66 (2016) 417–430. https://doi.org/10.1007/s12576-016-0440-9.

[141] J.F. Halling, S. Ringholm, M.M. Nielsen, P. Overby, H. Pilegaard, PGC-1α promotes exercise-induced autophagy in mouse skeletal muscle, Physiol. Rep. 4 (2016) e12698. https://doi.org/10.14814/phy2.12698.

[142] Y. Kim, M. Triolo, D.A. Hood, Regulation of Autophagy during Chronic Contractile Activity-Induced Muscle Adaptations, FASEB J. 31 (2017) 839.17-839.17. https://doi.org/10.1096/fasebj.31.1_supplement.839.17.

[143] D.L. Medina, S. Di Paola, I. Peluso, A. Armani, D. De Stefani, R. Venditti, S. Montefusco, A. Scotto-Rosato, C. Prezioso, A. Forrester, C. Settembre, W. Wang, Q. Gao, H. Xu, M. Sandri, R. Rizzuto, M.A. De Matteis, A. Ballabio, Lysosomal calcium signalling regulates autophagy through calcineurin and TFEB, Nat. Cell Biol. 17 (2015) 288–299. https://doi.org/10.1038/ncb3114.

[144] L. Mouchiroud, R.H. Houtkooper, N. Moullan, E. Katsyuba, D. Ryu, C. Cantó, A. Mottis, Y.-S. Jo, M. Viswanathan, K. Schoonjans, L. Guarente, J. Auwerx, The NAD(+)/Sirtuin Pathway Modulates Longevity through Activation of Mitochondrial UPR and FOXO Signaling, Cell. 154 (2013) 430–441. https://doi.org/10.1016/j.cell.2013.06.016.

[145] R.H. Houtkooper, L. Mouchiroud, D. Ryu, N. Moullan, E. Katsyuba, G. Knott, R.W. Williams, J. Auwerx, Mitonuclear protein imbalance as a conserved longevity mechanism, Nature. 497 (2013) 451–457. https://doi.org/10.1038/nature12188.

[146] C.J. Fiorese, A.M. Schulz, Y.-F. Lin, N. Rosin, M.W. Pellegrino, C.M. Haynes, The Transcription Factor ATF5 Mediates a Mammalian Mitochondrial UPR, Curr. Biol. CB. 26 (2016) 2037–2043. https://doi.org/10.1016/j.cub.2016.06.002.

[147] A. Mottis, V. Jovaisaite, J. Auwerx, The mitochondrial unfolded protein response in mammalian physiology, Mamm. Genome Off. J. Int. Mamm. Genome Soc. 25 (2014) 424–433. https://doi.org/10.1007/s00335-014-9525-z.

[148] Q. Zhao, J. Wang, I.V. Levichkin, S. Stasinopoulos, M.T. Ryan, N.J. Hoogenraad, A mitochondrial specific stress response in mammalian cells, EMBO J. 21 (2002) 4411–4419. https://doi.org/10.1093/emboj/cdf445.

[149] A.M. Nargund, M.W. Pellegrino, C.J. Fiorese, B.M. Baker, C.M. Haynes, Mitochondrial import efficiency of ATFS-1 regulates mitochondrial UPR activation, Science. 337 (2012) 587–590. https://doi.org/10.1126/science.1223560.

[150] A. Melber, C.M. Haynes, UPRmt regulation and output: a stress response mediated by mitochondrial-nuclear communication, Cell Res. 28 (2018) 281–295. https://doi.org/10.1038/cr.2018.16.

[151] C.J. Fiorese, A.M. Schulz, Y.-F. Lin, N. Rosin, M.W. Pellegrino, C.M. Haynes, The Transcription Factor ATF5 Mediates a Mammalian Mitochondrial UPR, Curr. Biol. CB. 26 (2016) 2037–2043. https://doi.org/10.1016/j.cub.2016.06.002.

[152] Y.T. Wang, Y. Lim, M.N. McCall, K.-T. Huang, C.M. Haynes, K. Nehrke, P.S. Brookes, Cardioprotection by the mitochondrial unfolded protein response requires ATF5, Am. J. Physiol. Heart Circ. Physiol. 317 (2019) H472–H478. https://doi.org/10.1152/ajpheart.00244.2019.

[153] M.B. Jensen, H. Jasper, Mitochondrial proteostasis in the control of aging and longevity, Cell Metab. 20 (2014) 214–225. https://doi.org/10.1016/j.cmet.2014.05.006.

[154] R.D. Martinus, G.P. Garth, T.L. Webster, P. Cartwright, D.J. Naylor, P.B. Høj, N.J. Hoogenraad, Selective induction of mitochondrial chaperones in response to loss of the mitochondrial genome, Eur. J. Biochem. 240 (1996) 98–103. https://doi.org/10.1111/j.1432-1033.1996.0098h.x.

[155] B.M. Baker, A.M. Nargund, T. Sun, C.M. Haynes, Protective coupling of mitochondrial function and protein synthesis via the eIF2α kinase GCN-2, PLoS Genet. 8 (2012) e1002760. https://doi.org/10.1371/journal.pgen.1002760.

[156] A.M. Nargund, C.J. Fiorese, M.W. Pellegrino, P. Deng, C.M. Haynes, Mitochondrial and nuclear accumulation of the transcription factor ATFS-1 promotes OXPHOS recovery during the UPR(mt), Mol. Cell. 58 (2015) 123–133. https://doi.org/10.1016/j.molcel.2015.02.008.

[157] T. Yoneda, C. Benedetti, F. Urano, S.G. Clark, H.P. Harding, D. Ron, Compartment-specific perturbation of protein handling activates genes encoding mitochondrial chaperones, J. Cell Sci. 117 (2004) 4055–4066. https://doi.org/10.1242/jcs.01275.

[158] I.M.N. Wortel, L.T. van der Meer, M.S. Kilberg, F.N. van Leeuwen, Surviving Stress: Modulation of ATF4-Mediated Stress Responses in Normal and Malignant Cells, Trends Endocrinol. Metab. TEM. 28 (2017) 794–806. https://doi.org/10.1016/j.tem.2017.07.003.

[159] C. Lai, J. Zhang, Z. Tan, L.F. Shen, R.R. Zhou, Y.Y. Zhang, Maf1 suppression of ATF5-dependent mitochondrial unfolded protein response contributes to rapamycin-induced radio-sensitivity in lung cancer cell line A549, Aging. 13 (2021) 7300–7313. https://doi.org/10.18632/aging.202584.

[160] D. Dluzen, G. Li, D. Tacelosky, M. Moreau, D.X. Liu, BCL-2 is a downstream target of ATF5 that mediates the prosurvival function of ATF5 in a cell type-dependent manner, J. Biol. Chem. 286 (2011) 7705–7713. https://doi.org/10.1074/jbc.M110.207639.

[161] X. Sun, J.M. Angelastro, D. Merino, Q. Zhou, M.D. Siegelin, L.A. Greene, Dominant-negative ATF5 rapidly depletes survivin in tumor cells, Cell Death Dis. 10 (2019) 709. https://doi.org/10.1038/s41419-019-1872-y.

[162] C. Mancini, P. Roncaglia, A. Brussino, G. Stevanin, N. Lo Buono, H. Krmac, F. Maltecca, E. Gazzano, A. Bartoletti Stella, M.A. Calvaruso, L. Iommarini, C. Cagnoli, S. Forlani, I. Le Ber, A.

Durr, A. Brice, D. Ghigo, G. Casari, A.M. Porcelli, A. Funaro, G. Gasparre, S. Gustincich, A. Brusco, Genome-wide expression profiling and functional characterization of SCA28 lymphoblastoid cell lines reveal impairment in cell growth and activation of apoptotic pathways, BMC Med. Genomics. 6 (2013) 22. https://doi.org/10.1186/1755-8794-6-22.

[163] C.M. Haynes, K. Petrova, C. Benedetti, Y. Yang, D. Ron, ClpP mediates activation of a mitochondrial unfolded protein response in C. elegans, Dev. Cell. 13 (2007) 467–480. https://doi.org/10.1016/j.devcel.2007.07.016.

[164] C.M. Haynes, Y. Yang, S.P. Blais, T.A. Neubert, D. Ron, The matrix peptide exporter HAF-1 signals a mitochondrial UPR by activating the transcription factor ZC376.7 in C. elegans, Mol. Cell. 37 (2010) 529–540. https://doi.org/10.1016/j.molcel.2010.01.015.

[165] C.J. Fiorese, C.M. Haynes, Integrating the UPRmt into the Mitochondrial Maintenance Network, Crit. Rev. Biochem. Mol. Biol. 52 (2017) 304–313. https://doi.org/10.1080/10409238.2017.1291577.

[166] E. Owusu-Ansah, W. Song, N. Perrimon, Muscle Mitohormesis Promotes Longevity via Systemic Repression of Insulin Signaling, Cell. 155 (2013) 699–712. https://doi.org/10.1016/j.cell.2013.09.021.

[167] D. Poveda-Huertes, S. Matic, A. Marada, L. Habernig, M. Licheva, L. Myketin, R. Gilsbach, S. Tosal-Castano, D. Papinski, P. Mulica, O. Kretz, C. Kücükköse, A.A. Taskin, L. Hein, C. Kraft, S. Büttner, C. Meisinger, F.-N. Vögtle, An Early mtUPR: Redistribution of the Nuclear Transcription Factor Rox1 to Mitochondria Protects against Intramitochondrial Proteotoxic Aggregates, Mol. Cell. 77 (2020) 180-188.e9. https://doi.org/10.1016/j.molcel.2019.09.026.

[168] C. Münch, The different axes of the mammalian mitochondrial unfolded protein response, BMC Biol. 16 (2018) 81. https://doi.org/10.1186/s12915-018-0548-x.

[169] N. Anderson, C.M. Haynes, Folding the Mitochondrial UPR into the Integrated Stress Response, Trends Cell Biol. 30 (2020) 428–439. https://doi.org/10.1016/j.tcb.2020.03.001.

[170] U. Topf, L. Wrobel, A. Chacinska, Chatty Mitochondria: Keeping Balance in Cellular Protein Homeostasis, Trends Cell Biol. 26 (2016) 577–586. https://doi.org/10.1016/j.tcb.2016.03.002.

[171] R. Iurlaro, C. Muñoz-Pinedo, Cell death induced by endoplasmic reticulum stress, FEBS J. 283 (2016) 2640–2652. https://doi.org/10.1111/febs.13598.

[172] K. Sasaki, T. Uchiumi, T. Toshima, M. Yagi, Y. Do, H. Hirai, K. Igami, K. Gotoh, D. Kang, Mitochondrial translation inhibition triggers ATF4 activation, leading to integrated stress response but not to mitochondrial unfolded protein response, Biosci. Rep. 40 (2020) BSR20201289. https://doi.org/10.1042/BSR20201289.

[173] T. Verfaillie, N. Rubio, A.D. Garg, G. Bultynck, R. Rizzuto, J.-P. Decuypere, J. Piette, C. Linehan, S. Gupta, A. Samali, P. Agostinis, PERK is required at the ER-mitochondrial contact sites to convey apoptosis after ROS-based ER stress, Cell Death Differ. 19 (2012) 1880–1891. https://doi.org/10.1038/cdd.2012.74.

[174] H. Zinszner, M. Kuroda, X. Wang, N. Batchvarova, R.T. Lightfoot, H. Remotti, J.L. Stevens, D. Ron, CHOP is implicated in programmed cell death in response to impaired function of the endoplasmic reticulum, Genes Dev. 12 (1998) 982–995. https://doi.org/10.1101/gad.12.7.982.

[175] R.D. Martinus, G.P. Garth, T.L. Webster, P. Cartwright, D.J. Naylor, P.B. Høj, N.J. Hoogenraad, Selective induction of mitochondrial chaperones in response to loss of the mitochondrial genome, Eur. J. Biochem. 240 (1996) 98–103. https://doi.org/10.1111/j.1432-1033.1996.0098h.x.

[176] T. Horibe, N.J. Hoogenraad, The Chop Gene Contains an Element for the Positive Regulation of the Mitochondrial Unfolded Protein Response, PLOS ONE. 2 (2007) e835. https://doi.org/10.1371/journal.pone.0000835.

[177] J.E. Aldridge, T. Horibe, N.J. Hoogenraad, Discovery of Genes Activated by the Mitochondrial Unfolded Protein Response (mtUPR) and Cognate Promoter Elements, PLOS ONE. 2 (2007) e874. https://doi.org/10.1371/journal.pone.0000874.

[178] A.N. Oliveira, D.A. Hood, Effect of Tim23 knockdown in vivo on mitochondrial protein import and retrograde signaling to the UPRmt in muscle, Am. J. Physiol. Cell Physiol. 315 (2018) C516–C526. https://doi.org/10.1152/ajpcell.00275.2017.

[179] E. Mick, D.V. Titov, O.S. Skinner, R. Sharma, A.A. Jourdain, V.K. Mootha, Distinct mitochondrial defects trigger the integrated stress response depending on the metabolic state of the cell, ELife. 9 (2020) e49178. https://doi.org/10.7554/eLife.49178.

[180] M. Molenaars, G.E. Janssens, E.G. Williams, A. Jongejan, J. Lan, S. Rabot, F. Joly, P.D. Moerland, B.V. Schomakers, M. Lezzerini, Y.J. Liu, M.A. McCormick, B.K. Kennedy, M. van Weeghel, A.H.C. van Kampen, R. Aebersold, A.W. MacInnes, R.H. Houtkooper, A Conserved Mito-Cytosolic Translational Balance Links Two Longevity Pathways, Cell Metab. 31 (2020) 549-563.e7. https://doi.org/10.1016/j.cmet.2020.01.011.

[181] S. Forsström, C.B. Jackson, C.J. Carroll, M. Kuronen, E. Pirinen, S. Pradhan, A. Marmyleva, M. Auranen, I.-M. Kleine, N.A. Khan, A. Roivainen, P. Marjamäki, H. Liljenbäck, L. Wang, B.J. Battersby, U. Richter, V. Velagapudi, J. Nikkanen, L. Euro, A. Suomalainen, Fibroblast Growth Factor 21 Drives Dynamics of Local and Systemic Stress Responses in Mitochondrial Myopathy with mtDNA Deletions, Cell Metab. 30 (2019) 1040-1054.e7. https://doi.org/10.1016/j.cmet.2019.08.019.

[182] Y.T. Wang, Y. Lim, M.N. McCall, K.-T. Huang, C.M. Haynes, K. Nehrke, P.S. Brookes, Cardioprotection by the mitochondrial unfolded protein response requires ATF5, Am. J. Physiol. Heart Circ. Physiol. 317 (2019) H472–H478. https://doi.org/10.1152/ajpheart.00244.2019.

[183] H. Zhang, D. Ryu, Y. Wu, K. Gariani, X. Wang, P. Luan, D. D'Amico, E.R. Ropelle, M.P. Lutolf, R. Aebersold, K. Schoonjans, K.J. Menzies, J. Auwerx, NAD^+ repletion improves mitochondrial and stem cell function and enhances life span in mice, Science. 352 (2016) 1436–1443. https://doi.org/10.1126/science.aaf2693.

[184] P. Bai, C. Cantó, H. Oudart, A. Brunyánszki, Y. Cen, C. Thomas, H. Yamamoto, A. Huber, B. Kiss, R.H. Houtkooper, K. Schoonjans, V. Schreiber, A.A. Sauve, J. Menissier-de Murcia, J. Auwerx, PARP-1 inhibition increases mitochondrial metabolism through SIRT1 activation, Cell Metab. 13 (2011) 461–468. https://doi.org/10.1016/j.cmet.2011.03.004.

[185] I. Smyrnias, S.P. Gray, D.O. Okonko, G. Sawyer, A. Zoccarato, N. Catibog, B. López, A. González, S. Ravassa, J. Díez, A.M. Shah, Cardioprotective Effect of the Mitochondrial Unfolded Protein Response During Chronic Pressure Overload, J. Am. Coll. Cardiol. 73 (2019) 1795–1806. https://doi.org/10.1016/j.jacc.2018.12.087.

[186] B. Zhang, Y. Tan, Z. Zhang, P. Feng, W. Ding, Q. Wang, H. Liang, W. Duan, X. Wang, S. Yu, J. Liu, D. Yi, Y. Sun, W. Yi, Novel PGC-1α/ATF5 Axis Partly Activates UPRmt and Mediates Cardioprotective Role of Tetrahydrocurcumin in Pathological Cardiac Hypertrophy, Oxid. Med. Cell. Longev. 2020 (2020) 9187065. https://doi.org/10.1155/2020/9187065.

[187] S. Aras, N. Purandare, S. Gladyck, M. Somayajulu-Nitu, K. Zhang, D.C. Wallace, L.I. Grossman, Mitochondrial Nuclear Retrograde Regulator 1 (MNRR1) rescues the cellular phenotype of MELAS by inducing homeostatic mechanisms, Proc. Natl. Acad. Sci. U. S. A. 117 (2020) 32056–32065. https://doi.org/10.1073/pnas.2005877117.

[188] P. Deng, C.M. Haynes, Mitochondrial dysfunction in cancer: Potential roles of ATF5 and the mitochondrial UPR, Semin. Cancer Biol. 47 (2017) 43–49. https://doi.org/10.1016/j.semcancer.2017.05.002.

[189] Y. Wang, H. Jasper, S. Toan, D. Muid, X. Chang, H. Zhou, Mitophagy coordinates the mitochondrial unfolded protein response to attenuate inflammation-mediated myocardial injury, Redox Biol. 45 (2021) 102049. https://doi.org/10.1016/j.redox.2021.102049.

[190] N. Al-Furoukh, A. Ianni, H. Nolte, S. Hölper, M. Krüger, S. Wanrooij, T. Braun, ClpX stimulates the mitochondrial unfolded protein response (UPRmt) in mammalian cells, Biochim. Biophys. Acta. 1853 (2015) 2580–2591. https://doi.org/10.1016/j.bbamcr.2015.06.016.

[191] T. Arnould, S. Michel, P. Renard, Mitochondria Retrograde Signaling and the UPRmt: Where Are We in Mammals?, Int. J. Mol. Sci. 16 (2015) 18224–18251. https://doi.org/10.3390/ijms160818224.

[192] S. Callegari, S. Dennerlein, Sensing the Stress: A Role for the UPRmt and UPRam in the Quality Control of Mitochondria, Front. Cell Dev. Biol. 6 (2018) 31. https://doi.org/10.3389/fcell.2018.00031.

[193] V. Jovaisaite, J. Auwerx, The mitochondrial unfolded protein response - synchronizing genomes, Curr. Opin. Cell Biol. 33 (2015) 74–81. https://doi.org/10.1016/j.ceb.2014.12.003.

[194] E. Rath, E. Berger, A. Messlik, T. Nunes, B. Liu, S.C. Kim, N. Hoogenraad, M. Sans, R.B. Sartor, D. Haller, Induction of dsRNA-activated protein kinase links mitochondrial unfolded protein response to the pathogenesis of intestinal inflammation, Gut. 61 (2012) 1269–1278. https://doi.org/10.1136/gutjnl-2011-300767.

[195] T.K. Rainbolt, N. Atanassova, J.C. Genereux, R.L. Wiseman, Stress-Regulated Translational Attenuation Adapts Mitochondrial Protein Import Through Tim17A Degradation, Cell Metab. 18 (2013) 908–919. https://doi.org/10.1016/j.cmet.2013.11.006.

[196] M.B. Hansen, C. Mitchelmore, K.M. Kjaerulff, T.E. Rasmussen, K.M. Pedersen, N.A. Jensen, Mouse Atf5: molecular cloning of two novel mRNAs, genomic organization, and odorant sensory neuron localization, Genomics. 80 (2002) 344–350. https://doi.org/10.1006/geno.2002.6838.

[197] L.A. Greene, H.Y. Lee, J.M. Angelastro, The Transcription Factor ATF5: Role In Neurodevelopment And Neural Tumors, J. Neurochem. 108 (2009) 11–22. https://doi.org/10.1111/j.1471-4159.2008.05749.x.

[198] M. Nishizawa, S. Nagata, cDNA clones encoding leucine-zipper proteins which interact with G-CSF gene promoter element 1-binding protein, FEBS Lett. 299 (1992) 36–38. https://doi.org/10.1016/0014-5793(92)80094-w.

[199] J. Al Sarraj, C. Vinson, G. Thiel, Regulation of asparagine synthetase gene transcription by the basic region leucine zipper transcription factors ATF5 and CHOP, Biol. Chem. 386 (2005) 873–879. https://doi.org/10.1515/BC.2005.102.

[200] Y.I. Shimizu, M. Morita, A. Ohmi, S. Aoyagi, H. Ebihara, D. Tonaki, Y. Horino, M. Iijima, H. Hirose, S. Takahashi, Y. Takahashi, Fasting induced up-regulation of activating transcription factor 5 in mouse liver, Life Sci. 84 (2009) 894–902. https://doi.org/10.1016/j.lfs.2009.04.002.

[201] R.P. Dalton, D.B. Lyons, S. Lomvardas, Co-opting the unfolded protein response to elicit olfactory receptor feedback, Cell. 155 (2013) 321–332. https://doi.org/10.1016/j.cell.2013.09.033.

[202] S.-Z. Wang, J. Ou, L.J. Zhu, M.R. Green, Transcription factor ATF5 is required for terminal differentiation and survival of olfactory sensory neurons, Proc. Natl. Acad. Sci. U. S. A. 109 (2012) 18589–18594. https://doi.org/10.1073/pnas.1210479109.

[203] D.X. Liu, D. Qian, B. Wang, J.-M. Yang, Z. Lu, p300-Dependent ATF5 acetylation is essential for Egr-1 gene activation and cell proliferation and survival, Mol. Cell. Biol. 31 (2011) 3906–3916. https://doi.org/10.1128/MCB.05887-11.

[204] D. Hu, Z. Liu, X. Qi, UPRmt activation protects against MPP+-induced toxicity in a cell culture model of Parkinson's disease, Biochem. Biophys. Res. Commun. 569 (2021) 17–22. https://doi.org/10.1016/j.bbrc.2021.06.079.

[205] Multi-omics analysis identifies ATF4 as a key regulator of the mitochondrial stress response in mammals | Journal of Cell Biology | Rockefeller University Press, (n.d.). https://rupress.org/jcb/article/216/7/2027/39040/Multi-omics-analysis-identifies-ATF4-as-a-key (accessed July 2, 2021).

[206] C. Vinson, M. Myakishev, A. Acharya, A.A. Mir, J.R. Moll, M. Bonovich, Classification of Human B-ZIP Proteins Based on Dimerization Properties, Mol. Cell. Biol. 22 (2002) 6321–6335. https://doi.org/10.1128/MCB.22.18.6321-6335.2002.

[207] D. Zhou, L.R. Palam, L. Jiang, J. Narasimhan, K.A. Staschke, R.C. Wek, Phosphorylation of eIF2 Directs ATF5 Translational Control in Response to Diverse Stress Conditions, J. Biol. Chem. 283 (2008) 7064–7073. https://doi.org/10.1074/jbc.M708530200.

[208] D. Brown, K. Ryan, Z. Daniel, M. Mareko, R. Talbot, J. Moreton, T.C.B. Giles, R. Emes, C. Hodgman, T. Parr, J.M. Brameld, The Beta-adrenergic agonist, Ractopamine, increases skeletal muscle expression of Asparagine Synthetase as part of an integrated stress response gene program, Sci. Rep. 8 (2018) 15915. https://doi.org/10.1038/s41598-018-34315-9.

[209] S.A. Dogan, C. Pujol, P. Maiti, A. Kukat, S. Wang, S. Hermans, K. Senft, R. Wibom, E.I. Rugarli, A. Trifunovic, Tissue-Specific Loss of DARS2 Activates Stress Responses Independently of Respiratory Chain Deficiency in the Heart, Cell Metab. 19 (2014) 458–469. https://doi.org/10.1016/j.cmet.2014.02.004.

[210] A. Melber, C.M. Haynes, UPRmt regulation and output: a stress response mediated by mitochondrial-nuclear communication, Cell Res. 28 (2018) 281–295. https://doi.org/10.1038/cr.2018.16.

[211] T. Arnould, S. Michel, P. Renard, Mitochondria Retrograde Signaling and the UPR: Where Are We in Mammals?, Int. J. Mol. Sci. 16 (2015) 18224–18251. https://doi.org/10.3390/ijms160818224.

[212] N.S. Anderson, C.M. Haynes, Folding the Mitochondrial UPR into the Integrated Stress Response, Trends Cell Biol. 30 (2020) 428–439. https://doi.org/10.1016/j.tcb.2020.03.001.

[213] D. Ron, P. Walter, Signal integration in the endoplasmic reticulum unfolded protein response, Nat. Rev. Mol. Cell Biol. 8 (2007) 519–529. https://doi.org/10.1038/nrm2199.

[214] S. Michel, M. Canonne, T. Arnould, P. Renard, Inhibition of mitochondrial genome expression triggers the activation of CHOP-10 by a cell signaling dependent on the integrated stress response but not the mitochondrial unfolded protein response, Mitochondrion. 21 (2015) 58–68. https://doi.org/10.1016/j.mito.2015.01.005.

[215] R.R. Koncha, G. Ramachandran, N.B.V. Sepuri, K.V.A. Ramaiah, CCCP-induced mitochondrial dysfunction - characterization and analysis of integrated stress response to cellular signaling and homeostasis, FEBS J. (2021). https://doi.org/10.1111/febs.15868.

[216] X. Guo, G. Aviles, Y. Liu, R. Tian, B.A. Unger, Y.-H.T. Lin, A.P. Wiita, K. Xu, M.A. Correia, M. Kampmann, Mitochondrial stress is relayed to the cytosol by an OMA1-DELE1-HRI pathway, Nature. 579 (2020) 427–432. https://doi.org/10.1038/s41586-020-2078-2.

[217] S.K. Young, R.C. Wek, Upstream Open Reading Frames Differentially Regulate Gene-specific Translation in the Integrated Stress Response, J. Biol. Chem. 291 (2016) 16927–16935. https://doi.org/10.1074/jbc.R116.733899.

[218] D. Zhou, L.R. Palam, L. Jiang, J. Narasimhan, K.A. Staschke, R.C. Wek, Phosphorylation of eIF2 directs ATF5 translational control in response to diverse stress conditions, J. Biol. Chem. 283 (2008) 7064–7073. https://doi.org/10.1074/jbc.M708530200.

[219] Z.S. Mesbah Moosavi, D.A. Hood, The unfolded protein response in relation to mitochondrial biogenesis in skeletal muscle cells, Am. J. Physiol. - Cell Physiol. 312 (2017) C583–C594. https://doi.org/10.1152/ajpcell.00320.2016.

[220] B.F. Teske, M.E. Fusakio, D. Zhou, J. Shan, J.N. McClintick, M.S. Kilberg, R.C. Wek, CHOP induces activating transcription factor 5 (ATF5) to trigger apoptosis in response to perturbations in protein homeostasis, Mol. Biol. Cell. 24 (2013) 2477–2490. https://doi.org/10.1091/mbc.E13-01-0067.

[221] M.C. Brearley, C. Li, Z.C.T.R. Daniel, P.T. Loughna, T. Parr, J.M. Brameld, Changes in expression of serine biosynthesis and integrated stress response genes during myogenic differentiation of C2C12 cells, Biochem. Biophys. Rep. 20 (2019) 100694. https://doi.org/10.1016/j.bbrep.2019.100694.

[222] A.V. Cordeiro, R.S. Brícola, R.R. Braga, L. Lenhare, V.R.R. Silva, C.P. Anaruma, C.K. Katashima, B.M. Crisol, F.M. Simabuco, A.S.R. Silva, D.E. Cintra, L.P. Moura, J.R. Pauli, E.R. Ropelle, Aerobic Exercise Training Induces the Mitonuclear Imbalance and UPRmt in the Skeletal Muscle of Aged Mice, J. Gerontol. A. Biol. Sci. Med. Sci. 75 (2020) 2258–2261. https://doi.org/10.1093/gerona/glaa059.

[223] B. Chabi, V. Ljubicic, K.J. Menzies, J.H. Huang, A. Saleem, D.A. Hood, Mitochondrial function and apoptotic susceptibility in aging skeletal muscle, Aging Cell. 7 (2008) 2–12. https://doi.org/10.1111/j.1474-9726.2007.00347.x.

[224] E. Pirinen, C. Canto, Y.-S. Jo, L. Morato, H. Zhang, K. Menzies, E.G. Williams, L. Mouchiroud, N. Moullan, C. Hagberg, W. Li, S. Timmers, R. Imhof, J. Verbeek, A. Pujol, B. van Loon, C. Viscomi, M. Zeviani, P. Schrauwen, A. Sauve, K. Schoonjans, J. Auwerx, Pharmacological Inhibition of Poly(ADP-Ribose) Polymerases Improves Fitness and Mitochondrial Function in Skeletal Muscle, Cell Metab. 19 (2014) 1034–1041. https://doi.org/10.1016/j.cmet.2014.04.002.

[225] S.B. Wilkinson, S.M. Phillips, P.J. Atherton, R. Patel, K.E. Yarasheski, M.A. Tarnopolsky, M.J. Rennie, Differential effects of resistance and endurance exercise in the fed state on signalling molecule phosphorylation and protein synthesis in human muscle, J. Physiol. 586 (2008) 3701–3717. https://doi.org/10.1113/jphysiol.2008.153916.

[226] D.I. Ogborn, B.R. McKay, J.D. Crane, G. Parise, M.A. Tarnopolsky, The unfolded protein response is triggered following a single, unaccustomed resistance-exercise bout, Am. J. Physiol. Regul. Integr. Comp. Physiol. 307 (2014) R664-669. https://doi.org/10.1152/ajpregu.00511.2013.

[227] J. Hentilä, J.P. Ahtiainen, G. Paulsen, T. Raastad, K. Häkkinen, A.A. Mero, J.J. Hulmi, Autophagy is induced by resistance exercise in young men, but unfolded protein response is induced regardless of age, Acta Physiol. Oxf. Engl. 224 (2018) e13069. https://doi.org/10.1111/apha.13069.

[228] A.T. Erlich, L.D. Tryon, M.J. Crilly, J.M. Memme, Z.S.M. Moosavi, A.N. Oliveira, K. Beyfuss, D.A. Hood, Function of specialized regulatory proteins and signaling pathways in exercise-induced muscle mitochondrial biogenesis, Integr. Med. Res. 5 (2016) 187–197. https://doi.org/10.1016/j.imr.2016.05.003.

[229] G. Uguccioni, D.A. Hood, The importance of PGC-1α in contractile activity-induced mitochondrial adaptations, Am. J. Physiol. Endocrinol. Metab. 300 (2011) E361-371. https://doi.org/10.1152/ajpendo.00292.2010.

[230] Y. Zhang, G. Uguccioni, V. Ljubicic, I. Irrcher, S. Iqbal, K. Singh, S. Ding, D.A. Hood, Multiple signaling pathways regulate contractile activity-mediated PGC-1α gene expression and activity in skeletal muscle cells, Physiol. Rep. 2 (2014) e12008. https://doi.org/10.14814/phy2.12008.

CHAPTER 2:

MANUSCRIPT

MANUSCRIPT AUTHOR CONTRIBUTIONS:

Mikhaela B. Slavin: Performed all exercise protocols and tissue collection for WT and ATF5 KO animals; mitochondrial isolations, respiration and ROS measurements; qPCR, cytochrome c oxidase assay and western blotting experiments; data analysis and interpretation; wrote the manuscript.

Dr. Rita Kumari: Assisted in tissue collection and performed nuclear/cytosolic fractionations.

Dr. David A. Hood: Supervised this project and is the principal investigator.

THE ROLE OF ATF5 IN MITOCHONDRIAL MAINTENANCE, BIOGENESIS AND UPR^{MT} SIGNALING FOLLOWING ACUTE EXERCISE IN SKELETAL MUSCLE

Mikhaela B. Slavin, Rita Kumari and David A. Hood

Muscle Health Research Centre, School of Kinesiology and Health Science, York University, Toronto, Ontario, M3J 1P3, Canada

To whom correspondence should be addressed: David A. Hood, Ph.D (dhood@yorku.ca)
Muscle Health Research Centre
School of Kinesiology and Health Science
York University, Toronto, ON
M3J 1P3, Canada

ABSTRACT

Over 99% of mitochondrial proteins require import into mitochondria, followed by their folding and intraorganellar sorting. Mitochondrial stress can result in the accretion of misfolded proteins, establishing a requirement for mitochondrial protein quality control (MQC) strategies. The Mitochondrial Unfolded Protein Response (UPR^{mt}) is a compartment-specific MQC mechanism that increases the expression of protective enzymes by ATF5 to restore mitochondrial function. Contractile activity during acute exercise is a stressor that has the potential to temporarily disrupt organellar protein homeostasis, however, the roles of ATF5 and the UPR^{mt} in basal mitochondrial maintenance and exercise-induced UPR^{mt} signaling in skeletal muscle are not known. To investigate this, we subjected WT and whole-body ATF5 KO mice to a bout of acute exercise and collected skeletal muscle tissue immediately after. ATF5 KO animals exhibited 2-fold increases in phosphorylated JNK protein levels, indicative of enhanced stress signaling. Muscle from these animals also displayed a more abundant, but dysfunctional, mitochondrial pool, with a 15% increase in mitochondrial content, 30-40% reductions in respiration, and a 20% increase in ROS emissions, corresponding with no changes in exercise performance. The UPR^{mt} proteins mtHSP70 and LONP were upregulated 20-30% in KO muscle in addition to 40-50% increases in nuclear and cytosolic PGC-1α protein. ATF4 mRNA was upregulated 2.5-3.7-fold in KO muscle, along with an 8% increase in its nuclear localization. Furthermore, KO muscle showed an impaired UPR^{mt} mRNA response to acute exercise, suggesting a regulatory role of ATF5 in basal mitochondrial upkeep and the mitochondrial gene expression response to acute exercise stress.

INTRODUCTION

Skeletal muscle is an extremely malleable tissue with a high degree of plasticity, being able to alter its structural, physiological and metabolic phenotype in response to altered external demands. Since skeletal muscle makes up approximately ~40% of human body mass, these changes elicit important modifications to whole-body metabolism, influencing overall health and susceptibility to disease [1–3]. Mitochondria produce cellular energy in the form of ATP, fulfilling their role as the "powerhouse of the cell". However, they are also influential in the maintenance of cellular homeostasis, acting as sensors of energy demand and cell stress and mediating retrograde signaling to the nucleus.

The plastic nature of skeletal muscle is largely due to the adaptability of the mitochondrial reticulum, which undergoes extensive remodeling, being a large contributor to improvements in muscle endurance from exercise [4,5]. Muscle contractions during voluntary exercise promote increases in mitochondrial content via mitochondrial biogenesis, and enhanced mitochondrial degradation via mitophagy, enhancing the quality of the mitochondrial pool in muscle [4,6–9]. At the onset of exercise in skeletal muscle, early signaling events involved in mitochondrial biogenesis are initiated, converging largely on the activation of the transcriptional co-activator PGC-1α [10–13]. This "master regulator of mitochondrial biogenesis" coordinates the transcription of mitochondrial genes encoded by the nuclear genome (NuGEMPs), which require import into the mitochondria via specialized PIM [14–16]. The mitochondrial proteome consists of ~1200 proteins, and over 99% of these are transcribed in the nucleus, while less than 1% are encoded by mtDNA [17]. The regulation of these proteins, including their proper translation, folding, and degradation is referred to as protein homeostasis or "proteostasis" [18,19]. Its

maintenance, in addition to the coordinated and synchronized expression of both genomes, are integral for biogenesis and for sustaining mitochondrial function.

The establishment of mitochondrial proteostasis relies on the equilibrium between the amount of misfolded proteins and the organelle's intrinsic folding capacity. This is determined by the amount of chaperone and protease enzymes, with the dedicated functions of refolding and degrading misfolded proteins, respectively. The stimulation of beneficial signaling pathways during exercise is dependent on the development of intracellular energetic and molecular imbalances. Likewise, unaccustomed exercise may additionally elicit a proteostatic imbalance, generated by an increase in misfolded proteins leading to acute organellar proteotoxic stress [20,21], ratifying a need for protein quality control strategies. As an adaptive mechanism, the cell activates a compartment-specific transcriptional program called the mitochondrial unfolded protein response (UPR^{mt}) [22–24], named in relation to the UPR^{er} [25]. Utilizing novel mitochondrial-nuclear communication, the transcription of UPR^{mt} genes, including mitochondrial-specific chaperones and proteases, are increased to restore proteostasis within the organelle [26–28].

Activating transcription factor 5 (ATF5) has been discovered to be a major regulator of the UPR^{mt} in mammalian cells, promoting the transcriptional induction of downstream UPR^{mt} targets during mitochondrial stress through promoter UPR^{mt} sites [29]. This is facilitated by its retrograde translocation to the nucleus in such conditions [29], while basally, is degraded in the mitochondrion, similar to ATFS-1 in *C. elegans* [28,29]. As part of the ATF/CREB family, the ATF5 protein retains a DNA-binding domain allowing it to interact with the promoters of target genes in the UPR^{mt}, in addition to a bZIP domain facilitating its interaction with other bZIP transcription factors through the formation of heterodimers [30,31]. Primarily abundant in the

liver, ATF5 has been investigated in a plethora of cellular conditions. It is known to be a responsive transcription factor during amino acid starvation [32–34], in mediating cell survival and proliferation in cancer and neurodegeneration [35–38], and retaining an influential role in the maturation of OSNs [39]. However, more evidence is beginning to emerge, supporting its role in mediating stress responses in muscle. ATF5 is upregulated in skeletal muscle during β-adrenergic stimulation [40], mitochondrial myopathy [41], and in myoblasts upon impaired protein translation [41] and during differentiation [42]. Furthermore, ATF5 has been found to be integral in UPR^{mt} activation and rescuing of mitochondrial function upon cardiac insult [43–45], providing opportunistic evidence for pursuing ATF5 function and UPR^{mt} activation in skeletal muscle.

The molecular mechanisms governing mitochondrial biogenesis in response to exercise are complex, and seminal work is beginning to reveal potential roles that acute mitochondrial proteotoxicity and the UPR^{mt} may have in mediating changes in cell signaling upon contractile activity [46–48]. Despite these findings, no work has focused on whether activation of the UPR^{mt} is required for mitochondrial biogenesis signaling following acute exercise, and whether ATF5 is required in this exercise-induced response, in addition to the maintenance of basal mitochondrial homeostasis. Therefore, our objectives were to: 1) assess the role of ATF5 in the maintenance of basal mitochondrial content and function; and 2) examine whether ATF5 and the UPR^{mt} is required for exercise-induced UPR^{mt} activation and mitochondrial biogenesis signaling.

METHODS

Animals and exercise protocols. ATF5 whole-body KO mice were generated by crossing $ATF5^{tm1(KOMP)}$ (Velocigene Project 11612) heterozygotes in a C57BL6/N background, generously provided by Stavros Lomvardas from Columbia University, with FVB WT females. Animals were

housed in a 12:12-h light-dark cycle and given food and water ad libitum. The ATF5(-/-) KO genotype causes semi-penetrant lethality in neonates, most likely due to improper development of olfactory epithelia, compromising pups' ability to compete for milk. Thus, ATF5(-/-) KO yields are lower than the assumed Mendelian ratios. To genotype progeny, ear clippings were obtained from each animal to make crude DNA extracts. They were subsequently mixed with JumpStart REDTaq polymerase (P0982, Sigma, Oakville, ON, Canada), forward and reverse primers (50 μM) (Table 1) for the WT and the altered ATF5 gene and subjected to amplification by PCR. Reaction products were run on a 1% agarose gel and visualized with the use of ethidium bromide. Experimental animals were used at 5.5-7 months of age and separated into either Control (CON) or Exercise (EX) groups (n=9-13/group).

Exercise protocols. Two different acute exercise protocols were used in this study, where animals ran at a fixed 10% slope in both, and acclimatized to the treadmill for three days prior to exercising. One was a bout of continuous exercise, where mice ran at a pace of 15 m/min for 60 minutes, followed by 18 m/min for 30 minutes. The other was exhaustive exercise, which was completed as follows: 0 m/min for 5 minutes, 5 m/min for 5 minutes. 10 m/min for 5 minutes, 15 m/min for 5 minutes, 20 m/min for 5 minutes, 25 m/min for 5 minutes, increasing the speed by 1 m/min every 3 minutes until exhaustion. Exhaustion was defined as the animal remaining on the shock pad for 10 seconds, despite encouragement to run. Using a small tail bleed, blood lactate was measured with a Lactate Scout+ analyzer (EKF Diagnostics, Magdeburg, Germany). Tissues were collected immediately after exercise and either used fresh or stored at -80°C until further analysis.

Cytochrome c oxidase activity. Activity of the cytochrome c oxidase (COX) enzyme was used as a marker of mitochondrial content in muscle. Using a portion of the TA, tissue lysates

were prepared in COX enzyme extraction buffer (100 mM Na-K-Phosphate, 2 mM EDTA, pH 7.2) and placed on ice. A test solution containing 20 mg of horse heart cytochrome c (C2506, Sigma, Oakville, ON, Canada) was prepared and incubated at 30°C. Using a multipipette, 240 µl of the test solution was added to 50 µl of whole muscle homogenate in a 96-well plate. The maximal oxidation rate of cytochrome c was then measured spectrophotometrically in a Synergy HT (Bio-Tek Instruments, Winooski, VT) plate reader, analyzing the change in absorbance at 550 nm and temperature of 30°C. For each sample, the COX activity measurement was determined as an average of three trials.

Nuclear and cytosolic fractionation. Nuclear and cytosolic fractions were prepared from one freshly extracted whole TA, using NE-PER Extraction Reagents (38835, Thermo Fisher Scientific) supplemented with phosphatase and protease inhibitors. Approximately ~30-50 mg of tissue was minced on ice and homogenized in CER-I. Homogenates were then left to stand on ice for 10 minutes. Following the addition of CER-II, samples were briefly vortexed and centrifuged at 16,000 g for 10 minutes at 4°C. The supernatant (cytosolic fraction) was collected. The remaining pellets, containing nuclei and cellular debris, were washed 3 times in cold 1 x PBS and resuspended in NER. Nuclear fractions were then sonicated 3 times for 3 seconds and incubated on ice for 40 minutes. Samples were vortexed every 10 minutes during the incubation then underwent centrifugation at 16, 000 g for 10 minutes. The resulting supernatants (nuclear fractions) were collected. Both cytosolic and nuclear subfractions were stored in -80°C until further analysis.

RNA isolation and reverse transcription. Approximately 50-70 mg of lysed gastrocnemius muscle tissue was combined with TRIzol® reagent (15596018, Life Technologies, Carlsbad, CA, USA) and mixed with chloroform. Samples were centrifuged at 16,000 g for 15 minutes at 4°C, and the upper aqueous phase was transferred into a new tube with isopropanol and

left overnight at -20°C to precipitate. Samples were once again centrifuged at 16,000 g for 10 minutes. The resulting supernatant fraction was discarded, and the pellet was suspended in 30 µl of molecular grade sterile H_2O. RNA concentrations and purities were measured using the NanoDrop 2000 (Thermo Fisher Scientific, Waltham, MA, USA). The Superscript III Reverse Transcriptase enzyme (Invitrogen, Waltham, MA, USA) was used to reverse-transcribe 1.5 µg of RNA into cDNA.

mRNA expression using real-time PCR. The mRNA expression of *ATF5, ATF4, CHOP, PGC-1α, COX-IV, HSP60, LONP, mtHSP70 and ClpP* was measured using the 7500 Real-Time PCR system (Applied Biosystems Inc., Foster City, CA, USA) and SYBR Green qPCR Master Mix (B21203, BiMake, Houston, TX, USA) in a 96-well plate. GAPDH and β-2 microglobulin were used as housekeeping genes for the normalization of transcript levels. Each well contained SYBR green, forward and reverse primers for the gene of interest (GOI) (20 µM) (Table 1), 10 ng of cDNA and sterile H_2O to yield a final reaction volume of each well of 25 µl. Primer optimizations were run beforehand to control for primer dimers and nonspecific amplification by analyzing melt curves generated by the instrument. All samples were run in duplicates in tandem with negative control wells that contained sterile H_2O in the place of cDNA.

Real-time PCR quantification. For the quantification of mRNA levels, the threshold cycle (C_T) value of the GOI was first subtracted from the average C_T value of both endogenous reference genes to obtain the ΔC_T value for the GOI: $\Delta C_T = C_T$ (GOI) - C_T (reference). Next, the ΔC_T value of the exercised tissue (EX) was subtracted from the ΔC_T value of the control tissue (CON) for each genotype to obtain the $\Delta\Delta C_T$ values for the WT EX, KO CON, and KO EX samples: $\Delta\Delta C_T = \Delta C_T$ (EX) - ΔC_T (CON). Results are expressed as fold changes above mRNA levels of WT CON animals using the $\Delta\Delta C_T$ method, calculated as $2^{-\Delta\Delta^{CT}}$.

Immunoblotting. Whole muscle protein extracts prepared from a portion of the gastrocnemius and isolated subfractions were separated on 10-15% SDS-PAGE gels via electrophoresis at 120 V for approximately ~90 minutes, and subsequently transferred onto nitrocellulose membranes, stained with Ponceau Red and cut at the appropriate molecular weights. Blots were blocked in a 5% skim milk solution in TBS-T (25 mM Tris-HCl, 1 mM NaCl, 0.1% Tween-20, pH 7.5) or 5% BSA in TBS-T for phosphorylated proteins for one hour at room temperature with gentle agitation. They were then coated with the appropriate primary antibodies (Table 2) and incubated overnight at 4°C. Membranes were then washed 3 x 5 minutes in TBS-T solution and incubated with HRP-linked secondary antibodies for one hour at room temperature. After another series of wash steps, blots were visualized with enhanced chemiluminescence using an iBright CL1500 Imaging System (Thermo Fisher Scientific, Waltham, MA, USA). Quantifications were carried out using ImageJ (NIH) software and normalized to the corresponding loading controls or Ponceau. Quantified values were additionally normalized over a 'Standard' sample that was run on every gel.

Mitochondrial isolations. Approximately 700-1000 mg of fresh skeletal muscle tissue (one gastrocnemius, two quadriceps, and two triceps) was extracted from anesthetized animals, placed in ice-cold buffer, and subsequently minced and homogenized. To separate SS and IMF mitochondria, homogenates were subjected to differential centrifugation at 800 g for 10 minutes. The IMF fraction was treated with the nagarse protease from *Bacillus lichenformis* (P5380, Sigma, Oakville, ON, Canada) to break down muscle fibres and liberate the mitochondrial pool. After additional centrifugation steps, both SS and IMF pellets were suspended in resuspension buffer (100 mM KCl, 10 mM MOPS, 0.2% BSA pH of 7.4). Protein concentrations were determined

using the Bradford method. Fresh mitochondrial fractions were utilized immediately to measure respiration and ROS emission.

Mitochondrial respiration. Oxygen consumption (O_2/mg/min) over time in SS and IMF mitochondria was measured using a Clark Electrode (Strathkelvin Instruments, North Lanakshire, UK). A small volume of either the SS or IMF fraction (50 µl) was incubated with 250 µl of VO_2 buffer (250 mM sucrose, 50 mM KCl, 25 mM Tris base, 10 mM K_2HPO_4, pH 7.4) while being continuously stirred at 30°C. Respiration rates were determined (nanoatoms O_2/min/mg) in the presence of 10 mM glutamate for State IV (passive) respiration, and 0.44 mM ADP for State III (active) respiration. Finally, NADH was added to test mitochondrial membrane integrity.

Mitochondrial ROS emission. SS and IMF mitochondria (75 µg) were incubated in a black polystyrene 96-well plate with VO_2 buffer and 50 mM H_2DCF-DA (D399, Thermo Fisher Scientific) at 37°C for 30 minutes. The fluorescence emission (480-520 nm) was measured in a Synergy HT (Biotek, Winooski, VT, USA) plate reader using Gen5 software. ROS emission was assessed with the addition of 10 mM glutamate in the absence (State IV) or presence (State III) of 0.44 mM ADP. Data were normalized to the corresponding respiration rates.

Statistical analysis. Data were analyzed using GraphPad Prism 8.0 software and values are reported as means $\pm$ SEM. Basal comparisons of WT and KO animals were carried out with unpaired student's t-tests. To compare control values with those of both exercise conditions, a 1-way ANOVA was performed, while a 2-way ANOVA was used in the comparisons of exercise conditions and genotypes, followed by a Bonferroni post-hoc test where necessary. Statistical significance was set at $P < 0.05$.

Table 1. List of primer oligonucleotide sequences used in PCR (genotyping) and real-time qPCR for *Mus Musculus.*

Gene	Forward Primer	Reverse Primer
WT (geno)	5'-GGC TGG CTG GTC ACT TGT C-3'	5'-GTC CCT GAG GAC TGT GCT TTA TC-3'
ATF5 mut (geno)	5'-GCA GCC TCT GTT CCA CAT ACA CTT CA-3'	5'-CAG AGT GGC TTC CTG CTT TAT-3'
PGC-1α	5'-TTC CAC CAA GAG CAA GTA T-3'	5'-CGC TGT CCC ATG AGG TAT T-3'
COX-IV	5'-CTC CAA CGA ATG GAA GAC AG-3'	5'-TGA CAA CCT TCT TAG GGA AC-3'
ATF5	5'-TGG AGC GGG AGA TCC AGT A-3'	5'-GAC GCT GGA GAC AGA CGT ACA-3'
ATF4	5'-GCC GGT TTA AGT TGT GTG CT-3'	5'-CTG GAT TCG AGG AAT GTG CT-3'
CHOP	5'-CAC CAC ACC TGA AAG CAG AA-3'	5'-AGG TGA AAG GCA GGG ACT CA-3'
HSP60	5'-CTG GGT GCA AGA GCC ATA TA-3'	5'-GAA AGG CTG CTT CTG AAC TCT-3'
mtHSP70	5'-TGG CTA TTA CTG CGG GTT CT-3'	5'-CAT CTG CTC CAC CTC CTC T-3'
LONP	5'-CGA CTT GCA CAG CCC TAT GT-3'	5'-CGA ATG TTC CCG TAT GGT AGA T-3'
ClpP	5'-CACACCAAGCAGAGCCTACA-3'	5'-CCCAGCAGAGGAAGTTTCAG-3'
GAPDH	5'-AAC ACT GAG CAT CTC CCT CA-3'	5'-GTG GGT GCA GCG AAC TTT AT-3'
β2-microglobulin	5'-GGT CTT TCT GGT GCT TGT CT-3'	5'-TAT GTT CGG CTT CCC ATT CT-3'

Table 2. List of antibodies used in Western Blotting.

Antibody	Manufacturer	Catalogue #
α-tubulin	Calbiochem (Millipore)	CP06-100µg
H2B	Cell Signaling	2934S
p-SAPK/JNK (T183)	Cell Signaling	4668S
t-SAPK/JNK	Cell Signaling	9252T
p-eIF2α (S51)	Invitrogen	44728G
t-eIF2α	Cell Signaling	9722S
ATF5	abcam	ab184923
ATF4/CREB2	Santa Cruz Biotechnology	sc-390063
VDAC1/Porin	abcam	ab14734
PGC-1α	EMD Millipore	AB3242
LONP1	Cell Signaling	28020S
HSP60	Enzo Life Sciences	ADI-SPA-806-D
mtHSP70	Enzo Life Sciences	ADI-SPS-825-F
Anti-Mouse HRP-linked 2°	Cell Signaling	7076S
Anti-Rabbit HRP-linked 2°	Cell Signaling	7074S

RESULTS

Confirmation of ATF5 KO mouse model. The ATF5 KO mouse model was confirmed with DNA genotyping, through the presence of the mutant ATF5 allele and the absence of the WT allele (Fig. 1A) [44]. It was additionally confirmed with the abolishing of the ATF5 transcript in KO muscle (Fig. 1B).

ATF5 KO animals exhibit reduced body weight and no changes in exercise tolerance. The phenotypic characteristics of ATF5 KO mice have been described previously [44]. In our study, deletion of the ATF5 gene resulted in a reduction in body weight of approximately 21% ($P < 0.0001$) (Fig. 2A) without any changes occurring in muscle mass, observed by comparing TA weight and body weight (Fig. 2B). To examine the involvement of ATF5 in determining endurance capacity, WT and ATF5 KO mice were subjected to an acute bout of exhaustive, incremental exercise. No changes in exercise tolerance were observed between genotypes, represented by the distance run by the animal until exhaustion (Fig. 2C). Both genotypes experienced significant anaerobic challenge during the exhaustive test, with significantly greater blood lactate levels post-exercise ($P < 0.0001$).

Exercise stimulates the phosphorylation of eIF2α and JNK. The phosphorylation of the α subunit of ribosomal eIF2 at Serine 51 is a pivotal event during ISR activation, inhibiting global protein translation and selectively translating mRNAs with uORFs. These include the transcription factors ATF5, ATF4 and CHOP, which induce the transcription of mitochondrial-protective genes in the nucleus. On the other hand, JNK is a kinase that is highly responsive to acute exercise and has been identified to be implicated in UPR^{mt} signaling during mitochondrial stress. Thus, we sought to investigate whether there are discrepancies in acute-exercise induced UPR^{mt} upstream signaling, represented by eIF2α and JNK phosphorylation.

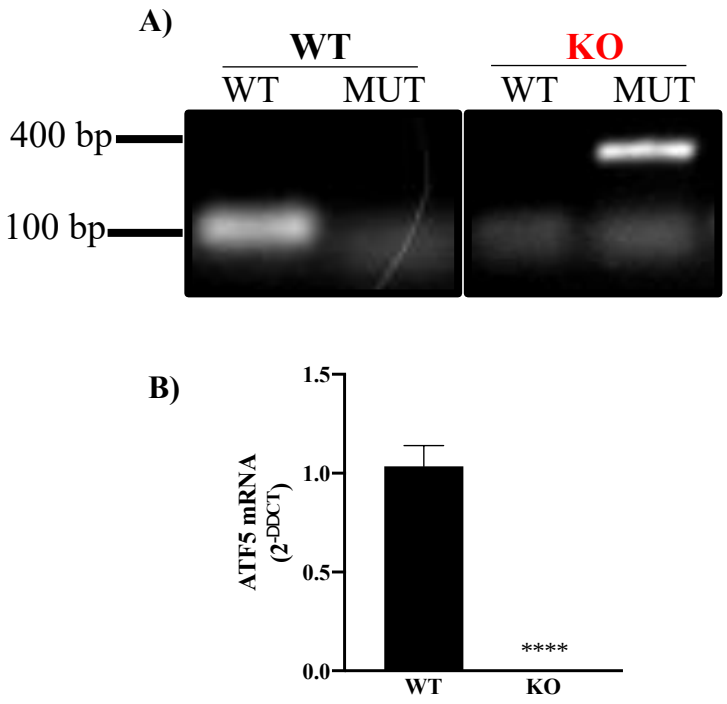

Figure 1. Genotyping of ATF5 KO animals and mRNA levels. A) Genotyping of WT and ATF5 KO animals was performed by probing for the ATF5 WT (100 bp) and MUT (400 bp) alleles with designated primer sets. Animals were identified as a WT or KO, with WT mice retaining only the WT allele, and KO mice having only the MUT allele. The KO mouse model was further confirmed upon the measurement of **B)** ATF5 mRNA, with the complete abolishment of the ATF5 transcript in KO muscle. ****P<0.0001, WT vs. KO, unpaired t-test. WT: n=16, KO: n=23. WT, wild-type; MUT, mutant.

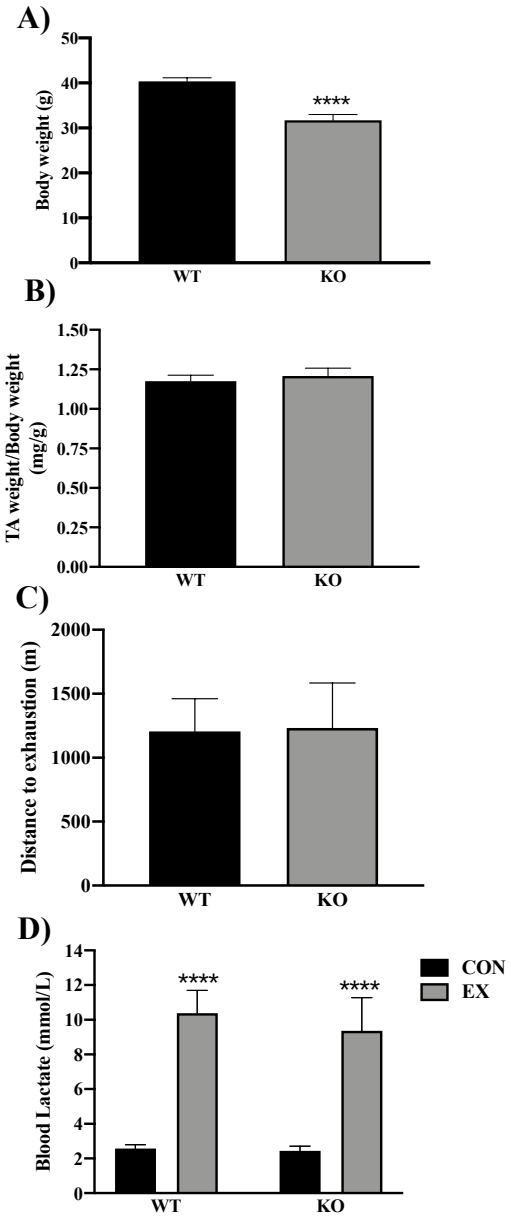

Figure 2. Animal characteristics and response to exercise. A) Differences in body weight and **B)** TA weight/body weight between WT (n=18) and ATF5 KO (n=26-27) animals. ***P<0.0001, Unpaired t-test, WT vs. KO. Exercise performance was established in an incremental exhaustive exercise test on the treadmill by recording **C)** Distance to exhaustion, and **D)** Blood lactate levels measured before and after exercise. In lactate levels, there was an effect of exercise, but no effect of genotype. ****P<0.0001, CON vs. EX, 2-way ANOVA. WT: n=4, KO: n=7.

Following continuous exercise, no significant changes were observed in phosphorylated eIF2α in both WT and KO muscle (Fig. 3A,B). However, KO muscle appeared to have 20% less phosphorylated eIF2α relative to WT ($P = 0.08$) (Fig. 3A,B). Interestingly, exhaustive exercise elicited greater increases in eIF2α phosphorylation, increasing by 17% in WT muscle and by 47% in KO animals ($P = 0.07$) (Fig. 3A,B). In contrast, KO muscle retained higher basal levels of phosphorylated JNK by 31% and increased 2-fold post-exercise in both protocols ($P < 0.05$) (Fig. 3C,D). WT muscle exhibited increases of 2.3-fold following exhaustive exercise ($P < 0.05$), but no changes were observed with continuous exercise (Fig. 3C,D). These JNK results indicate increased stress signaling with exhaustive exercise, in addition to enhanced stress signaling basally in the absence of ATF5.

Acute exercise is not a sufficient stimulus for the induction of ATF5 nuclear translocation. The subcellular localizations of PGC-1α and ATF4 were measured in nuclear and cytosolic fractions isolated from WT and KO muscle following the exhaustive exercise test, while ATF5 expression was observed in fractions from WT animals only. Additionally, localization of transcription factors was compared between the two exercise protocols in WT muscle. No changes were observed in the proportions of nuclear ATF5 and protein levels in nuclear and cytosolic compartments (Fig. 4A, B, C). In contrast, the percentage of nuclear PGC-1α tended to increase by 2-fold from 3.5 to 7% of total PGC-1α after one bout of continuous exercise in WT animals ($P = 0.09$). However, these changes were not observed following a bout of exhaustive exercise in WT or KO muscle (Fig. 5C). Nuclear and cytosolic PGC-1α protein levels were elevated in KO muscle in comparison to WT muscle by 50% and 40%, respectively ($P < 0.05$) (Fig. 5B), although, proportions of nuclear PGC-1α relative to total PGC-1α did not differ significantly between genotypes (Fig. 5C). The localization of ATF4, another transcription factor activated by cellular stress was also evaluated.

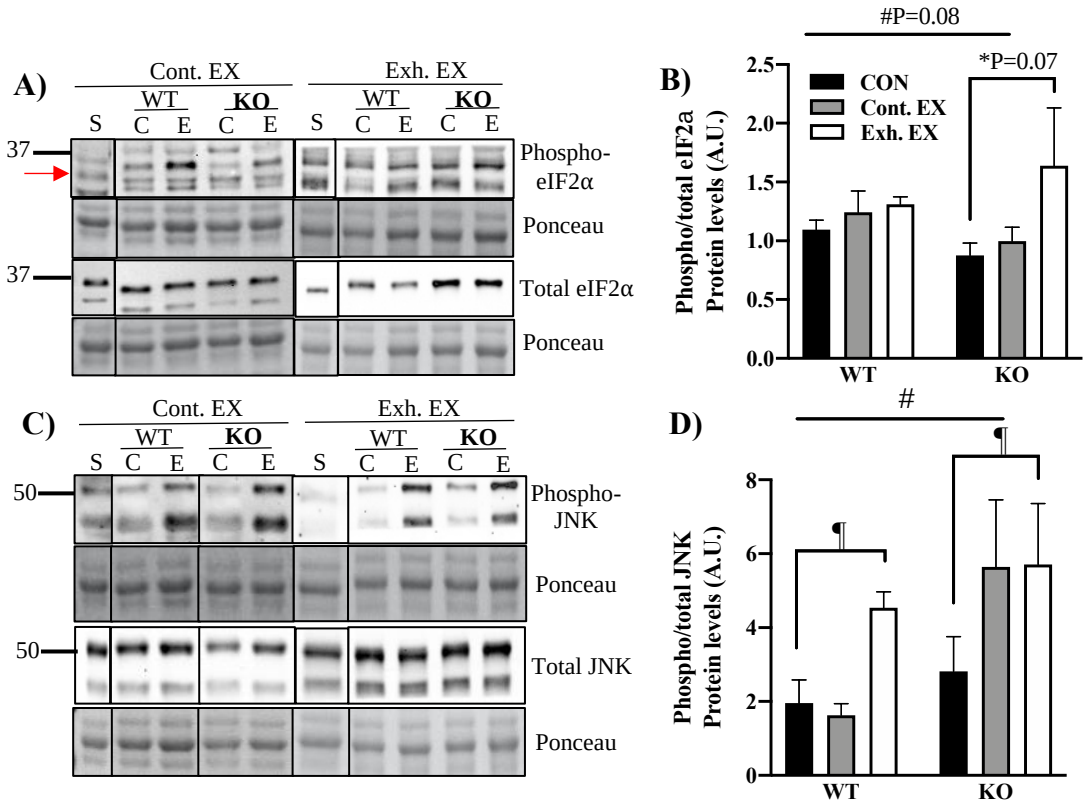

Figure 3. Effects of acute continuous and exhaustive exercise on upstream signaling, represented by eIF2α and JNK phosphorylation in WT and KO muscle. A) Immunoblots of phosphorylated and total eIF2α with corresponding Ponceaus. **B)** Quantification of phosphorylated/total eIF2α protein in WT and KO muscle in response to exercise. **C)** Immunoblots of phosphorylated and total JNK with corresponding Ponceau-stained gels. **D)** Quantification of phosphorylated/total JNK in WT and KO muscle in response to exercise. Dividing lines on immunoblots indicate where samples were spliced together from the same blot for direct comparisons of WT and KO samples. ¶P<0.05, main effect of exercise, #P<0.05, main effect of genotype, 2-way ANOVA; *P<0.05, KO CON vs. KO EX (Exh.), unpaired t-test. WT CON: n=8, WT EX (Cont.): n=5, WT EX (Exh.): n=3, KO CON: n=12, KO EX (Cont.): n=5, KO EX (Exh.): n=7. S, standard; Cont., continuous; Exh., exhaustive.

Similar to ATF5, its nuclear translocation was not observed after either continuous or exhaustive exercise (Fig. 6D). Nuclear and cytosolic ATF4 protein levels were also not different following exercise in both animal models and were not different basally between genotypes (Fig. 6B). However, 19% and 24% of total ATF4 was observed in the nucleus in KO muscle compared to 10% and 14% in WT in control and exercised samples, respectively. This potentially indicates compensatory nuclear trafficking of ATF4 in the absence of ATF5 ($P < 0.05$) (Fig. 6C).

Basal protein expression of UPR^{mt} markers is augmented in the absence of ATF5. Since it has been suggested that ATF5 is required for the expression of its downstream UPR^{mt} targets during mitochondrial stress [29], it was of interest to investigate the requirement of ATF5 in the basal expression of these proteins (Fig. 7). Interestingly, protein levels of LONP (Fig. 7E) and mtHSP70 (Fig. 7D) were increased by 23% and 31% (Fig. 7D) ($P<0.05$), respectively, while HSP60 tended to increase (Fig. 7B,8C,D). No changes were observed in the expression of the transcription factor ATF4 (Fig. 7E,F).

The muscle of ATF5 KO animals display enhanced mitochondrial content. Mitochondrial content was measured in the skeletal muscle of WT and ATF5 KO animals via the quantification of COX enzyme activity and mitochondrial yield calculations from mitochondrial isolations. Protein expression of the mitochondrial marker VDAC was also measured (Fig. 8C,D). KO muscle exhibited 12% greater COX activity relative to WT muscle ($P < 0.05$) (Fig. 8A) and an increased mitochondrial yield of 19% ($P < 0.01$) (Fig. 8B).

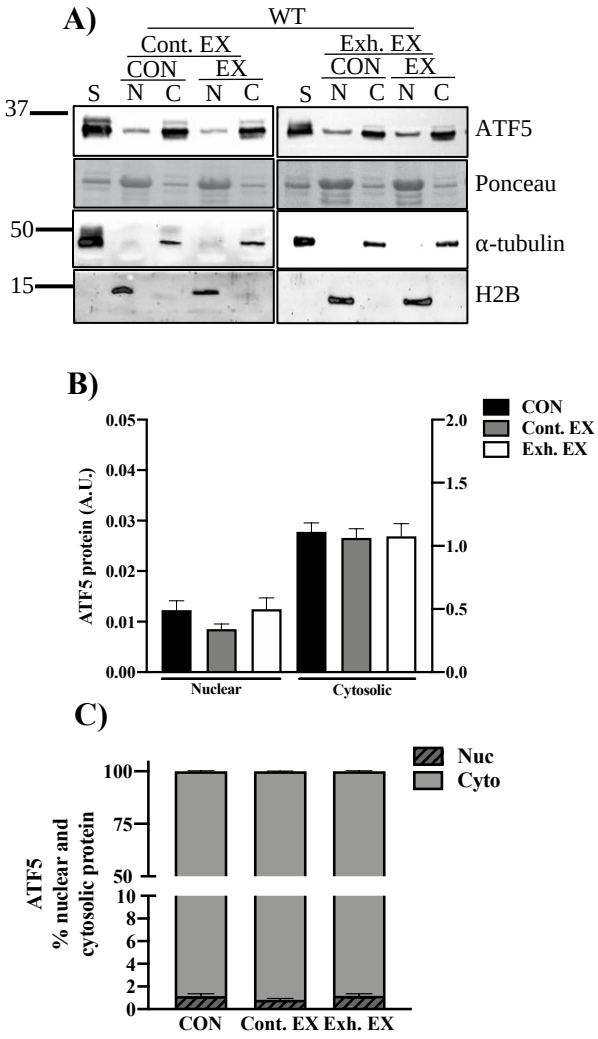

Figure 4. Subcellular localization of ATF5 following acute continuous and exhaustive exercise in WT animals. A,B) ATF5 protein expression was measured in nuclear and cytosolic fractions in WT animals basally and following acute continuous and exhaustive exercise. **C)** % of nuclear ATF5 relative to total ATF5 did not change with acute exercise, indicating that acute exercise stress does not induce ATF5 nuclear translocation. WT CON: n=9, WT EX (Cont.): n=5, WT EX (Exh.): n=4. CON, control; EX, exercise; Cont., continuous; Exh., exhaustive; N, nuclear; C, cytosolic; S, standard. Blots were normalized to the Ponceau stains. α-tubulin and H2B blots are shown to indicate sample purity. Micrograms of protein loaded: Nuclear, 60; Cytosolic, 10. Approximate molecular weights of proteins in kilodaltons (kDa) are shown on blots.

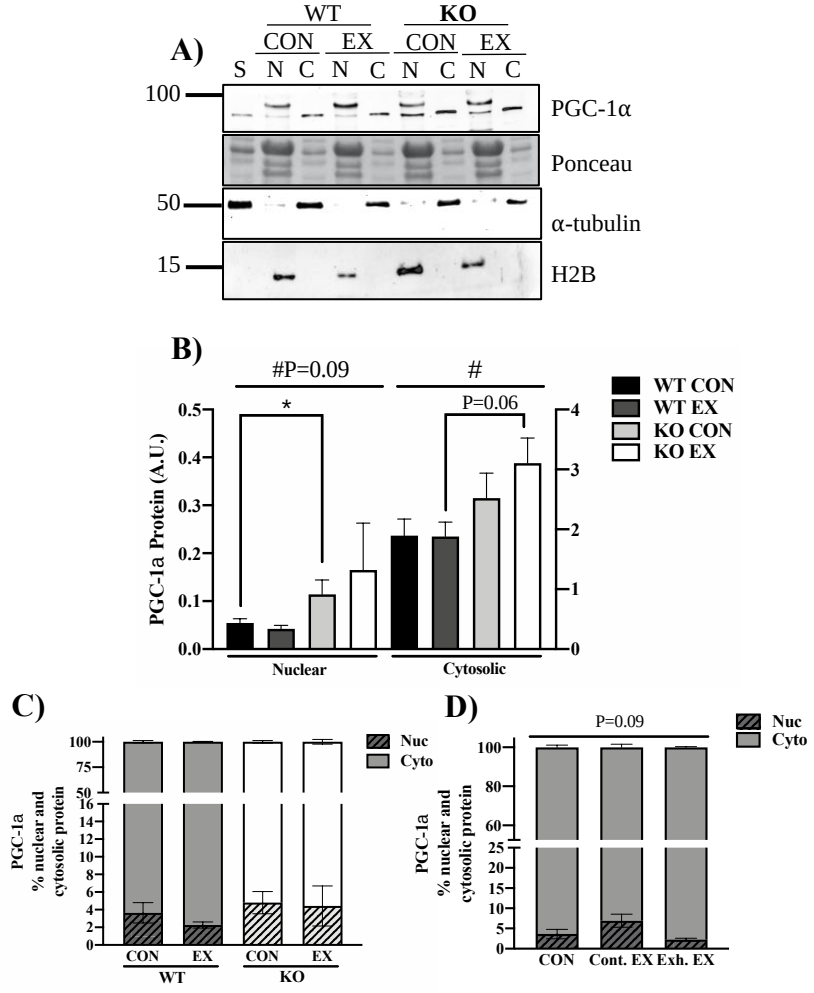

Figure 5. Subcellular localization of PGC-1α following acute continuous and exhaustive exercise in WT and KO animals. A,B) PGC-1α protein expression in nuclear and cytosolic fractions in WT and KO muscle. A genotype effect was significant in cytosolic samples. **C)** PGC-1α % nuclear protein basally and after exhaustive exercise in WT and KO animals**. D)** PGC-1α % nuclear protein basally and following both exercise protocols in WT animals. WT CON: n=9, WT EX (Cont.): n=5, WT EX (Exh.): n=4, KO CON: n=6, KO EX, n=6. #P<0.05, main effect of genotype, 2-way ANOVA. Blots were normalized to the Ponceau stains. α-tubulin and H2B blots are shown to indicate sample purity. Micrograms of protein loaded: Nuclear, 60; Cytosolic, 10. Approximate molecular weights of proteins in kilodaltons (kDa) are shown on blots. CON, control; EX, exercise; Cont., continuous; Exh., exhaustive; N, nuclear; C, cytosolic; S, standard.

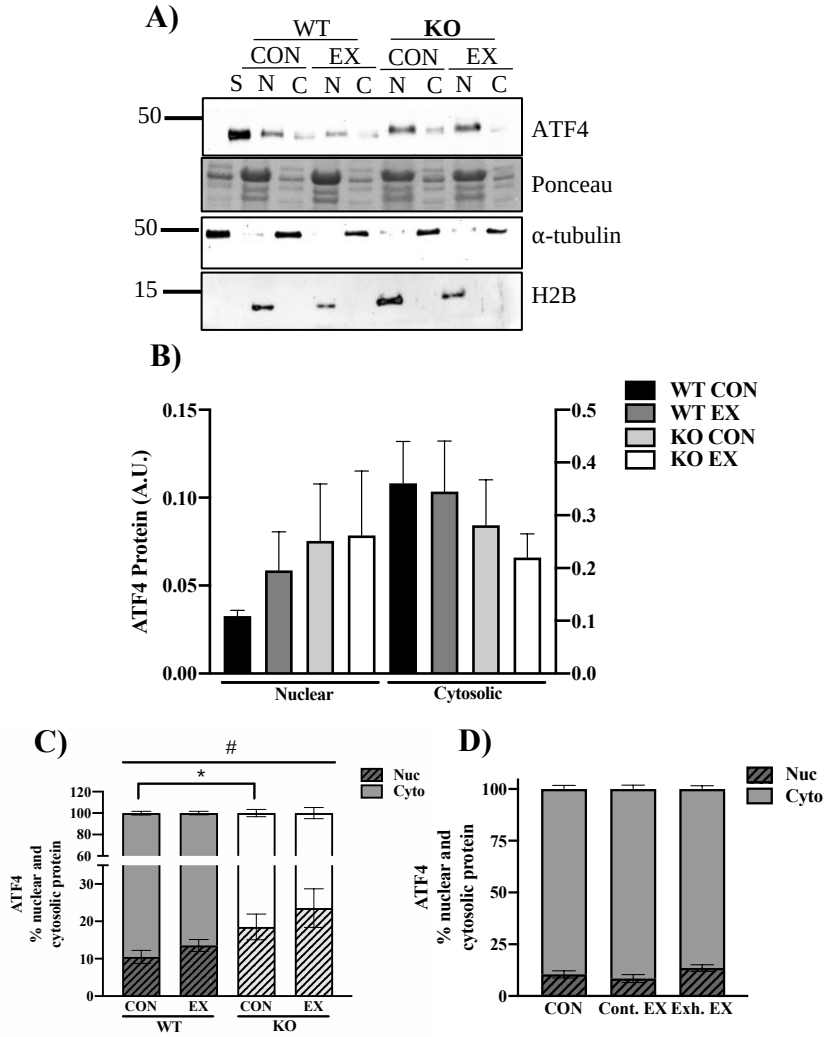

Figure 6. Subcellular localization of ATF4 following acute continuous and exhaustive exercise in WT and KO animals. A,B) ATF4 protein levels, **C)** ATF4 % nuclear protein in WT and KO mice, and in **D)** WT mice only. WT CON: n=9, WT EX (Cont.): n=5, WT EX (Exh.): n=4, KO CON: n=6, KO EX, n=6. *P<0.05, WT CON vs. KO CON, unpaired t-test. #P<0.05, main effect of genotype, 2-way ANOVA. Blots were normalized to the Ponceau stains. α-tubulin and H2B blots are shown to indicate sample purity. Micrograms of protein loaded: Nuclear, 60; Cytosolic, 10. Approximate molecular weights of proteins in kilodaltons (kDa) are shown on blots. CON, control; EX, exercise; Cont., continuous; Exh., exhaustive; N, nuclear; C, cytosolic; S, standard.

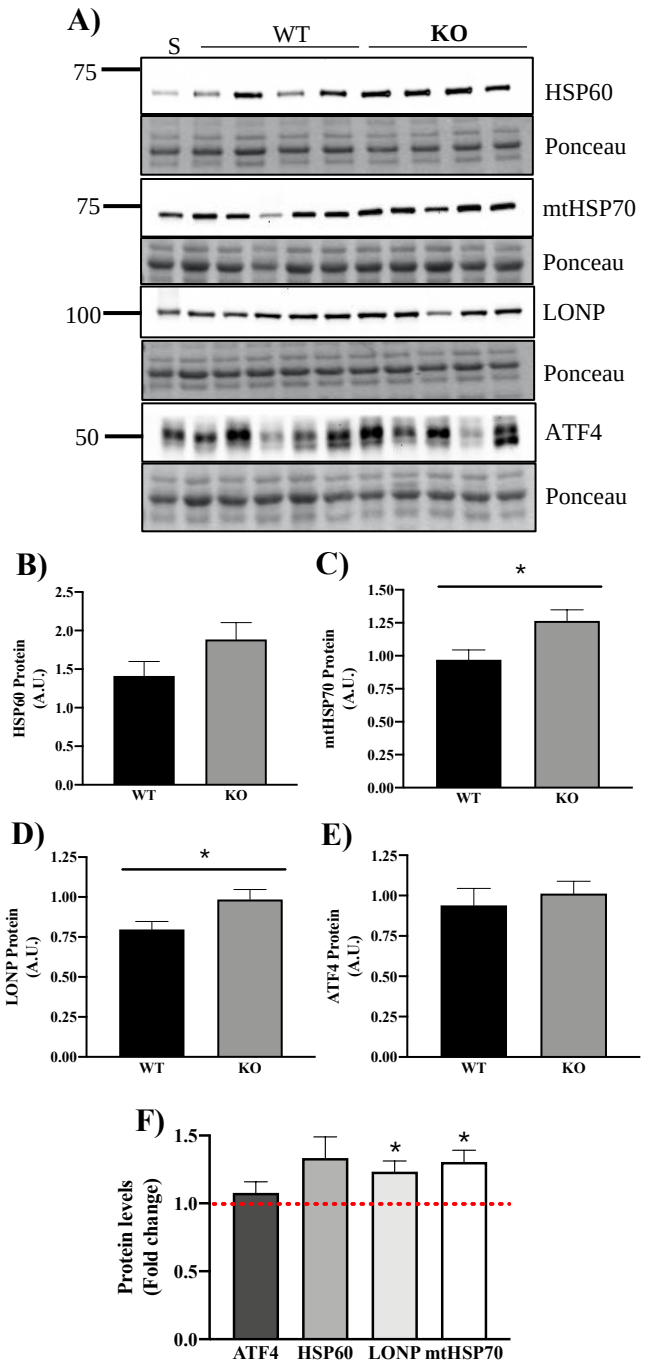

Figure 7. Basal protein expression in WT and KO muscle. A) Blots indicating protein of the UPR^{mt} markers HSP60, mtHSP70, LONP and the transcription factor ATF4 with corresponding Ponceau stains. **B-E)** Graphical representation of protein levels between WT and KO muscle. **F)** Protein levels of KO muscle expressed as fold changes relative to WT. *P<0.05, WT vs. KO, unpaired t-test. WT: n=15-16, KO: n=22. S, standard.

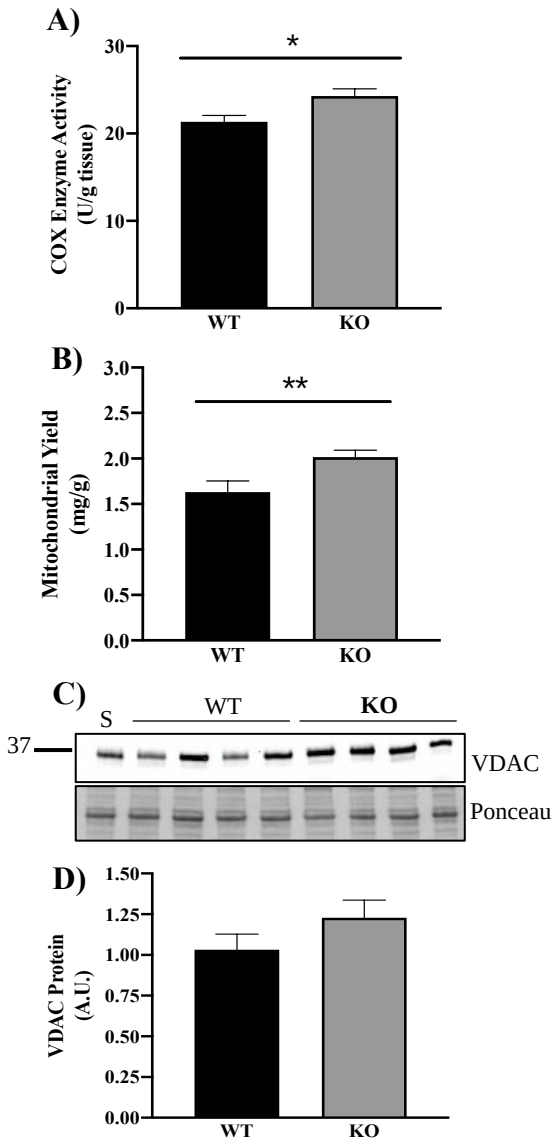

Figure 8. ATF5 KO muscle exhibits a greater mitochondrial pool. A) COX activity measurements in WT and KO muscle. WT: n=9, KO: n=10. **B)** Total mitochondrial yield (SS and IMF) calculated from mitochondrial isolation experiments. WT: n=18, KO: n=27. **C)** VDAC protein blot with its corresponding Ponceau stain. WT: n=16, KO n=22. *P<0.05, **P<0.01, WT vs. KO, unpaired t-test. S, standard.

ATF5 is required for the maintenance of basal mitochondrial function. To investigate whether ATF5 retains a role in mitochondrial function in mammalian muscle, we measured oxygen consumption and ROS emission in SS and IMF mitochondria isolated from the skeletal muscle of WT and ATF5 KO animals (Fig. 9). In the absence of ATF5, significant reductions in mitochondrial respiration were observed in both mitochondrial fractions derived from KO muscle. In State IV (passive) respiratory conditions, oxygen consumption was reduced by 39% in SS mitochondria ($P < 0.05$) (Fig. 9A), while in State III (active) respiration, there was reduction of 40% and 32% in SS ($P < 0.01$) (Fig. 9A) and IMF ($P < 0.01$) (Fig. 9B) fractions, respectively, in comparison to WT animals. However, no alterations were observed in the Respiratory Control Ratios (RCRs) between genotypes in both subfractions. Furthermore, IMF mitochondria from KO animals exhibited a 20% increase in ROS emission under State III conditions ($P < 0.01$) (Fig. 9D), without any significant changes observed in the SS fraction (Fig. 9C).

Changes in acute exercise-induced signaling in the absence of ATF5. In mammalian cells and cardiac injury in rodents, ATF5 is known to be required for the stress-induced transcriptional activation of its downstream targets, including HSP60, LONP and mtHSP70 [29,44]. Thus, we investigated whether ATF5 KO animals exhibit impaired transcriptional signaling through the measurement of mRNA levels post-exercise (Fig. 10). mRNA data from the continuous exercise protocol is shown. Indicative of mitochondrial biogenesis signaling, PGC-1α mRNA was enhanced in both animal models after an acute bout of continuous exercise, increasing by 5.7-fold and 3-fold in WT and KO animals, respectively ($P < 0.05$) (Fig. 10A). However, a 44% reduction in COX-IV mRNA was observed in KO muscle post-exercise ($P < 0.01$) with no changes occurring in WT animals (Fig. 10B).

No significant changes were observed in ATF5 and ATF4 mRNA with exercise (Fig. 10C,E). However, ATF4 mRNA was found to be upregulated 2.6-fold and 3.7-fold in KO control and exercised samples, respectively, relative to WT mice ($P < 0.05$) (Fig. 10E). No changes in CHOP mRNA were observed between WT and KO mice basally and with exercise (Fig. 10D). mRNA levels of the mitochondrial chaperone HSP60 were increased in both animal models with exercise ($P < 0.05$), but even more so in KO mice, by 30% and 36% in WT and KO mice, respectively (Fig. 10F). In addition, there was a trending main effect of genotype, with 24% more HSP60 mRNA in KO muscle ($P = 0.07$).

The gene expression response of UPR^{mt} markers downstream of ATF5 were evaluated in WT and KO animals to examine the role of ATF5 in acute exercise-induced proteostatic signaling. In contrast to what was observed with HSP60, mRNA levels of these UPR^{mt} markers increased slightly or did not change with exercise in WT animals but were reduced upon acute exercise in KO muscle. Significant interaction effects were seen with exercise in all three genes, where mRNA levels of LONP ($P < 0.01$) (Fig. 10H), mtHSP70 ($P < 0.05$) (Fig. 10G) and ClpP ($P < 0.05$) (Fig. 10I) were reduced by 18%, 22% and 19%, respectively. mRNA levels of LONP, mHSP70 and ClpP are also collectively represented as overall changes in UPR^{mt} downstream targets (Fig. 10J). Combined, the gene expression of these targets increased by 21% post-exercise in WT animals, while basally, KO muscle displayed a 16% increase compared to WT and a 20% reduction in mRNA levels with exercise ($P < 0.05$) (Fig. 10J).

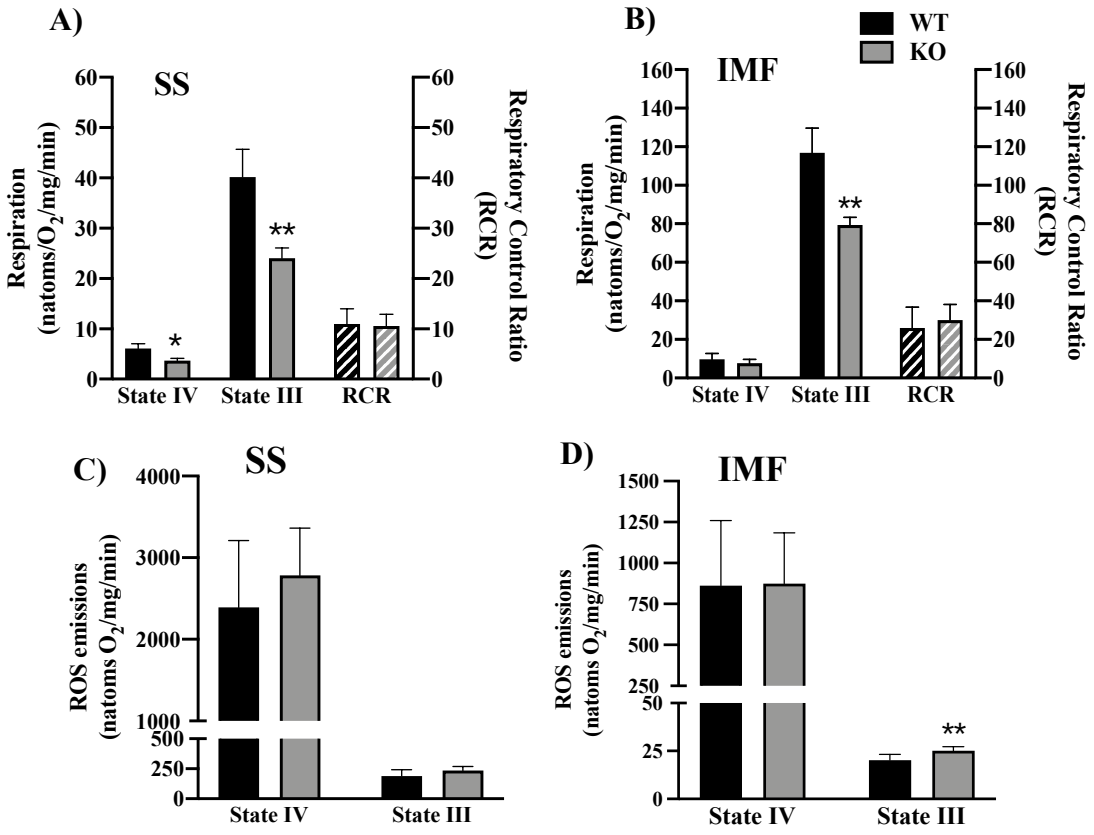

Figure 9. Diminished function in mitochondria from ATF5 KO muscle. Mitochondrial function was assessed in the skeletal muscle of WT and ATF5 KO mice through the measurements of oxygen consumption (respiration) and ROS emission in isolated organelles. Respiration rates in **A)** SS and **B)** IMF mitochondria in State IV and III conditions. RCR measurements (State III/State IV) are also indicated for both genotypes in SS and IMF mitochondria. ROS emission was also measured in **C)** SS and **D)** IMF mitochondria in passive and active respiratory states. *P<0.05, **P<0.01, WT vs. KO in given respiratory condition, unpaired t-test. WT: n=16-18, KO: n=24-27.

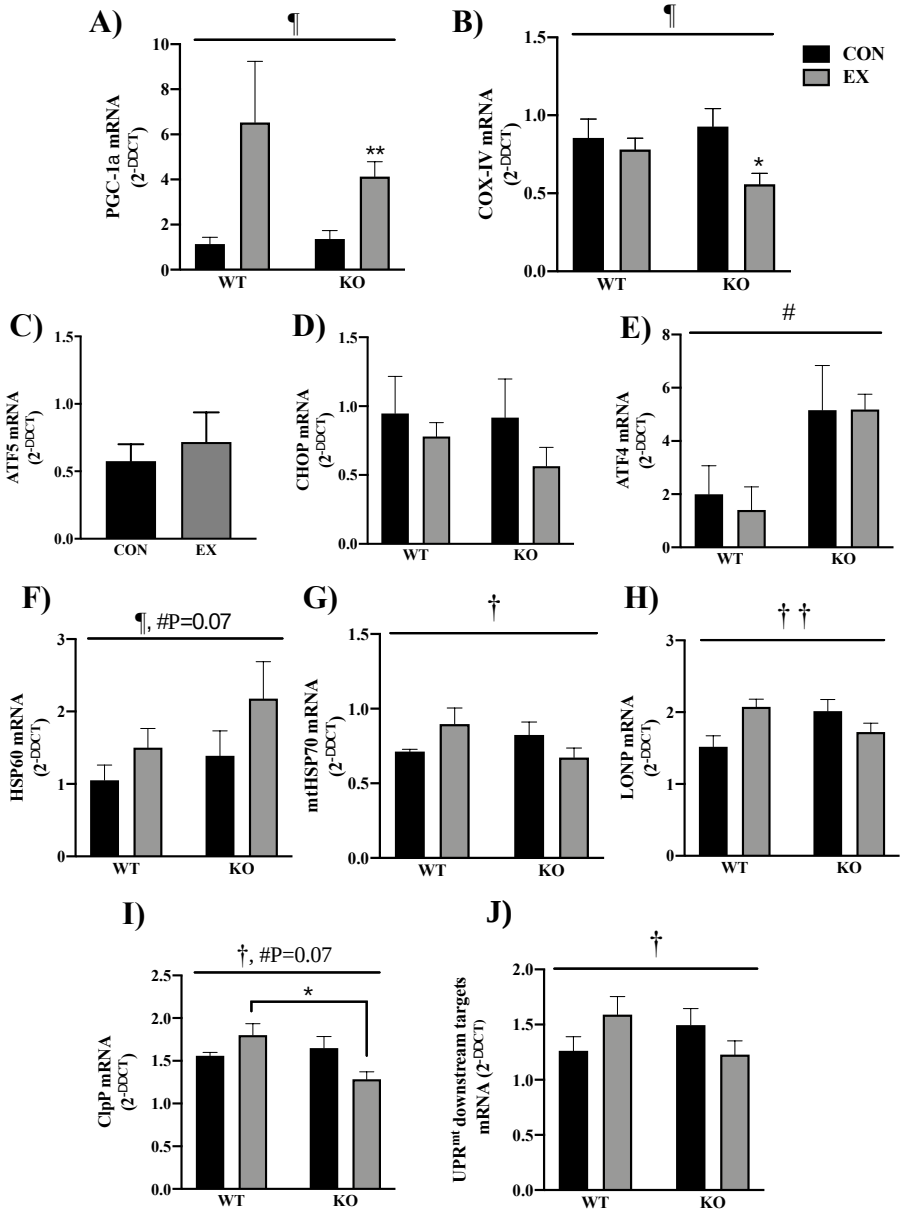

Fig 10. Changes in mRNA levels in response to acute continuous exercise in WT and KO animals. Transcript levels were measured for mitochondrial biogenesis markers **A)** PGC-1α and **B)** COX-IV, in addition to transcription factors involved in the UPR^{mt} such as **C)** ATF5 (WT mice only), **D)** CHOP and **E)** ATF4. mRNA levels of the UPR^{mt} chaperones **F)** HSP60 and **G)** mtHSP70. mRNA levels of the UPR^{mt} proteases, including **H)** LONP and **I)** ClpP; *P<0.05, WT EX vs. KO EX, Bonferroni post-hoc. WT: n=4. KO: n=5. **J)** mRNA of UPR^{mt} downstream targets with similar trends (LONP, mtHSP70 and ClpP combined). WT: n=12, KO: n=15. #P<0.05, main effect of genotype; ¶P<0.05, main effect of exercise; †P<0.05, ††P<0.01, interaction effect, 2-way ANOVA; *P<0.05, **P<0.01, EX vs. CON of same genotype unless indicated otherwise, unpaired t-test.

DISCUSSION

The maintenance of a healthy mitochondrial pool is essential for the regulation of cellular homeostasis. Despite being separated from the cytosol by a double-membraned barrier, mitochondria are tightly integrated into the cellular milieu, lying at the crossroads of a multitude of bidirectional signaling cascades with the nucleus. Mitochondria monitor their own function and coordinate retrograde (mitochondria-nuclear) communication to induce specific transcriptional programs to preserve the organelle network [52,53]. The mitochondrial proteome is mostly comprised of proteins with nuclear origins. These proteins are integrated within the mitochondrial network via an import process, followed by their folding and shuttling to their appropriate organellar destinations. These events require extensive coordination, and any dysregulation can incite the accretion of misfolded proteins, disrupting protein homeostasis and causing proteotoxic stress, leading to the activation of the mitochondrial unfolded protein response (UPR^{mt}). This involves the nuclear translocation of ATF5 to stimulate the transcription of additional mitochondrial chaperones and proteases [29,54]. The result is an improvement in the protein folding environment of the matrix, which determines mitochondrial recovery [29]. Our previous research in this area has shown that an induction of UPR^{mt} occurs in response to muscle contractile activity, and that this actually precedes signaling towards mitochondrial biogenesis during a time-course of muscle adaptations in a rodent model [46]. This suggests the importance of upregulating the expression of proteostatic machinery, possibly via the action of ATF5, for mitochondrial adaptations to exercise to occur. However, the role of ATF5 in 1) the maintenance of basal mitochondrial content and function in muscle, as well as in 2) acute exercise signaling to organelle biogenesis, have yet to be determined. Thus, we sought to investigate these functions using whole-body ATF5 KO animals.

Given the role of ATF5 in regulating the UPR^{mt}, we originally hypothesized that the absence of this transcription factor would result in a decrease in mitochondrial content. However, our findings indicate that the muscle of ATF5 KO animals displayed increased mitochondrial content in comparison to WT animals. We then assessed whether these mitochondria were equally functional, by measuring respiration and ROS emission in isolated mitochondria. Our data show that mitochondria from ATF5 KO muscle displayed reduced rates of oxygen consumption along with specific substrate-induced increases in ROS emission, in comparison to mitochondria from WT animals. These findings support other work that measured mitochondrial respiration in the absence of ATF5 in a mammalian cell model [29]. Thus, this novel finding indicates that in the absence of ATF5, skeletal muscle possesses a larger mitochondrial pool comprised of more dysfunctional mitochondria. The result of this compensatory adaptation is little to no change in exercise capacity between the two genotypes. Whether this altered mitochondrial content and function is a result of inherent differences in the habitual activity / inactivity level of the KO animals remains to be determined.

To investigate the possible underlying reasons for this increase in organelle content, we sought to examine the expression and localization of PGC-1α, a potent transcriptional co-activator that stimulates mitochondrial biogenesis. We found increased expression in both nuclear and cytosolic fractions isolated from ATF5 KO muscle, relative to WT samples. This potentially reveals an increased drive for mitochondrial biogenesis in the absence of ATF5, contributing to a larger mitochondrial pool, albeit composed of more dysfunctional organelles.

An accumulation of poor quality mitochondria in the absence of ATF5 may be an indicator of impaired mitophagy, the process whereby defective mitochondria are degraded and processed by the lysosomes [55]. Although we have not investigated the role of ATF5 in mitophagy in the

current study, the involvement of this protein in mitochondrial degradations is suggested by the fact that ATF5 levels are increased upon the inhibition of mitophagy in the myocardium, along with other UPR^{mt} proteins, possibly playing a compensatory role in the maintenance of mitochondrial homeostasis during cardiac stress [56]. It will be of interest in the future to consider whether ATF5 acts in the nucleus to induce the transcription of autophagic or mitophagic genes, serving to maintain mitochondrial quality via this degradative pathway.

Among the many cellular events that encompass the physiological response to the stress of acute exercise, the activation (phosphorylation) of stress-inducible kinases is at the forefront of this molecular cascade. Our data show that acute exercise increases JNK activation, a member of the MAPK family of kinases, that has been shown to contribute to increases in PGC-1α gene expression following exercise [10,57,58]. Further, the JNK activation response is exaggerated in ATF5 KO muscle and is accompanied by enhanced eIF2α phosphorylation post-exercise. As JNK activation is highly responsive to ROS production [50,59–61], this could be a consequence of the elevated ROS levels that we observed in IMF mitochondria during State III respiration and is similar to what has been found previously in cardiac muscle from ATF5 KO animals [43].

In contrast to our initial hypothesis, protein markers previously established to be downstream targets of ATF5 [29] such as mitochondrial chaperones and proteases were increased basally in ATF5 KO muscle. To investigate the reason for this, we studied the expression and localization of ATF4, a well-established transcription that regulates the UPR^{ER} [62]. Sharing close homology with ATF5, ATF4 controls the transcription of ATF5, is activated by endoplasmic reticulum (ER) and mitochondrial stress [63,64], and its protein levels have been found to be upregulated in mammalian cells in the absence of ATF5 [65]. Whether ATF4 truly regulates the transcription of chaperones and proteases of the UPR^{mt} remains a controversial topic [64], however

our results indicate that muscle from ATF5 KO animals exhibited enhanced ATF4 mRNA levels, in addition to its increased nuclear localization. These changes suggest that ATF5 negatively regulates ATF4 by suppressing its expression. Moreover, in conjunction with the enhanced stress signaling and mitochondrial ROS emissions observed in ATF5 KO muscle, the increased expression and nuclear trafficking of ATF4 could represent the induction of a protective cellular program to counteract mitochondrial dysfunction in the absence of ATF5, resulting in the increased expression of UPR^{mt} targets [63].

Previous research has identified that the expression of UPR^{mt} markers, including chaperones and proteases, is extremely responsive to inducible mitochondrial stressors, in an ATF5-dependent manner [29]. Thus, we sought to investigate whether acute exercise elicits this same effect in skeletal muscle. The exercise conditions that we chose were sufficiently stressful to provoke large increases in blood lactate levels, as well as augment the transcript levels of PGC-1α equally well in both genotypes. These data have been reported by us and others [9,12,13,66], confirming the magnitude of the exercise stress, and additionally indicating that ATF5 is not required for the induction of PGC-1α signaling following acute exercise. However, our results also indicate that acute exercise, either prolonged or exhaustive, is not a sufficient stimulus to mediate an increase in the nuclear localization of ATF5 in WT animals. Thus, despite its relatively low abundance detected in the nuclear fractions, these levels are clearly sufficient to induce an exercise stress response in WT animals, which is absent in KO muscle. This is evident from the markedly divergent exercise-induced changes in mRNA transcripts of the downstream markers mtHSP70, LONP and ClpP. These results coincide with the concept that ATF5 may be part of a team of transcription factors that regulates the basal expression of UPR^{mt} markers [29], but that it is required for normal stress-induced changes in these downstream proteins. Interestingly, digressing

from this collective response is the change in HSP60 gene expression, an established UPR^{mt} chaperone which is clearly extremely responsive to acute exercise. However, these changes occurred in WT animals, and were even more pronounced in the absence of ATF5, suggesting redundancies in the transcriptional regulation of HSP60 during exercise stress that do not obligate the presence of ATF5.

Taken together, our results indicate that the skeletal muscle of ATF5 KO animals exhibits 1) enhanced basal and acute exercise-induced stress signaling, 2) increased basal expression of UPR^{mt} proteins, PGC-1α and ATF4, 3) a more abundant mitochondrial pool, with reduced mitochondrial function, and 4) an altered gene expression response of UPR^{mt} downstream targets to acute exercise. Further investigation is required to understand the potential role of ATF5 in mediating changes in mitochondrial degradation via the mitophagy pathway in order to preserve the health of the muscle mitochondrial pool.

ACKNOWLEDGEMENTS

This work was supported by funding from the Natural Sciences and Engineering Research Council of Canada (NSERC) to D.A. Hood. D.A. Hood is also the holder of a Canada Research Chair in Cell Physiology.

REFERENCES

[1] P.J. Adhihetty, M.F.N. O'Leary, D.A. Hood, Mitochondria in skeletal muscle: adaptable rheostats of apoptotic susceptibility, Exerc. Sport Sci. Rev. 36 (2008) 116–121. https://doi.org/10.1097/JES.0b013e31817be7b7.

[2] D.A. Hood, I. Irrcher, V. Ljubicic, A.-M. Joseph, Coordination of metabolic plasticity in skeletal muscle, J. Exp. Biol. 209 (2006) 2265–2275. https://doi.org/10.1242/jeb.02182.

[3] D.A. Hood, L.D. Tryon, H.N. Carter, Y. Kim, C.C.W. Chen, Unravelling the mechanisms regulating muscle mitochondrial biogenesis, Biochem. J. 473 (2016) 2295–2314. https://doi.org/10.1042/BCJ20160009.

[4] R.A. Jacobs, D. Flück, T.C. Bonne, S. Bürgi, P.M. Christensen, M. Toigo, C. Lundby, Improvements in exercise performance with high-intensity interval training coincide with an increase in skeletal muscle mitochondrial content and function, J. Appl. Physiol. Bethesda Md 1985. 115 (2013) 785–793. https://doi.org/10.1152/japplphysiol.00445.2013.

[5] J.A. Calvo, T.G. Daniels, X. Wang, A. Paul, J. Lin, B.M. Spiegelman, S.C. Stevenson, S.M. Rangwala, Muscle-specific expression of PPARgamma coactivator-1alpha improves exercise performance and increases peak oxygen uptake, J. Appl. Physiol. Bethesda Md 1985. 104 (2008) 1304–1312. https://doi.org/10.1152/japplphysiol.01231.2007.

[6] J.O. Holloszy, Biochemical Adaptations in Muscle, J. Biol. Chem. 242 (1967) 2278–2282. https://doi.org/10.1016/S0021-9258(18)96046-1.

[7] C.C.W. Chen, A.T. Erlich, D.A. Hood, Role of Parkin and endurance training on mitochondrial turnover in skeletal muscle, Skelet. Muscle. 8 (2018) 10. https://doi.org/10.1186/s13395-018-0157-y.

[8] Y. Dun, S. Liu, W. Zhang, M. Xie, L. Qiu, Exercise Combined with Rhodiola sacra Supplementation Improves Exercise Capacity and Ameliorates Exhaustive Exercise-Induced Muscle Damage through Enhancement of Mitochondrial Quality Control, Oxid. Med. Cell. Longev. 2017 (2017) e8024857. https://doi.org/10.1155/2017/8024857.

[9] K. Beyfuss, A.T. Erlich, M. Triolo, D.A. Hood, The Role of p53 in Determining Mitochondrial Adaptations to Endurance Training in Skeletal Muscle, Sci. Rep. 8 (2018) 14710. https://doi.org/10.1038/s41598-018-32887-0.

[10] T. Akimoto, S.C. Pohnert, P. Li, M. Zhang, C. Gumbs, P.B. Rosenberg, R.S. Williams, Z. Yan, Exercise stimulates Pgc-1alpha transcription in skeletal muscle through activation of the p38 MAPK pathway, J. Biol. Chem. 280 (2005) 19587–19593. https://doi.org/10.1074/jbc.M408862200.

[11] N. Brandt, T.P. Gunnarsson, M. Hostrup, J. Tybirk, L. Nybo, H. Pilegaard, J. Bangsbo, Impact of adrenaline and metabolic stress on exercise-induced intracellular signaling and PGC-1α mRNA response in human skeletal muscle, Physiol. Rep. 4 (2016) e12844. https://doi.org/10.14814/phy2.12844.

[12] H. Pilegaard, B. Saltin, P.D. Neufer, Exercise induces transient transcriptional activation of the PGC-1alpha gene in human skeletal muscle, J. Physiol. 546 (2003) 851–858. https://doi.org/10.1113/jphysiol.2002.034850.

[13] A. Vainshtein, L.D. Tryon, M. Pauly, D.A. Hood, Role of PGC-1α during acute exercise-induced autophagy and mitophagy in skeletal muscle, Am. J. Physiol. Cell Physiol. 308 (2015) C710-719. https://doi.org/10.1152/ajpcell.00380.2014.

[14] D.A. Hood, P.J. Adhihetty, M. Colavecchia, J.W. Gordon, I. Irrcher, A.-M. Joseph, S.T. Lowe, A.A. Rungi, Mitochondrial biogenesis and the role of the protein import pathway, Med. Sci. Sports Exerc. 35 (2003) 86–94. https://doi.org/10.1097/00005768-200301000-00015.

[15] D.A. Hood, A.-M. Joseph, Mitochondrial assembly: protein import, Proc. Nutr. Soc. 63 (2004) 293–300. https://doi.org/10.1079/PNS2004342.

[16] N.J. Hoogenraad, M.T. Ryan, Translocation of proteins into mitochondria, IUBMB Life. 51 (2001) 345–350. https://doi.org/10.1080/152165401753366096.

[17] I. Garcia, E. Jones, M. Ramos, W. Innis-Whitehouse, R. Gilkerson, The little big genome: the organization of mitochondrial DNA, Front. Biosci. Landmark Ed. 22 (2017) 710–721.

[18] V. Romanello, M. Sandri, The connection between the dynamic remodeling of the mitochondrial network and the regulation of muscle mass, Cell. Mol. Life Sci. CMLS. 78 (2021) 1305–1328. https://doi.org/10.1007/s00018-020-03662-0.

[19] A.N. Oliveira, D.A. Hood, Effect of Tim23 knockdown in vivo on mitochondrial protein import and retrograde signaling to the UPRmt in muscle, Am. J. Physiol. Cell Physiol. 315 (2018) C516–C526. https://doi.org/10.1152/ajpcell.00275.2017.

[20] C.M. Haynes, D. Ron, The mitochondrial UPR – protecting organelle protein homeostasis, J. Cell Sci. 123 (2010) 3849–3855. https://doi.org/10.1242/jcs.075119.

[21] V. Jovaisaite, J. Auwerx, The mitochondrial unfolded protein response - synchronizing genomes, Curr. Opin. Cell Biol. 33 (2015) 74–81. https://doi.org/10.1016/j.ceb.2014.12.003.

[22] C.J. Fiorese, C.M. Haynes, Integrating the UPRmt into the Mitochondrial Maintenance Network, Crit. Rev. Biochem. Mol. Biol. 52 (2017) 304–313. https://doi.org/10.1080/10409238.2017.1291577.

[23] N. Anderson, C.M. Haynes, Folding the Mitochondrial UPR into the Integrated Stress Response, Trends Cell Biol. 30 (2020) 428–439. https://doi.org/10.1016/j.tcb.2020.03.001.

[24] A. Melber, C.M. Haynes, UPRmt regulation and output: a stress response mediated by mitochondrial-nuclear communication, Cell Res. 28 (2018) 281–295. https://doi.org/10.1038/cr.2018.16.

[25] D. Ron, P. Walter, Signal integration in the endoplasmic reticulum unfolded protein response, Nat. Rev. Mol. Cell Biol. 8 (2007) 519–529. https://doi.org/10.1038/nrm2199.

[26] Q. Zhao, J. Wang, I.V. Levichkin, S. Stasinopoulos, M.T. Ryan, N.J. Hoogenraad, A mitochondrial specific stress response in mammalian cells, EMBO J. 21 (2002) 4411–4419. https://doi.org/10.1093/emboj/cdf445.

[27] J.E. Aldridge, T. Horibe, N.J. Hoogenraad, Discovery of Genes Activated by the Mitochondrial Unfolded Protein Response (mtUPR) and Cognate Promoter Elements, PLOS ONE. 2 (2007) e874. https://doi.org/10.1371/journal.pone.0000874.

[28] R.D. Martinus, G.P. Garth, T.L. Webster, P. Cartwright, D.J. Naylor, P.B. Høj, N.J. Hoogenraad, Selective induction of mitochondrial chaperones in response to loss of the mitochondrial genome, Eur. J. Biochem. 240 (1996) 98–103. https://doi.org/10.1111/j.1432-1033.1996.0098h.x.

[29] C.J. Fiorese, A.M. Schulz, Y.-F. Lin, N. Rosin, M.W. Pellegrino, C.M. Haynes, The Transcription Factor ATF5 Mediates a Mammalian Mitochondrial UPR, Curr. Biol. CB. 26 (2016) 2037–2043. https://doi.org/10.1016/j.cub.2016.06.002.

[30] M.B. Hansen, C. Mitchelmore, K.M. Kjaerulff, T.E. Rasmussen, K.M. Pedersen, N.A. Jensen, Mouse Atf5: molecular cloning of two novel mRNAs, genomic organization, and odorant sensory neuron localization, Genomics. 80 (2002) 344–350. https://doi.org/10.1006/geno.2002.6838.

[31] L.A. Greene, H.Y. Lee, J.M. Angelastro, The Transcription Factor ATF5: Role In Neurodevelopment And Neural Tumors, J. Neurochem. 108 (2009) 11–22. https://doi.org/10.1111/j.1471-4159.2008.05749.x.

[32] J. Al Sarraj, C. Vinson, G. Thiel, Regulation of asparagine synthetase gene transcription by the basic region leucine zipper transcription factors ATF5 and CHOP, Biol. Chem. 386 (2005) 873–879. https://doi.org/10.1515/BC.2005.102.

[33] T. Yamazaki, A. Ohmi, H. Kurumaya, K. Kato, T. Abe, H. Yamamoto, N. Nakanishi, R. Okuyama, M. Umemura, T. Kaise, R. Watanabe, Y. Okawa, S. Takahashi, Y. Takahashi, Regulation of the human CHOP gene promoter by the stress response transcription factor ATF5 via the AARE1 site in human hepatoma HepG2 cells, Life Sci. 87 (2010) 294–301. https://doi.org/10.1016/j.lfs.2010.07.006.

[34] Y.I. Shimizu, M. Morita, A. Ohmi, S. Aoyagi, H. Ebihara, D. Tonaki, Y. Horino, M. Iijima, H. Hirose, S. Takahashi, Y. Takahashi, Fasting induced up-regulation of activating transcription factor 5 in mouse liver, Life Sci. 84 (2009) 894–902. https://doi.org/10.1016/j.lfs.2009.04.002.

[35] C. Lai, J. Zhang, Z. Tan, L.F. Shen, R.R. Zhou, Y.Y. Zhang, Maf1 suppression of ATF5-dependent mitochondrial unfolded protein response contributes to rapamycin-induced radio-sensitivity in lung cancer cell line A549, Aging. 13 (2021) 7300–7313. https://doi.org/10.18632/aging.202584.

[36] X. Sun, J.M. Angelastro, D. Merino, Q. Zhou, M.D. Siegelin, L.A. Greene, Dominant-negative ATF5 rapidly depletes survivin in tumor cells, Cell Death Dis. 10 (2019) 709. https://doi.org/10.1038/s41419-019-1872-y.

[37] D. Hu, Z. Liu, X. Qi, UPRmt activation protects against MPP+-induced toxicity in a cell culture model of Parkinson's disease, Biochem. Biophys. Res. Commun. 569 (2021) 17–22. https://doi.org/10.1016/j.bbrc.2021.06.079.

[38] I.H. Hernández, J. Torres-Peraza, M. Santos-Galindo, E. Ramos-Morón, M.R. Fernández-Fernández, M.J. Pérez-Álvarez, A. Miranda-Vizuete, J.J. Lucas, The neuroprotective transcription factor ATF5 is decreased and sequestered into polyglutamine inclusions in Huntington's disease, Acta Neuropathol. (Berl.). 134 (2017) 839–850. https://doi.org/10.1007/s00401-017-1770-2.

[39] R.P. Dalton, D.B. Lyons, S. Lomvardas, Co-opting the unfolded protein response to elicit olfactory receptor feedback, Cell. 155 (2013) 321–332. https://doi.org/10.1016/j.cell.2013.09.033.

[40] D. Brown, K. Ryan, Z. Daniel, M. Mareko, R. Talbot, J. Moreton, T.C.B. Giles, R. Emes, C. Hodgman, T. Parr, J.M. Brameld, The Beta-adrenergic agonist, Ractopamine, increases skeletal muscle expression of Asparagine Synthetase as part of an integrated stress response gene program, Sci. Rep. 8 (2018) 15915. https://doi.org/10.1038/s41598-018-34315-9.

[41] S. Forsström, C.B. Jackson, C.J. Carroll, M. Kuronen, E. Pirinen, S. Pradhan, A. Marmyleva, M. Auranen, I.-M. Kleine, N.A. Khan, A. Roivainen, P. Marjamäki, H. Liljenbäck, L. Wang, B.J. Battersby, U. Richter, V. Velagapudi, J. Nikkanen, L. Euro, A. Suomalainen, Fibroblast Growth Factor 21 Drives Dynamics of Local and Systemic Stress Responses in Mitochondrial Myopathy with mtDNA Deletions, Cell Metab. 30 (2019) 1040-1054.e7. https://doi.org/10.1016/j.cmet.2019.08.019.

[42] M.C. Brearley, C. Li, Z.C.T.R. Daniel, P.T. Loughna, T. Parr, J.M. Brameld, Changes in expression of serine biosynthesis and integrated stress response genes during myogenic differentiation of C2C12 cells, Biochem. Biophys. Rep. 20 (2019) 100694. https://doi.org/10.1016/j.bbrep.2019.100694.

[43] B. Zhang, Y. Tan, Z. Zhang, P. Feng, W. Ding, Q. Wang, H. Liang, W. Duan, X. Wang, S. Yu, J. Liu, D. Yi, Y. Sun, W. Yi, Novel PGC-1α/ATF5 Axis Partly Activates UPRmt and Mediates Cardioprotective Role of Tetrahydrocurcumin in Pathological Cardiac Hypertrophy, Oxid. Med. Cell. Longev. 2020 (2020) 9187065. https://doi.org/10.1155/2020/9187065.

[44] Y.T. Wang, Y. Lim, M.N. McCall, K.-T. Huang, C.M. Haynes, K. Nehrke, P.S. Brookes, Cardioprotection by the mitochondrial unfolded protein response requires ATF5, Am. J. Physiol. Heart Circ. Physiol. 317 (2019) H472–H478. https://doi.org/10.1152/ajpheart.00244.2019.

[45] I. Smyrnias, S.P. Gray, D.O. Okonko, G. Sawyer, A. Zoccarato, N. Catibog, B. López, A. González, S. Ravassa, J. Díez, A.M. Shah, Cardioprotective Effect of the Mitochondrial Unfolded Protein Response During Chronic Pressure Overload, J. Am. Coll. Cardiol. 73 (2019) 1795–1806. https://doi.org/10.1016/j.jacc.2018.12.087.

[46] J.M. Memme, A.N. Oliveira, D.A. Hood, Chronology of UPR activation in skeletal muscle adaptations to chronic contractile activity, Am. J. Physiol. - Cell Physiol. 310 (2016) C1024–C1036. https://doi.org/10.1152/ajpcell.00009.2016.

[47] J. Wu, J.L. Ruas, J.L. Estall, K.A. Rasbach, J.H. Choi, L. Ye, P. Boström, H.M. Tyra, R.W. Crawford, K.P. Campbell, D.T. Rutkowski, R.J. Kaufman, B.M. Spiegelman, The unfolded protein response mediates adaptation to exercise in skeletal muscle through a PGC-1α /ATF6α complex, Cell Metab. 13 (2011) 160–169. https://doi.org/10.1016/j.cmet.2011.01.003.

[48] A.V. Cordeiro, R.S. Brícola, R.R. Braga, L. Lenhare, V.R.R. Silva, C.P. Anaruma, C.K. Katashima, B.M. Crisol, F.M. Simabuco, A.S.R. Silva, D.E. Cintra, L.P. Moura, J.R. Pauli, E.R. Ropelle, Aerobic Exercise Training Induces the Mitonuclear Imbalance and UPRmt in the Skeletal Muscle of Aged Mice, J. Gerontol. A. Biol. Sci. Med. Sci. 75 (2020) 2258–2261. https://doi.org/10.1093/gerona/glaa059.

[49] M. Umemura, Y. Kaneko, R. Tanabe, Y. Takahashi, ATF5 deficiency causes abnormal cortical development, Sci. Rep. 11 (2021) 7295. https://doi.org/10.1038/s41598-021-86442-5.

[50] A. Vainshtein, L. Kazak, D. Hood, Effects of endurance training on apoptotic susceptibility in striated muscle, J. Appl. Physiol. Bethesda Md 1985. 110 (2011) 1638–45. https://doi.org/10.1152/japplphysiol.00020.2011.

[51] K.J. Menzies, K. Singh, A. Saleem, D.A. Hood, Sirtuin 1-mediated effects of exercise and resveratrol on mitochondrial biogenesis, J. Biol. Chem. 288 (2013) 6968–6979. https://doi.org/10.1074/jbc.M112.431155.

[52] S. Callegari, S. Dennerlein, Sensing the Stress: A Role for the UPRmt and UPRam in the Quality Control of Mitochondria, Front. Cell Dev. Biol. 6 (2018) 31. https://doi.org/10.3389/fcell.2018.00031.

[53] M.T. Ryan, N.J. Hoogenraad, Mitochondrial-Nuclear Communications, Annu. Rev. Biochem. 76 (2007) 701–722. https://doi.org/10.1146/annurev.biochem.76.052305.091720.

[54] A.M. Nargund, M.W. Pellegrino, C.J. Fiorese, B.M. Baker, C.M. Haynes, Mitochondrial import efficiency of ATFS-1 regulates mitochondrial UPR activation, Science. 337 (2012) 587–590. https://doi.org/10.1126/science.1223560.

[55] D.A. Hood, L.D. Tryon, A. Vainshtein, J. Memme, C. Chen, M. Pauly, M.J. Crilly, H. Carter, Exercise and the Regulation of Mitochondrial Turnover, Prog. Mol. Biol. Transl. Sci. 135 (2015) 99–127. https://doi.org/10.1016/bs.pmbts.2015.07.007.

[56] Y. Wang, H. Jasper, S. Toan, D. Muid, X. Chang, H. Zhou, Mitophagy coordinates the mitochondrial unfolded protein response to attenuate inflammation-mediated myocardial injury, Redox Biol. 45 (2021) 102049. https://doi.org/10.1016/j.redox.2021.102049.

[57] L.J. Goodyear, P.Y. Chang, D.J. Sherwood, S.D. Dufresne, D.E. Moller, Effects of exercise and insulin on mitogen-activated protein kinase signaling pathways in rat skeletal muscle, Am. J. Physiol. 271 (1996) E403-408. https://doi.org/10.1152/ajpendo.1996.271.2.E403.

[58] M. Whitham, M.H.S. Chan, M. Pal, V.B. Matthews, O. Prelovsek, S. Lunke, A. El-Osta, H. Broenneke, J. Alber, J.C. Brüning, F.T. Wunderlich, G.I. Lancaster, M.A. Febbraio, Contraction-induced interleukin-6 gene transcription in skeletal muscle is regulated by c-Jun terminal kinase/activator protein-1, J. Biol. Chem. 287 (2012) 10771–10779. https://doi.org/10.1074/jbc.M111.310581.

[59] H. Enslen, H. Tokumitsu, P.J. Stork, R.J. Davis, T.R. Soderling, Regulation of mitogen-activated protein kinases by a calcium/calmodulin-dependent protein kinase cascade, Proc. Natl. Acad. Sci. 93 (1996) 10803–10808. https://doi.org/10.1073/pnas.93.20.10803.

[60] Y. Wang, E. Yamada, H. Zong, J.E. Pessin, Fyn Activation of mTORC1 Stimulates the IRE1α-JNK Pathway, Leading to Cell Death *, J. Biol. Chem. 290 (2015) 24772–24783. https://doi.org/10.1074/jbc.M115.687020.

[61] S. Damiano, E. Muscariello, G. La Rosa, M. Di Maro, P. Mondola, M. Santillo, Dual Role of Reactive Oxygen Species in Muscle Function: Can Antioxidant Dietary Supplements Counteract Age-Related Sarcopenia?, Int. J. Mol. Sci. 20 (2019) 3815. https://doi.org/10.3390/ijms20153815.

[62] J. Han, S.H. Back, J. Hur, Y.-H. Lin, R. Gildersleeve, J. Shan, C.L. Yuan, D. Krokowski, S. Wang, M. Hatzoglou, M.S. Kilberg, M.A. Sartor, R.J. Kaufman, ER-stress-induced transcriptional regulation increases protein synthesis leading to cell death, Nat. Cell Biol. 15 (2013) 481–490. https://doi.org/10.1038/ncb2738.

[63] D. Jiang, H. Cui, N. Xie, S. Banerjee, R.-M. Liu, H. Dai, V.J. Thannickal, G. Liu, ATF4 Mediates Mitochondrial Unfolded Protein Response in Alveolar Epithelial Cells, Am. J. Respir. Cell Mol. Biol. 63 (2020) 478–489. https://doi.org/10.1165/rcmb.2020-0107OC.

[64] Multi-omics analysis identifies ATF4 as a key regulator of the mitochondrial stress response in mammals | Journal of Cell Biology | Rockefeller University Press, (n.d.). https://rupress.org/jcb/article/216/7/2027/39040/Multi-omics-analysis-identifies-ATF4-as-a-key (accessed July 2, 2021).

[65] B.F. Teske, M.E. Fusakio, D. Zhou, J. Shan, J.N. McClintick, M.S. Kilberg, R.C. Wek, CHOP induces activating transcription factor 5 (ATF5) to trigger apoptosis in response to perturbations in protein homeostasis, Mol. Biol. Cell. 24 (2013) 2477–2490. https://doi.org/10.1091/mbc.E13-01-0067.

[66] A.T. Erlich, D.M. Brownlee, K. Beyfuss, D.A. Hood, Exercise induces TFEB expression and activity in skeletal muscle in a PGC-1α-dependent manner, Am. J. Physiol. Cell Physiol. 314 (2018) C62–C72. https://doi.org/10.1152/ajpcell.00162.2017.

FUTURE DIRECTIONS

1. Given the role of ATF5 in mediating the UPR^{mt} mRNA response to acute exercise, it is worth investigating whether ATF5 and UPR^{mt} activation are required for mitochondrial adaptations to a chronic endurance training protocol. These adaptations include mitochondrial biogenesis, slight improvements in organellar quality, and improved mitophagic signaling. Furthermore, it is worthwhile to examine the response of trained muscle in WT and ATF5 KO animals to an acute bout of exercise, as trained muscle tends to present an attenuated gene expression response to acute exercise. This would characterize the involvement of ATF5 in the muscular adaptations to training and whether UPR^{mt} activation is required in conferring resistance to exercise stress during subsequent exercise bouts. Colchicine injections can also be employed to measure autophagy flux. This project can additionally be carried out in a cell model, employing a long-term chronic contractile activity (CCA) protocol in myotubes expressing an ATF5 siRNA and bafilomycin treatment to assess flux.
2. In contrast to knocking out ATF5, the impact of its overexpression and enhanced UPR^{mt} activation on the level of mitochondrial adaptations to chronic exercise can also be assessed. This can be carried out by virally overexpressing ATF5 in animals and cells, and treating animals with the NAD^+ precursor Nicotinamide Riboside (NR) or conversely, PARP inhibitors, to increase muscular NAD+ pools, known inducers of the UPR^{mt}. The effects of ATF5 overexpression can be assessed on UPR^{mt} activation, mitochondrial biogenesis, autophagy/mitophagy, protein synthesis and apoptotic susceptibility of mitochondria.

3. Our data showed a significant increase in ATF4 gene expression and its nuclear localization in the muscle of ATF5 KO animals. This is indicative of either a compensatory mechanism in an attempt to induce the expression of UPR^{mt} targets basally and in response to acute exercise in the absence of ATF5, or, suggestive of ATF5 being a negative regulator of ATF4 and suppressing its cellular expression. As our lab is also breeding ATF4 KO (-/-) animals, double KO (dKO) animals can be bred to yield mice colonies lacking the expression of both ATF5 and ATF4. Establishing a robust deficiency in the UPR^{mt} without both transcription factors will allow us to determine whether their mutual interaction is required for UPR^{mt} activation and mitochondrial adaptations to training.
4. Taking a more mechanistic approach, investigating the molecular mechanisms responsible for the cellular localization of ATF5 and downstream UPR^{mt} activation during various forms of mitochondrial stress are of great interest. From what has been observed in mammalian cells, multiple mitochondrial stressors can induce the proteolytic activity of ClpP to cause the transport of peptides into the cytosol. This stress-induced peptide efflux is thought to be the mechanism responsible for inhibiting the mitochondrial import of ATF5, prompting its subsequent nuclear trafficking. Manipulating mitochondrial protein import by either using a Tim23-KD model previously used in our lab, or a small-molecule inhibitor of import, can be used to identify whether blocked import truly induces the nuclear translocation of ATF5, its binding to the promoters of target UPR^{mt} genes and their transcription. Inducing multiple forms of mitochondrial stress will also allow us to assess how different forms of mitochondrial dysfunction and proteotoxicity can influence the intracellular movement of ATF5 and UPR^{mt} activation on mitochondrial function. ETC inhibitors, including oligomycin and rotenone can be used to induce organellar

dysfunction, and transfecting cells with a mutated form of MPP (mitochondrial-processing peptidase), the enzyme responsible for cleavage of presequences from imported proteins in the matrix, can be employed to cause the accumulation of precursor proteins and induce proteotoxicity. These observations could contribute greatly to the characterization of the UPR^{mt} pathways in response to stress in muscle.

APPENDIX A: DATA AND STATISTICAL ANALYSIS

Table 1A. Animal body weights.

	Body weight (g)	
N	WT	KO
1	35.5	27
2	45	26.4
3	45	34.75
4	38	29.27
5	39.2	29.3
6	37.3	24.6
7	34.7	39.13
8	45.42	31.93
9	38.13	23.2
10	41.2	36.2
11	41.3	25.6
12	44.9	23.7
13	41.6	22.4
14	38.1	32.18
15	36.8	47.8
16	42.6	43.34
17	42.2	35.5
18	39.3	28.8
19		27.3
20		35.5
21		25.6
22		33.7
23		36.7
24		25.7
25		44.1
26		30.6
27		35.6
X	40.34722222	31.7
SEM	0.824816559	1.297040901

UNPAIRED T-TEST: Body weight	
P value	<0.0001
P value summary	****
Significantly different (P < 0.05)?	Yes

Table 1B. TA weights/Body weights.

	TA weights/Body weights (mg/g)	
N	WT	KO
1	1.262	1.226
2	1.111	1.402
3	1.053	1.071
4	0.934	1.151
5	1.156	1.072
6	1.075	1.492
7	1.349	0.767
8	1.004	0.626
9	1.191	1.560
10	1.002	1.166
11	1.194	1.352
12	1.096	1.308
13	1.195	1.304
14	1.381	0.929
15	1.590	0.933
16	1.080	0.754
17	1.187	1.290
18	1.300	1.267
19		1.414
20		1.223
21		1.301
22		1.377
23		1.180
24		1.790
25		1.154
26		1.301
X	1.17548718	1.207999476
SEM	0.038589784	0.050500178

UNPAIRED T-TEST: TA weights/Body weights	
P value	0.6369
P value summary	ns
Significantly different (P < 0.05)?	No

Table 1C. Distance to exhaustion during the incremental, exhaustive exercise test.

	Distance to exhaustion (m)	
N	WT	KO
1	1740	453
2	1151	507
3	1398	2238
4	534	534
5		857
6		2784
7		1255
X	1205.75	1232.571429
SEM	254.3994153	351.2413942

UNPAIRED T-TEST: Distance to exhaustion	
P value	0.9592
P value summary	ns
Significantly different (P < 0.05)?	No

Table 1D. Blood lactate levels before and immediately after exhaustive exercise.

	Blood lactate (mmol/L)			
	WT		KO	
N	CON	EX	CON	EX
1	3	11.5	2	20.2
2	2.5	10	2	8.7
3	4.2	6.9	1.9	8.3
4	2.1	13.1	2.6	8.7
5	2.9		1.1	8.3
6	3		3	3.8
7	2.9		2.9	7.5
8	2.3		1.7	
9	1.8		1.8	
10	1.8		2.7	
11	1.8		1.7	
12			4.8	
13			3.6	
X	2.572727273	10.375	2.44615385	9.35714286
SEM	0.219954916	1.319958964	0.27165575	1.92104351

2-WAY ANOVA			
Source of Variation	P value	P value summary	Significant?
Interaction	0.6365	ns	No
Genotype	0.5444	ns	No
Exercise	<0.0001	****	Yes

POST-HOC TEST				
Bonferroni	Mean Difference	Significant?	Summary	Adjusted P Value
WT:CON vs. WT:EX	-7.802	Yes	****	<0.0001
WT:CON vs. KO:CON	0.1266	No	ns	>0.9999
WT:CON vs. KO:EX	-6.784	Yes	****	<0.0001
WT:EX vs. KO:CON	7.929	Yes	****	<0.0001
WT:EX vs. KO:EX	1.018	No	ns	>0.9999
KO:CON vs. KO:EX	-6.911	Yes	****	<0.0001

Table 2A. Phosphorylated/total eIF2α protein levels following acute continuous and exhaustive exercise.

	Phospho/total eIF2α Protein (A.U.) - Cont. EX			
	WT		KO	
N	CON	EX	CON	EX
1	1.006	1.089	0.707	0.676
2	0.877	0.908	0.511	1.231
3	0.883	1.903	0.716	1.230
4	1.167	0.970	0.665	0.755
5	0.835	1.343	0.652	1.091
6	1.479		1.359	
7	1.291		1.453	
8	1.221		1.530	
9			0.814	
10			0.599	
11			0.861	
12			0.658	
X	1.09491934	1.24227465	0.87694682	0.99661858
SEM	0.08188344	0.18110541	0.10313517	0.11815426

2-WAY ANOVA			
Source of Variation	P value	P value summary	Significant?
Interaction	0.9134	ns	No
Genotype	0.0773	ns	No
Exercise	0.2991	ns	No

UNPAIRED T-TEST: WT CON vs. KO CON	
P value	0.1462
P value summary	ns
Significantly different (P < 0.05)?	No

	Phospho/total eIF2α Protein (A.U.) - Exh. EX			
	WT		KO	
N	CON	EX	CON	EX
1	1.006	1.374	0.707	0.957
2	0.877	1.373	0.511	4.112
3	0.883	1.184	0.716	2.768
4	1.167		0.665	1.223
5	0.835		0.652	0.790
6	1.479		1.359	0.845
7	1.291		1.453	0.774
8	1.221		1.530	
9			0.814	
10			0.599	
11			0.861	
12			0.658	
X	1.09491934	1.31057806	0.87694682	1.63862248
SEM	0.08188344	0.06314768	0.10313517	0.49105312

2-WAY ANOVA			
Source of Variation	P value	P value summary	Significant?
Interaction	0.3389	ns	No
Genotype	0.8458	ns	No
Exercise	0.093	ns	No

UNPAIRED T-TEST: WT CON vs. WT EX	
P value	0.1648
P value summary	ns
Significantly different (P < 0.05)?	No

UNPAIRED T-TEST: KO CON vs. KO EX	
P value	0.0686
P value summary	ns
Significantly different (P < 0.05)?	No

Table 2B. Phosphorylated/total JNK protein levels following acute continuous and exhaustive exercise.

	Phospho/total JNK Protein (A.U.) - Cont. EX			
	WT		KO	
N	CON	EX	CON	EX
1	0.626	1.511	1.060	1.770
2	0.495	0.534	0.711	1.784
3	0.568	1.674	4.449	9.637
4	0.934	2.393	1.865	5.008
5	0.866	2.026	1.423	10.025
6	3.370		1.938	
7	4.676		12.122	
8	4.117		2.634	
9			0.648	
10			5.012	
11			0.793	
12			1.109	
X	1.95666425	1.62762925	2.81368379	5.64491057
SEM	0.62858321	0.31280936	0.94135483	1.80905467

2-WAY ANOVA			
Source of Variation	P value	P value summary	Significant?
Interaction	0.1624	ns	No
Genotype	0.0355	*	Yes
Exercise	0.2654	ns	No

POST-HOC TEST				
Bonferroni	Mean Difference	Significant?	Summary	Adjusted P Value
WT:CON vs. WT:EX	0.329	No	ns	>0.9999
WT:CON vs. KO:CON	-0.857	No	ns	>0.9999
WT:CON vs. KO:EX	-3.688	No	ns	0.1801
WT:EX vs. KO:CON	-1.186	No	ns	>0.9999
WT:EX vs. KO:EX	-4.017	No	ns	0.1972
KO:CON vs. KO:EX	-2.831	No	ns	0.422

	Phospho/total JNK Protein (A.U.) - Exh. EX			
	WT		KO	
N	CON	EX	CON	EX
1	0.626	4.669	1.060	11.380
2	0.495	3.741	0.711	4.590
3	0.568	5.208	4.449	10.091
4	0.934		1.865	1.538
5	0.866		1.423	3.447
6	3.370		1.938	3.205
7	4.676		12.122	
8	4.117		2.634	
9			0.648	
10			5.012	
11			0.793	
12			1.109	
X	1.95666425	4.53970439	2.81368379	5.70847872
SEM	0.62858321	0.42841634	0.94135483	1.64710959

2-WAY ANOVA			
Source of Variation	P value	P value summary	Significant?
Interaction	0.902	ns	No
Genotype	0.4264	ns	No
Exercise	0.0384	*	Yes

POST-HOC TEST				
Bonferroni	Mean Difference	Significant?	Summary	Adjusted P Value
WT:CON vs. WT:EX	-2.583	No	ns	>0.9999
WT:CON vs. KO:CON	-0.857	No	ns	>0.9999
WT:CON vs. KO:EX	-3.752	No	ns	0.1678
WT:EX vs. KO:CON	1.726	No	ns	>0.9999
WT:EX vs. KO:EX	-1.169	No	ns	>0.9999
KO:CON vs. KO:EX	-2.895	No	ns	0.3789

UNPAIRED T-TEST: WT CON vs. WT EX	
P value	0.1648
P value summary	ns
Significantly different (P < 0.05)?	No

UNPAIRED T-TEST: KO CON vs. KO EX	
P value	0.1196
P value summary	ns
Significantly different (P < 0.05)?	No

Table 3A. Protein levels of PGC-1α in nuclear and cytosolic fractions basally and after exhaustive exercise in WT and KO mice.

	PGC-1α Protein (A.U.)							
	WT				KO			
	CON		EX		CON		EX	
N	Nuc	Cyto	Nuc	Cyto	Nuc	Cyto	Nuc	Cyto
1	0.025	1.716	0.041	1.458	0.118	1.661	0.041	1.748
2	0.046	1.703	0.030	2.310	0.049	2.173	0.035	2.486
3	0.032	1.456	0.035	1.481	0.090	2.048	0.062	2.497
4	0.063	2.622	0.063	2.275	0.254	2.329	0.650	3.483
5	0.027	1.738			0.110	2.350	0.086	3.928
6	0.078	2.729			0.066	4.553	0.117	4.477
7	0.105	3.140						
8	0.070	1.619						
9	0.046	0.319						
X	0.054508625	1.893372079	0.042195084	1.88094651	0.114330573	2.519016607	0.165120444	3.103323917
SEM	0.008935599	0.279435509	0.007222829	0.237704494	0.029850836	0.419530958	0.097715366	0.420207516

2-WAY ANOVA: PGC-1α Nuclear Protein			
Source of Variation	P value	P value summary	Significant?
Interaction	0.5459	ns	No
Genotype	0.0899	ns	No
Exercise	0.7119	ns	No

2-WAY ANOVA: PGC-1α Cytosolic Protein			
Source of Variation	P value	P value summary	Significant?
Interaction	0.4334	ns	No
Genotype	0.022	*	Yes
Exercise	0.4525	ns	No

POST-HOC TEST				
Bonferroni	Mean Difference	Significant?	Summary	Adjusted P Value
WT:CON vs. WT:EX	0.01243	No	ns	>0.9999
WT:CON vs. KO:CON	-0.6256	No	ns	>0.9999
WT:CON vs. KO:EX	-1.21	No	ns	0.1093
WT:EX vs. KO:CON	-0.638	No	ns	>0.9999
WT:EX vs. KO:EX	-1.222	No	ns	0.2809
KO:CON vs. KO:EX	-0.5843	No	ns	>0.9999

UNPAIRED T-TEST: PGC-1α Nuclear WT CON vs. KO CON	
P value	0.0408
P value summary	*
Significantly different (P < 0.05)?	Yes

UNPAIRED T-TEST: PGC-1α Nuclear WT EX vs. KO EX	
P value	0.3442
P value summary	ns
Significantly different (P < 0.05)?	No

UNPAIRED T-TEST: PGC-1α Cytosolic WT CON vs. KO CON	
P value	0.2174
P value summary	ns
Significantly different (P < 0.05)?	No

UNPAIRED T-TEST: PGC-1α Cytosolic WT EX vs. KO EX	
P value	0.0598
P value summary	ns
Significantly different (P < 0.05)?	No

Table 3B. % nuclear PGC-1α protein basally and after exhaustive exercise in WT and KO mice.

	PGC-1α % nuclear protein			
	WT		KO	
N	CON	EX	CON	EX
1	1.439	2.754	6.640	2.299
2	2.615	1.263	2.185	1.384
3	2.120	2.329	4.218	2.416
4	2.331	2.680	9.823	15.722
5	1.514		4.464	2.142
6	2.770		1.421	2.549
7	3.247			
8	4.139			
9	12.601			
X	3.641895505	2.256371429	4.791794794	4.418736557
SEM	0.249250306	0.343974875	1.25587648	2.26673522

2-WAY ANOVA: PGC-1α % nuclear Protein			
Source of Variation	P value	P value summary	Significant?
Interaction	0.7506	ns	No
Genotype	0.304	ns	No
Exercise	0.5818	ns	No

Table 3C. % nuclear PGC-1α protein basally and after continuous and exhaustive exercise in WT mice.

	PGC-1α % nuclear protein		
N	CON	Cont. EX	Exh. EX
1	1.439	3.848	2.754
2	2.615	4.137	1.263
3	2.120	5.953	2.329
4	2.331	8.141	2.680
5	1.514	12.584	
6	2.770		
7	3.247		
8	4.139		
9	12.601		
X	3.641895505	6.932477372	2.256371429
SEM	1.15409411	1.60766217	0.343974875

1-WAY ANOVA: PGC-1α % nuclear protein	
P value	0.0941
P value summary	ns
Significantly different (P < 0.05)?	No

Table 4A. Protein levels of ATF4 in nuclear and cytosolic fractions basally and after exhaustive exercise in WT and KO mice.

	ATF4 Protein (A.U.)							
	WT				KO			
	CON		EX		CON		EX	
N	Nuc	Cyto	Nuc	Cyto	Nuc	Cyto	Nuc	Cyto
1	0.046	0.198	0.047	0.395	0.101	0.566	0.047	0.166
2	0.039	0.220	0.118	0.565	0.041	0.133	0.043	0.307
3	0.040	0.353	0.057	0.316	0.043	0.185	0.062	0.272
4	0.027	0.159	0.013	0.103	0.225	0.536	0.259	0.363
5	0.017	0.409			0.005	0.111	0.016	0.134
6	0.039	0.449			0.037	0.155	0.044	0.078
7	0.027	0.919						
8	0.021	0.152						
9	0.037	0.384						
X	0.03263364	0.360455578	0.058683984	0.344831503	0.075420883	0.281047785	0.078500898	0.219852266
SEM	0.003267486	0.079291632	0.021913872	0.095733676	0.032429788	0.086153892	0.036643469	0.045123529

2-WAY ANOVA: ATF4 Nuclear Protein			
Source of Variation	P value	P value summary	Significant?
Interaction	0.6564	ns	No
Genotype	0.2324	ns	No
Exercise	0.5732	ns	No

2-WAY ANOVA: ATF4 Cytosolic Protein			
Source of Variation	P value	P value summary	Significant?
Interaction	0.788	ns	No
Genotype	0.2354	ns	No
Exercise	0.6508	ns	No

Table 4B. % nuclear ATF4 protein basally and after exhaustive exercise in WT and KO mice.

	ATF4 % nuclear protein			
	WT		KO	
N	CON	EX	CON	EX
1	4.074	10.697	15.165	22.050
2	8.050	17.291	23.524	12.341
3	2.845	15.164	18.924	18.497
4	18.797	11.040	29.518	41.686
5	14.965		4.550	10.729
6	10.265		19.430	36.021
7	14.451			
8	12.194			
9	8.801			
X	10.493	13.54803006	18.51862546	23.55391819
SEM	1.732406455	1.608187012	3.4322219	5.171220322

2-WAY ANOVA: ATF4 % nuclear Protein			
Source of Variation	P value	P value summary	Significant?
Interaction	0.774	ns	No
Genotype	0.0151	*	Yes
Exercise	0.2482	ns	No

POST-HOC TEST				
Bonferroni	Mean Difference	Significant?	Summary	Adjusted P Value
WT:CON vs. WT:EX	-3.055	No	ns	>0.9999
WT:CON vs. KO:CON	-8.025	No	ns	0.459
WT:CON vs. KO:EX	-13.06	Yes	*	0.038
WT:EX vs. KO:CON	-4.971	No	ns	>0.9999
WT:EX vs. KO:EX	-10.01	No	ns	0.4303
KO:CON vs. KO:EX	-5.035	No	ns	>0.9999

UNPAIRED T-TEST: WT CON vs. KO CON	
P value	0.0386
P value summary	*
Significantly different (P < 0.05)?	Yes

Table 4C. % nuclear ATF4 protein basally and after continuous and exhaustive exercise in WT mice.

	ATF4 % nuclear protein		
N	CON	Cont. EX	Exh. EX
1	4.074	14.367	10.697
2	8.050	9.500	17.291
3	2.845	4.076	15.164
4	18.797	4.646	11.040
5	14.965	9.675	
6	10.265		
7	14.451		
8	12.194		
9	8.801		
X	10.49348072	8.4528568	13.54803006
SEM	1.732406455	1.887047181	1.608187012

1-WAY ANOVA: ATF4 % nuclear protein	
P value	0.2855
P value summary	ns
Significantly different (P < 0.05)?	No

Table 5A. Protein levels of ATF5 in nuclear and cytosolic fractions basally after continuous and exhaustive exercise in WT.

	ATF5 Protein (A.U.)					
	CON		Continuous EX		Exhaustive EX	
N	Nuc	Cyto	Nuc	Cyto	Nuc	Cyto
1	0.011	0.907	0.012	0.860	0.009	1.069
2	0.005	1.269	0.007	1.051	0.012	0.796
3	0.006	1.150	0.007	0.963	0.019	1.247
4	0.012	1.193	0.007	1.194	0.009	1.190
5	0.010	1.247	0.010	1.252		
6	0.023	1.050				
7	0.014	0.752				
8	0.018	0.996				
9	0.011	1.447				
X	0.012269461	1.112406109	0.008508696	1.063992786	0.012462025	1.075483185
SEM	0.001871269	0.069942367	0.001021861	0.072226985	0.00223787	0.10032082

1-WAY ANOVA: ATF5 Nuclear Protein	
P value	0.3317
P value summary	ns
Significantly different (P < 0.05)?	No

1-WAY ANOVA: ATF5 Cytosolic Protein	
P value	0.8935
P value summary	ns
Significantly different (P < 0.05)?	No

Table 5B. % nuclear ATF5 protein basally and after continuous and exhaustive exercise in WT mice.

	ATF5 % nuclear protein		
N	CON	Cont. EX	Exh. EX
1	1.188	1.323	0.867
2	0.415	0.630	1.528
3	0.477	0.692	1.487
4	0.982	0.604	0.777
5	0.823	0.823	
6	2.107		
7	1.887		
8	1.821		
9	0.754		
X	1.161599614	0.814219515	1.164864505
SEM	0.210701615	0.132693632	0.198920362

1-WAY ANOVA: ATF5 % nuclear protein	
P value	0.4605
P value summary	ns
Significantly different (P < 0.05)?	No

Table 6A. Basal protein expression of the mitochondrial protein VDAC in WT and KO muscle.

	VDAC Protein (A.U.)	
N	WT	KO
1	0.789	1.730
2	1.167	1.385
3	0.721	1.305
4	1.178	0.883
5	1.326	1.098
6	1.108	1.299
7	1.035	0.796
8	1.293	1.236
9	1.833	0.438
10	1.662	1.308
11	0.893	0.428
12	0.769	1.171
13	0.852	1.481
14	0.567	1.815
15	0.345	2.282
16	0.971	2.486
17		0.980
18		0.950
19		1.026
20		0.964
21		1.193
22		0.762
X	1.031787681	1.227914432
SEM	0.099037478	0.108664457

UNPAIRED T-TEST	
P value	0.2039
P value summary	ns
Significantly different (P < 0.05)?	No

Table 6B. Basal protein expression of the transcription factor ATF4 in WT and KO muscle.

	ATF4 Protein (A.U.)	
N	WT	KO
1	0.653	1.466
2	0.474	1.299
3	1.659	0.845
4	0.570	0.755
5	0.662	1.172
6	1.386	1.243
7	0.859	0.945
8	1.219	1.501
9	0.717	0.363
10	1.189	0.832
11	0.416	1.324
12	0.660	1.575
13	0.812	0.770
14	1.609	1.104
15	1.210	0.444
16		1.443
17		0.564
18		0.867
19		1.015
20		0.575
21		0.826
22		1.341
X	0.939562477	1.012135045
SEM	0.108704802	0.076494237

UNPAIRED T-TEST	
P value	0.5708
P value summary	ns
Significantly different (P < 0.05)?	No

Table 6C. Basal protein expression of the UPR^{mt} chaperone HSP60 in WT and KO muscle.

	HSP60 Protein (A.U.)	
N	WT	KO
1	1.635	3.974
2	3.301	4.251
3	1.727	3.934
4	2.973	3.342
5	0.972	1.380
6	1.057	1.374
7	1.068	1.730
8	1.129	0.591
9	0.979	1.275
10	0.712	1.476
11	1.401	2.176
12	0.978	1.668
13	0.885	1.245
14	1.506	1.583
15	0.637	1.484
16	1.631	1.247
17		1.425
18		1.563
19		1.322
20		0.902
21		2.061
22		1.465
X	1.411980259	1.88479235
SEM	0.194047076	0.21845425

UNPAIRED T-TEST	
P value	0.1268
P value summary	ns
Significantly different (P < 0.05)?	No

Table 6D. Basal protein expression of the UPR^{mt} chaperone mtHSP70 in WT and KO muscle.

	mtHSP70 Protein (A.U.)	
N	WT	KO
1	0.438	1.038
2	0.712	0.986
3	0.840	0.878
4	0.915	0.521
5	0.822	1.147
6	1.162	1.656
7	1.284	1.693
8	1.398	1.674
9	1.080	0.761
10	0.741	1.508
11	1.469	1.966
12	1.296	1.843
13	0.927	1.359
14	0.983	1.662
15	0.500	1.598
16	0.937	1.177
17		0.981
18		1.163
19		1.029
20		0.721
21		1.370
22		1.090
X	0.969052104	1.264546333
SEM	0.077538251	0.083983605

UNPAIRED T-TEST	
P value	0.0166
P value summary	*
Significantly different (P < 0.05)?	Yes

Table 6E. Basal protein expression of the UPR^{mt} protease LONP in WT and KO muscle.

	LONP Protein (A.U.)	
N	WT	KO
1	0.940	1.010
2	0.789	1.133
3	0.963	0.779
4	0.901	0.719
5	0.616	0.766
6	0.529	0.811
7	0.629	0.774
8	0.699	0.445
9	1.025	0.664
10	0.780	0.756
11	1.125	1.356
12	0.955	1.348
13	0.701	1.218
14	0.894	1.252
15	0.382	1.125
16	0.839	1.152
17		0.999
18		0.984
19		0.905
20		0.625
21		1.140
22		1.702
X	0.797874833	0.984752668
SEM	0.050731629	0.062798147

UNPAIRED T-TEST	
P value	0.0341
P value summary	*
Significantly different (P < 0.05)?	Yes

Table 6F. Fold changes of protein levels (KO/WT).

	Fold Changes				
N	VDAC	ATF4	HSP60	LONP	mtHSP70
1	1.677	1.560	2.814	1.266	1.072
2	1.343	1.383	3.011	1.421	1.018
3	1.265	0.899	2.786	0.976	0.906
4	0.856	0.804	2.367	0.901	0.537
5	1.065	1.247	0.977	0.960	1.184
6	1.259	1.323	0.973	1.016	1.708
7	0.771	1.005	1.226	0.970	1.747
8	1.198	1.598	0.419	0.558	1.727
9	0.424	0.387	0.903	0.833	0.785
10	1.268	0.886	1.045	0.947	1.556
11	0.414	1.409	1.541	1.700	2.029
12	1.135	1.676	1.181	1.689	1.902
13	1.435	0.820	0.881	1.526	1.402
14	1.759	1.174	1.121	1.570	1.715
15	2.211	0.472	1.051	1.410	1.650
16	2.410	1.536	0.883	1.444	1.215
17	0.950	0.601	1.009	1.252	1.012
18	0.920	0.922	1.107	1.234	1.200
19	0.994	1.080	0.936	1.134	1.062
20	0.935	0.612	0.639	0.784	0.744
21	1.156	0.879	1.459	1.429	1.414
22	0.738	1.427	1.038	2.133	1.125
X	1.212	1.07724081	1.33485744	1.234	1.30493121
SEM	0.10779506	0.08141474	0.1547148	0.08055894	0.08666573

Table 7A. COX Activity in WT and KO muscle.

	COX Activity (U/g muscle)	
N	WT	KO
1	22.01	27.28
2	24.71	27.33
3	20.04	27.86
4	22.25	20.45
5	20.38	22.92
6	20.95	25.24
7	22.17	22.62
8	22.75	21.61
9	16.74	24.63
10		23
X	21.33333333	24.294
SEM	0.782965117	0.817872851

UNPAIRED T-TEST	
P value	0.0163
P value summary	*
Significantly different (P < 0.05)?	Yes

Table 7B. Mitochondrial yields from mitochondrial isolations of WT and KO muscle.

	Mitochondrial Yield (mg/g)	
N	WT	KO
1	1.1	2
2	1.32	2.43
3	0.96	1.52
4	1.02	2.11
5	1.14	2.33
6	1.43	2.37
7	1.5	2.19
8	1.53	2.12
9	1.4	2.34
10	1.23	1.9
11	2.03	2.36
12	1.47	2.03
13	2.03	2.36
14	2.2	1.44
15	2.17	1.55
16	2.95	2.23
17	1.79	2.21
18	2.08	2.25
19		2.83
20		1.86
21		1.98
22		1.38
23		1.30
24		2.30
25		1.58
26		1.48
27		2.03
X	1.630555556	2.017193681
SEM	0.126852971	0.074572175

UNPAIRED T-TEST	
P value	0.0067
P value summary	**
Significantly different (P < 0.05)?	Yes

Table 8A. Respiration of SS mitochondria isolated from WT and KO muscle.

	SS mitochondria: Respiration (natoms O2/mg/min)			
	WT		KO	
N	State IV	State III	State IV	State III
1	14.33	89.69	8.93	18.02
2	9.18	80.28	4.27	35.29
3	9.11	58.98	8.93	23.07
4	9.27	42.08	1.6	18.74
5	10.27	52.61	7.89	27.07
6	9.94	44.5	6.44	5.08
7	8.96	43	5.19	6.63
8	7.61	55.07	3.95	40.58
9	3.68	60.68	2.58	30.81
10	7.58	42.05	4.2	14.04
11	3.67	22.56	3.58	34.67
12	0.66	32.5	3.6	34.18
13	3.82	17.72	3.1	16.93
14	1.26	16.99	0.97	18.66
15	5.55	19.44	0.32	9.71
16	1.23	5.06	1.79	19.97
17	0.6	23.26	1.2	25.49
18	2.19	17.07	3.87	32.63
19			4.64	19.29
20			1.36	21.32
21			3.44	27.33
22			1.78	21.04
23			2.64	37.44
24			3.16	38.67
25			3.88	
26			2.78	
X	6.050555556	40.19666667	3.695769231	24.0275
SEM	0.957606791	5.464821783	0.447018903	2.049878244

UNPAIRED T-TEST: SS State IV respiration	
P value	0.0182
P value summary	*
Significantly different (P < 0.05)?	Yes

UNPAIRED T-TEST: SS State III respiration	
P value	0.0039
P value summary	**
Significantly different (P < 0.05)?	Yes

Table 8B. Respiration of IMF mitochondria isolated from WT and KO muscle.

	IMF mitochondria: Respiration (natoms O2/mg/min)			
	WT		KO	
N	State IV	State III	State IV	State III
1	47.74	236.99	48.41	93.18
2	16.14	183.19	6.91	81.27
3	23.56	185.85	6.72	88.55
4	36.22	93.14	6.79	76.44
5	-3.15	179.64	11	63.42
6	1.32	157.6	9.78	69.18
7	4.04	118.04	28.45	74.2
8	7.19	137.81	4.01	65.02
9	6	133	7.74	96.74
10	5.74	128.72	7.13	74.91
11	5.72	77.4	3.84	70.04
12	3.87	76.92	4.69	72.04
13	4.45	75.09	0.5	53.94
14	4.37	75.8	7.02	81.2
15	4.1	62.22	8.05	114.46
16	0.31	49.98	1.37	50.88
17	2.54	67.95	3.49	70.28
18	3.89	64.38	0.33	50.22
19			3.11	58.09
20			12.36	84.28
21			2.26	76
22			5.39	90.8
23			5.95	87.7
24			0.4	66.7
25			2.79	76.05
26			3.7	141.03
27			6.41	117.19
X	9.669444444	116.8733333	7.725925926	79.40037037
SEM	3.129721058	12.75503558	1.880986228	3.968896862

UNPAIRED T-TEST: IMF State IV respiration	
P value	0.5745
P value summary	ns
Significantly different (P < 0.05)?	No

UNPAIRED T-TEST: IMF State III respiration	
P value	0.0021
P value summary	**
Significantly different (P < 0.05)?	Yes

Table 8C. Respiratory Control Ratios (RCR) of SS and IMF mitochondria isolated from WT and KO muscle.

	Respiratory Control Ratio (RCR)			
	WT		KO	
N	SS	IMF	SS	IMF
1	6.26	4.96	-0.12	1.92
2	8.75	11.35	4.22	11.75
3	6.47	7.89	-0.12	13.18
4	4.54	2.57	22	11.25
5	5.12	-57	2.93	5.76
6	4.48	119	2.91	7.07
7	4.8	29.2	5.21	2.61
8	7.24	19.17	1.29	16.2
9	16.5	22.17	2.57	12.5
10	5.55	22.44	9.67	10.5
11	6.14	13.52	8.6	18.22
12	49.56	19.88	3.9	15.36
13	4.64	16.87	11.17	108.85
14	13.5	17.33	35.33	11.56
15	3.5	15.16	53.56	14.22
16	4.11	159.13	10.4	37.19
17	38.84	26.8	8.12	20.12
18	7.78	16.55	5.16	151
19			5.5	18.66
20			24	6.82
21			5.6	33.63
22			12	16.83
23			10.36	14.73
24			6.67	166.97
25			9.64	27.29
26			13.92	38.12
27				18.27
X	10.98777778	25.94388889	10.55730769	30.02148148
SEM	2.984570185	10.76170763	2.321008637	8.139074086

2-WAY ANOVA			
Source of Variation	P value	P value summary	Significant?
Interaction	0.7467	ns	No
Genotype	0.7938	ns	No
Mitochondrial Fraction	0.0154	*	Yes

POST-HOC TEST				
Bonferroni	Mean Difference	Significant?	Summary	Adjusted P Value
WT:SS vs. WT:IMF	-14.96	No	ns	>0.9999
WT:SS vs. KO:SS	0.4305	No	ns	>0.9999
WT:SS vs. KO:IMF	-19.03	No	ns	0.3326
WT:IMF vs. KO:SS	15.39	No	ns	0.7376
WT:IMF vs. KO:IMF	-4.078	No	ns	>0.9999
KO:SS vs. KO:IMF	-19.46	No	ns	0.1834

Table 9A. ROS production in SS mitochondria isolated from WT and KO muscle.

	SS mitochondria: ROS production (natoms O2/mg/min)			
	WT		KO	
N	State IV	State III	State IV	State III
1	432.66	27.35	855.54	138.36
2	374.73	27.4	818.11	81.23
3	446.4	52	1550	105.19
4	501.98	115.65	336.29	64.75
5	754.3	105.18	345.76	71.91
6	308.52	73.41	447.01	548.56
7	446.43	78.14	850.63	629.46
8	208.5	65.86	2118.86	75.57
9	898.55	38.23	682.54	170.51
10	489.01	87.2	1322.16	341.88
11	2906.45	352.25	1581.48	221.52
12	13858.59	220.31	2408.6	185.29
13	1769.63	307	9209.62	239.42
14	3650.79	258.19	12500	220.79
15	1403	251.71	2905	313.08
16	4780.49	982.87	2800	146.89
17	7688.89	138.72	819.98	7.85
18	2100.46	233.55	5143.68	199.41
19			5588.24	367.03
20			2961.24	448.41
21			4411.99	265.4
22			3277.78	562.1
23			3962.03	123.93
24			1312.71	105.16
25			1366.91	
26				
27				
X	2389.965556	189.7233333	2783.0464	234.7375
SEM	818.969876	52.46652205	577.7891843	34.83976919

UNPAIRED T-TEST: SS State IV ROS	
P value	0.6881
P value summary	ns
Significantly different (P < 0.05)?	No

UNPAIRED T-TEST: SS State III ROS	
P value	0.4622
P value summary	ns
Significantly different (P < 0.05)?	No

Table 9B. ROS production in IMF mitochondria isolated from WT and KO muscle.

	IMF mitochondria: ROS production (natoms O2/mg/min)			
	WT		KO	
N	State IV	State III	State IV	State III
1	25.14	4.05	310.66	20.75
2	85.91	8.15	202.38	19.69
3	49.8	5.17	216	14.61
4	44.17	16.18	153.94	20.23
5	1454.55	6.01	167.69	27.96
6	330.03	10.15	30.46	26.02
7	174.32	9.49	229.43	9.7
8	475.56	9.77	180.88	13.33
9	459.93	18.15	102.85	13.37
10	529.14	20.1	430.56	9.61
11	833.76	33.94	449.18	26.27
12	443.45	40.39	5040	26.1
13	414.95	16.51	326.69	50.18
14	702.44	22.87	453.83	28.08
15	7053.56	30.64	1226.28	26.21
16	986.88	42.15	638.01	33.28
17	596.4	29.63	6989.9	16.13
18		39.76	441.59	37.97
19			226.54	22.95
20			1498.53	29.11
21			917.75	30.18
22			661.06	40.38
23			845.88	51.84
24			677.48	25.19
25			276.65	30.51
26				14.09
27				14.11
X	862.3523529	20.17277778	907.7688	25.10555556
SEM	397.5236517	3.055914848	320.4810409	2.123329934

UNPAIRED T-TEST: IMF State IV ROS	
P value	0.6694
P value summary	ns
Significantly different (P < 0.05)?	No

UNPAIRED T-TEST: IMF State III ROS	
P value	0.0038
P value summary	**
Significantly different (P < 0.05)?	Yes

Table 10A. mRNA levels of PGC-1α basally and following continuous exercise in WT and KO muscle.

	PGC-1α mRNA (2-ΔCT)			
	WT		KO	
N	CON	Cont. EX	CON	Cont. EX
1	0.127	0.318	0.133	0.544
2	0.076	1.178	0.058	0.263
3	0.040	0.084	0.056	0.215
4	0.161	0.738	0.121	0.384
5			0.238	0.426
X	0.10098959	0.57940287	0.1210228	0.36654738
SEM	0.02677288	0.24095275	0.03310058	0.05876189

2-WAY ANOVA			
Source of Variation	P value	P value summary	Significant?
Interaction	0.3208	ns	No
Genotype	0.4084	ns	No
Exercise	0.0064	**	Yes

POST-HOC TEST				
Bonferroni	Mean Difference	Significant?	Summary	Adjusted P Value
WT:CON vs. WT:EX	-0.4784	No	ns	0.0791
WT:CON vs. KO:CON	-0.02004	No	ns	>0.9999
WT:CON vs. KO:EX	-0.2656	No	ns	0.7149
WT:EX vs. KO:CON	0.4584	No	ns	0.0748
WT:EX vs. KO:EX	0.2129	No	ns	>0.9999
KO:CON vs. KO:EX	-0.2455	No	ns	0.7552

UNPAIRED T-TEST: WT CON vs. EX	
P value	0.095901
P value summary	ns
Significantly different (P < 0.05)?	No

UNPAIRED T-TEST: KO CON vs. EX	
P value	0.006585
P value summary	**
Significantly different (P < 0.05)?	Yes

UNPAIRED T-TEST: WT CON vs. KO CON	
P value	0.6647
P value summary	ns
Significantly different (P < 0.05)?	No

Table 10B. mRNA levels of COX-IV basally and following continuous exercise in WT and KO muscle.

	COX-IV mRNA (2-ΔCT)			
	WT		KO	
N	CON	Cont. EX	CON	Cont. EX
1	0.002	0.003	0.003	0.002
2	0.004	0.002	0.002	0.002
3	0.002	0.002	0.002	0.001
4	0.003	0.002	0.003	0.001
5			0.004	0.002
X	0.00258713	0.00236287	0.00280841	0.00168705
SEM	0.00036263	0.00021573	0.00034842	0.00021389

2-WAY ANOVA			
Source of Variation	P value	P value summary	Significant?
Interaction	0.1521	ns	No
Genotype	0.457	ns	No
Exercise	0.0388	*	Yes

POST-HOC TEST				
Bonferroni	Mean Difference	Significant?	Summary	Adjusted P Value
WT:CON vs. WT:EX	0.0002266	No	ns	>0.9999
WT:CON vs. KO:CON	-0.000222	No	ns	>0.9999
WT:CON vs. KO:EX	0.0009019	No	ns	0.2956
WT:EX vs. KO:CON	-0.0004486	No	ns	>0.9999
WT:EX vs. KO:EX	0.0006753	No	ns	0.7757
KO:CON vs. KO:EX	0.001124	No	ns	0.0778

UNPAIRED T-TEST: WT CON vs. EX	
P value	0.61038
P value summary	ns
Significantly different (P < 0.05)?	No

UNPAIRED T-TEST: KO CON vs. EX	
P value	0.02483
P value summary	*
Significantly different (P < 0.05)?	Yes

Table 10C. mRNA levels of ATF5 basally and after continuous exercise in WT and KO muscle.

	ATF5 mRNA (2-ΔCT)			
	WT		KO	
N	CON	Cont. EX	CON	Cont. EX
1	0.022	0.032	0.000	0.000
2	0.008	0.010	0.000	0.000
3	0.025	0.035	0.000	0.000
4	0.015	0.011	0.000	0.000
5			0.000	0.000
X	0.01750048	0.02181574	3.7122E-05	3.8681E-05
SEM	0.00381981	0.00670085	2.5796E-05	1.9388E-05

UNPAIRED T-TEST: WT vs. KO	
P value	<0.0001
P value summary	****
Significantly different (P < 0.05)?	Yes

UNPAIRED T-TEST: WT CON vs. EX	
P value	0.5961
P value summary	ns
Significantly different (P < 0.05)?	No

Table 10D. mRNA levels of ATF4 basally and after continuous exercise in WT and KO muscle.

	ATF4 mRNA (2-ΔCT)			
	WT		KO	
N	CON	Cont. EX	CON	Cont. EX
1	0.109	0.023	0.106	0.179
2	0.016	0.021	0.373	0.224
3	0.201	0.169	0.404	0.282
4	0.009	0.025	0.086	0.151
5			0.115	0.253
X	0.08374374	0.05923194	0.21667782	0.21775575
SEM	0.04531735	0.03649148	0.07046043	0.0239251

2-WAY ANOVA			
Source of Variation	P value	P value summary	Significant?
Interaction	0.7991	ns	No
Genotype	0.0104	*	Yes
Exercise	0.8156	ns	No

POST-HOC TEST				
Bonferroni	Mean Difference	Significant?	Summary	Adjusted P Value
WT:CON vs. WT:EX	0.02451	No	ns	>0.9999
WT:CON vs. KO:CON	-0.1329	No	ns	0.4645
WT:CON vs. KO:EX	-0.134	No	ns	0.4518
WT:EX vs. KO:CON	-0.1574	No	ns	0.243
WT:EX vs. KO:EX	-0.1585	No	ns	0.236
KO:CON vs. KO:EX	-0.001076	No	ns	>0.9999

Table 10E. mRNA levels of CHOP basally and after continuous exercise in WT and KO muscle.

	CHOP mRNA (2-ΔCT)			
	WT		KO	
N	CON	Cont. EX	CON	Cont. EX
1	0.013	0.008	0.015	0.007
2	0.007	0.007	0.006	0.003
3	0.007	0.004	0.007	0.006
4	0.003	0.006	0.002	0.002
5			0.004	0.004
X	0.00739329	0.00608829	0.00715366	0.00440728
SEM	0.00209436	0.00078197	0.00219194	0.00106242

2-WAY ANOVA			
Source of Variation	P value	P value summary	Significant?
Interaction	0.6767	ns	No
Genotype	0.5798	ns	No
Exercise	0.2521	ns	No

Table 10F. mRNA levels of HSP60 basally and after continuous exercise in WT and KO muscle.

	HSP60 mRNA (2-ΔCT)			
	WT		KO	
N	CON	Cont. EX	CON	Cont. EX
1	0.179	0.210	0.229	0.339
2	0.204	0.352	0.526	0.588
3	0.354	0.464	0.406	0.799
4	0.159	0.254	0.148	0.433
5			0.169	0.160
X	0.22403441	0.3197514	0.29569952	0.46382181
SEM	0.04433941	0.05639823	0.07324447	0.10865033

2-WAY ANOVA			
Source of Variation	P value	P value summary	Significant?
Interaction	0.3267	ns	No
Genotype	0.0664	ns	No
Exercise	0.0363	*	Yes

POST-HOC TEST				
Bonferroni	Mean Difference	Significant?	Summary	Adjusted P Value
WT:CON vs. WT:EX	-0.09571	No	ns	>0.9999
WT:CON vs. KO:CON	-0.07167	No	ns	>0.9999
WT:CON vs. KO:EX	-0.3157	No	ns	0.0626
WT:EX vs. KO:CON	0.02405	No	ns	>0.9999
WT:EX vs. KO:EX	-0.22	No	ns	0.345
KO:CON vs. KO:EX	-0.244	No	ns	0.1798

Table 10G. mRNA levels of LONP basally and after continuous exercise in WT and KO muscle.

	LONP mRNA (2-ΔCT)			
	WT		KO	
N	CON	Cont. EX	CON	Cont. EX
1	0.011	0.017	0.015	0.011
2	0.010	0.015	0.019	0.016
3	0.016	0.017	0.020	0.016
4	0.013	0.019	0.013	0.014
5			0.016	0.014
X	0.01242141	0.01696307	0.01648463	0.01411516
SEM	0.00125615	0.00088465	0.00132048	0.00099096

2-WAY ANOVA			
Source of Variation	P value	P value summary	Significant?
Interaction	0.0097	**	Yes
Genotype	0.6053	ns	No
Exercise	0.3625	ns	No

POST-HOC TEST				
Bonferroni	Mean Difference	Significant?	Summary	Adjusted P Value
WT:CON vs. WT:EX	-0.004541	No	ns	0.1165
WT:CON vs. KO:CON	-0.004064	No	ns	0.1556
WT:CON vs. KO:EX	-0.001696	No	ns	>0.9999
WT:EX vs. KO:CON	0.0004762	No	ns	>0.9999
WT:EX vs. KO:EX	0.002844	No	ns	0.6195
KO:CON vs. KO:EX	0.002368	No	ns	0.8763

Table 10H. mRNA levels of mtHSP70 basally and after continuous exercise in WT and KO muscle.

	mtHSP70 mRNA (2-ΔCT)			
	WT		KO	
N	CON	Cont. EX	CON	Cont. EX
1	0.006	0.010	0.008	0.007
2	0.006	0.009	0.009	0.005
3	0.006	0.006	0.007	0.007
4	0.006	0.006	0.005	0.005
5			0.006	0.005
X	0.00607972	0.00764924	0.0070233	0.00574241
SEM	0.00012899	0.00090783	0.00074262	0.00053846

2-WAY ANOVA			
Source of Variation	P value	P value summary	Significant?
Interaction	0.0479	*	Yes
Genotype	0.4756	ns	No
Exercise	0.8298	ns	No

POST-HOC TEST				
Bonferroni	Mean Difference	Significant?	Summary	Adjusted P Value
WT:CON vs. WT:EX	-0.00157	No	ns	0.7902
WT:CON vs. KO:CON	-0.0009434	No	ns	>0.9999
WT:CON vs. KO:EX	0.0003381	No	ns	>0.9999
WT:EX vs. KO:CON	0.0006263	No	ns	>0.9999
WT:EX vs. KO:EX	0.001908	No	ns	0.3568
KO:CON vs. KO:EX	0.001282	No	ns	0.9961

Table 10I. mRNA levels of ClpP basally and after continuous exercise in WT and KO muscle.

	ClpP mRNA (2-ΔCT)			
	WT		KO	
N	CON	Cont. EX	CON	Cont. EX
1	1.208	1.601	1.383	1.051
2	1.068	1.277	1.408	0.873
3	1.138	1.182	1.297	1.104
4	1.138	1.200	0.952	0.916
5			0.981	0.742
X	1.13800781	1.31518256	1.20416071	0.93711265
SEM	0.02842075	0.09748367	0.09888644	0.06463916

2-WAY ANOVA			
Source of Variation	P value	P value summary	Significant?
Interaction	0.0153	*	Yes
Genotype	0.073	ns	No
Exercise	0.5854	ns	No

POST-HOC TEST				
Bonferroni	Mean Difference	Significant?	Summary	Adjusted P Value
WT:CON vs. WT:EX	-0.1772	No	ns	0.9708
WT:CON vs. KO:CON	-0.06615	No	ns	>0.9999
WT:CON vs. KO:EX	0.2009	No	ns	0.5957
WT:EX vs. KO:CON	0.111	No	ns	>0.9999
WT:EX vs. KO:EX	0.3781	Yes	*	0.0302
KO:CON vs. KO:EX	0.267	No	ns	0.1561

Table 10J. mRNA levels of UPR^{mt} downstream targets (LONP, mtHSP70, ClpP) basally and after continuous exercise in WT and KO muscle.

	UPRmt downstream targets mRNA (2-ΔCT)			
	WT		KO	
N	CON	Cont. EX	CON	Cont. EX
1	0.011	0.017	0.015	0.011
2	0.010	0.015	0.019	0.016
3	0.016	0.017	0.020	0.016
4	0.013	0.019	0.013	0.014
5	0.006	0.010	0.016	0.014
6	0.006	0.009	0.008	0.007
7	0.006	0.006	0.009	0.005
8	0.006	0.006	0.007	0.007
9	1.208	1.601	0.005	0.005
10	1.068	1.277	0.006	0.005
11	1.237	0.767	1.383	1.051
12	1.283	1.083	1.408	0.873
13			1.297	1.104
14			0.952	0.916
15			0.981	0.742
X	0.40588421	0.40216684	0.40922291	0.31899066
SEM	0.1697025	0.17440338	0.15330154	0.1185093

2-WAY ANOVA			
Source of Variation	P value	P value summary	Significant?
Interaction	0.043	*	Yes
Genotype	0.6508	ns	No
Exercise	0.8386	ns	No

POST-HOC TEST				
Bonferroni	Mean Difference	Significant?	Summary	Adjusted P Value
WT:CON vs. WT:EX	-0.3273	No	ns	0.7932
WT:CON vs. KO:CON	-0.2326	No	ns	>0.9999
WT:CON vs. KO:EX	0.03595	No	ns	>0.9999
WT:EX vs. KO:CON	0.09468	No	ns	>0.9999
WT:EX vs. KO:EX	0.3632	No	ns	0.4766
KO:CON vs. KO:EX	0.2685	No	ns	0.999

APPENDIX B: ADDITIONAL DATA
(STATISTIC TABLES NOT SHOWN)

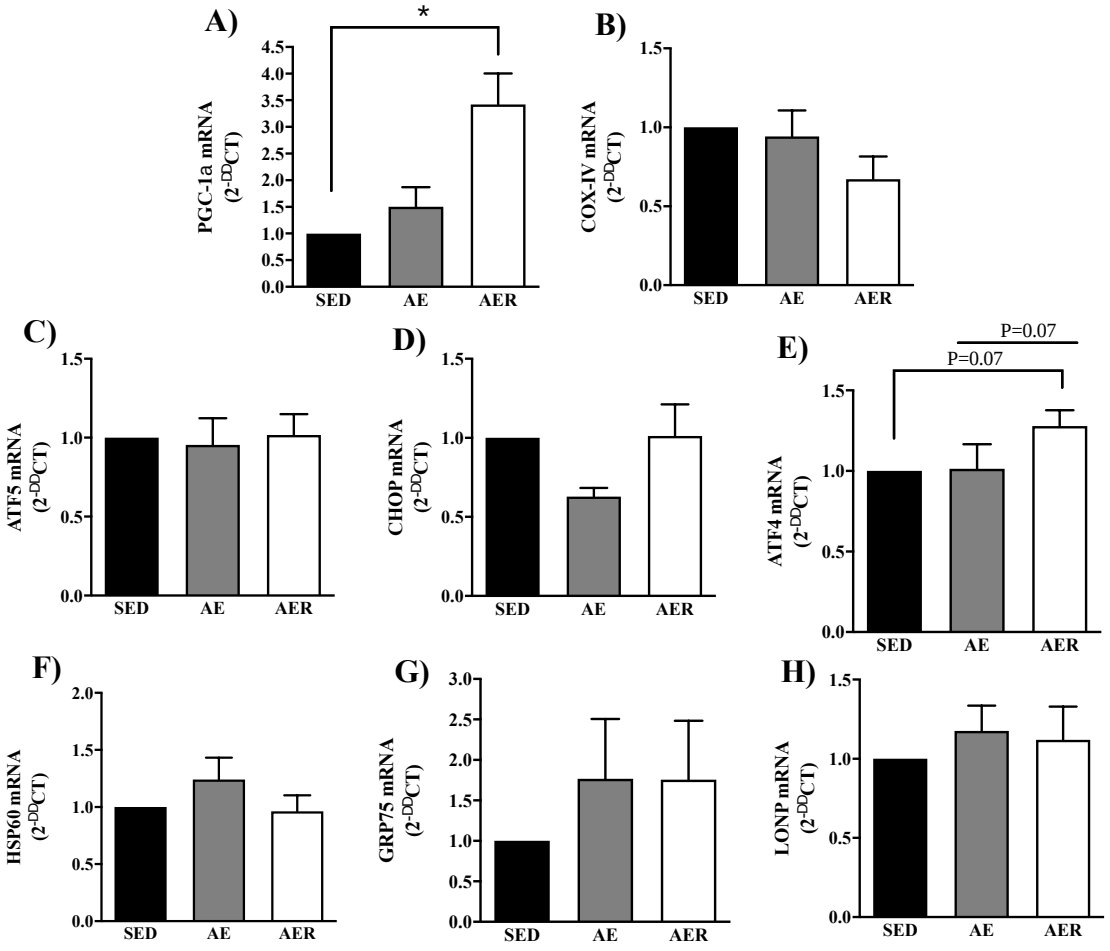

Figure S1. Changes in gene expression in WT muscle immediately after exercise and following 3 hours of recovery. mRNA levels of the mitochondrial transcriptional co-activator **A)** PGC-1α and the mitochondrial gene **B)** COX-IV were measured, in addition to the UPR^{mt} transcription factors **C)** ATF5**, D)** CHOP and **E)** ATF4. Gene expression of UPR^{mt} downstream targets include **F)** HSP60, **G)** GRP75 (mtHSP70), **H)** LONP. (n=4/group). *P<0.05, 1-way ANOVA. SED, sedentary; AE, acute exercise; AER, acute exercise + 3 hours of recovery. Data are expressed as fold changes using the $2^{-\Delta\Delta CT}$ method.

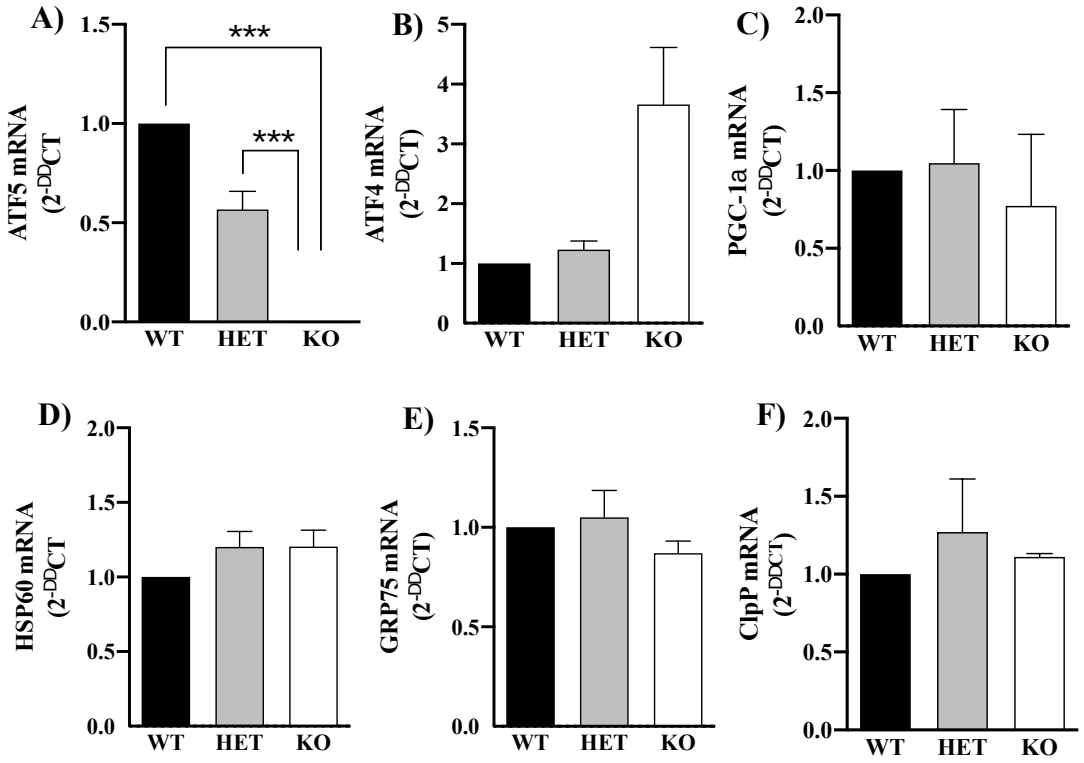

Figure S2. Basal mRNA levels in WT, HET and ATF5 KO mice. mRNA levels of the UPR^{mt} transcription factors **A)** ATF5**, B)** ATF4 and the mitochondrial transcriptional co-activator PGC-1α. Gene expression of UPR^{mt} downstream targets include **D)** HSP60, **E)** GRP75 (mtHSP70) and **F)** ClpP. WT: n=3-4, HET: n=3-4, KO: n=2-3. *P<0.05, ***P<0.001. 1-way ANOVA. WT, wild-type; HET, heterozygous KO; KO, homozygous KO. Data are expressed as fold changes using the $2^{-}\Delta\Delta^{CT}$ method.

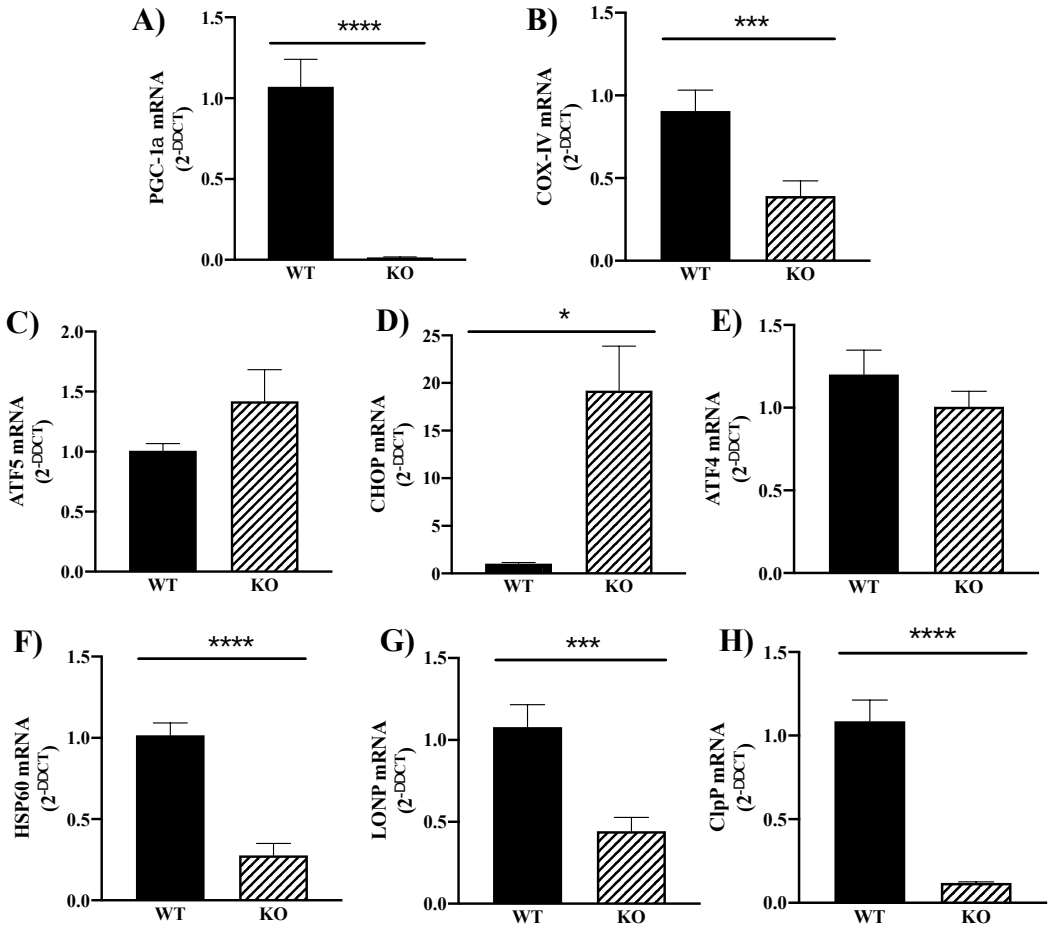

Figure S3. Basal mRNA levels in WT and PGC-1α KO mice. mRNA levels of **A)** PGC-1α and its downstream target **B)** COX-IV. Gene expression of UPR^{mt} transcription factors include **C)** ATF5, **D)** CHOP and **E)** ATF4. mRNA for downstream targets: **F)** HSP60, **G)** LONP, **H)** ClpP. WT: n=6, KO: n=10. *P<0.05, ***P<0.001, ****P<0.0001, unpaired t-test. Data are expressed as fold changes using the $2^{-}\Delta\Delta^{CT}$ method.

APPENDIX C: LABORATORY METHODS AND PROTOCOLS

CYTOCHROME C OXIDASE (COX) ACTIVITY FOR MICROPLATE READER

THEORY:

Tissue extract containing cytochrome c oxidase is added to the test solution containing fully reduced cytochrome c. The rate of cytochrome c oxidation is measured over time as a reduction in absorbance at 550 nm. The reaction is carried out at 30° C.

REAGENTS:

1. 20 mM KCN; MW= 65.12, 13.02 mg/10 ml dH_2O

2. 100 mM K-Phosphate Buffer

- make up 0.1 M KH_2PO_4; MW= 136.09
  = 13.6 g/1000 ml
  (pH approx. 5)
  (rm. temp)
- make up 0.1 M $K_2HPO_4.3H_2O$; MW= 174.18
  = 17.4 g/1000 ml
  (pH approx. 8)
  (rm. temp)
- mix in equal proportions, pH to 7.0

3. 10 mM K-Phosphate Buffer

- dilute 0.1 M KPO_4 Buffer prepared above 1:10 with ddH_2O (eg. 10 ml buffer + 90 ml ddH_2O)

4. Extraction Buffer (100 mM Na-K-Phosphate, 2 mM EDTA; pH 7.2)

- 500 ml 0.1 M $Na_2HPO_4.2H_2O$;

  Combine 8.9 g sodium phosphate with 0.372 g EDTA up to 500 ml.

- 200 ml 0.1 M KH_2PO_4;

  Combine 2.7 g potassium phosphate with 0.149 g EDTA up to 200 ml.

- combine both solutions and pH to 7.2

5. Test Solution (reduced cytochrome c, 2 mg/ml), for 10 ml (enough for 36 microplate wells);
- weigh out 20 mg of horse heart cytochrome c (Sigma, C-2506) in a scintillation vial

- add 1 ml of 10 mM KPO_4 buffer and dissolve cytochrome c

- make up a small volume of 10 mg/ml sodium dithionite-10 mM KPO_4 stock solution (make fresh each experiment and use within twenty minutes)

- add 40 μl of the dithionite stock solution to the test solution and observe red-orange colour change

- add 8 ml of ddH_2O

- add 1 ml of 100 mM KPO_4 buffer.

PROCEDURE:

1. Place powdered muscle samples in liquid N_2.

2. Add 50 μl of extraction Buffer to 1.5 ml Eppendorf tubes in the aluminum block on ice. (One Eppendorf per sample).

3. Add 5-7.5 mg tissue to each tube, recording exact tissue mass. Mix by tapping.

4. Add the volume of Extraction Buffer required to obtain a 20-fold dilution.

5. Add a stir bar and mix for 15 min. Make up Test Solution during this time and wrap in foil.

6. Sonicate each tube 3 x 3 seconds, cleaning the probe between samples.

7. Pipette some of 20-fold sample extract into new Eppendorf tube and add volume of Extraction Buffer required to obtain an 80-fold dilution. (eg. 50 μl of 20-fold extract + 150 μl Ext. Buffer = 200 μl of 80-fold sample extract). Keep 80-fold sample extract tube on ice for duration of experiment

8. Add 270 μl of Test Solution into 4-8 wells of 96-well microplate and incubate at 30°C for 10 minutes to stabilize the temperature and absorbance.

9. Open KC4 plate reader program (on Triton). Select CONTROL icon, then PRE-HEATING tab, enter 30°C and select ON. (Do not run assay until KC4 temperature has reached 30°C.)

10. Select WIZARD icon, then READING PARAMETERS icon.

    - Select Kinetic for Reading Type.
    - Select Absorbance for Reader and 550 nm for wavelength (drop-down menu).
    - Select Sweep for Read Mode.
    - Select 96 Well Plate (default) for Plate Type.
    - Enter first and last well to be read (eg. A1 and A4 if reading 4 samples

simultaneously).

- Select Yes and Pre-heating and enter 30 for Temperature Control.
- For Shaking enter 0 for both intensity and duration (shaking is not necessary and it will delay the first reading).
- Do not select either of the two options for Pre-reading.
- Click on the KINETIC… rectangular tile to open the Kinetic window.
- Enter run time (1 minute is recommended) and select MINIMUM for Interval time (under these conditions the minimum Interval time should be 3 seconds).
- Select Allow Well Zoom During Read to see data in real time (optional).
- Under Scales, checkmarks should appear for both Auto check boxes. Do not select Individual Well Auto Scaling.
- Press OK to return to Reading Parameters window. Press OK to return to Wizard window. Press OK. Do not save the protocol.

11. Set the multipipette to 250 μl and secure 4-8 yellow tips on the white projections (make sure they are on tight and all at the same height).

12. In a second, clean 96 well plate, pipette samples into 4-8 empty wells (start with A1). Recommended volumes: 30 μl of 80-fold extract for Mixed Gastroc, 10 μl for Heart. Adjust volumes according to oxidative capacity of the tissue. (eg. 25 μl for Red Gastrocnemius and 35 μl for White Gastrocnemius).

13. Remove microplate with Test Solution in 4-8 wells from the incubator (as long as it has been incubating for 10 minutes). Place this plate beside the plate with the sample extracts in it.

14. On KC4 program, select the READ icon and press the START READING icon, then press the READ PLATE button. A box will appear that says, "Insert plate and start reading". Do not press OK yet, but move the mouse so that the cursor hovers over the OK button.

15. Using the multipipette (set to 250 μl) carefully draw up the Test Solution. Make sure the volume is equal in all the pipette tips, and that no significant air bubbles have entered any of the tips.

16. Pipette the Test Solution into the wells with the sample extracts (the second plate). As soon as all the Test Solution has been expelled from the tips (do not wait for the second push from the multipipette), place the plate onto the tray of the plate reader and with the other hand on the mouse, press the OK button. (Speed at this point is paramount, as there is an unavoidable latency period between the time of pressing the OK button and the time of the first reading.)

17. If desired, add 5 μl KCN to one of the wells to measure any absorbance changes in the presence of the CYTOX inhibitor.

18. Once reading is complete, hold the CTRL key on the keyboard, and use the mouse to click once on each of the squares corresponding to a well that had sample in it. Once all the desired wells have been highlighted by a black square (up to a maximum of 8 wells), let go of the CTRL key and a large graph will appear with lines on it representing each sample.

19. To obtain the rate of change of absorbance over different time periods, select Options and enter the amount of time for which you would like a rate of change of absorbance to be calculated. The graph, along with one rate (at whichever time interval is selected) for each sample can be printed on a single sheet of paper, and the results can be saved.

20. The delta absorbance will appear in units of mOD/min and the number given will be negative. Convert this to OD/min by dividing by 1000 and omit the negative sign in the calculation. (eg. if Mean V: -394.8 mOD/mn, then use 0.395 OD/min)

CALCULATION: CYTOX activity (μmole/min/g tissue)

$$= \frac{\text{delta absorbance/min x total volume (ml) x 80 (dilution)}}{\text{18.5 (}\mu\text{mol/ml extinction coeff.) x sample vol (ml)}}$$

Example Calculation:

30 μl of 80-fold sample extract
250 μl of Test Solution
Mean V: -284.2 mOD/mn

$$\text{COX activity} = \frac{(.284)(.280)(80)}{(18.5)(.030)}$$

= 11.5 μmol/min/g tissue

= 11.5 U/g tissue

Filename: COX ASSAY MICROPLATE

Tissue	**Heart**	**Mixed Gastroc**
Weight (mg)	5 mg	7.5 mg
Vol. for 20-fold	100 μl	150 μl
Remove, put in new Eppendorf	50 μl	75 μl
Vol. needed for 80-fold	Add 150 μl of extract. buffer	Add 225 μl of extract. buffer
Final Volume of 80-fold	200 μl	300 μl
Vol. of 80-fold per well	10 μl	30 μl

WESTERN BLOTTING: ELECTROPHORESIS WITH SDS-PAGE GELS AND PROTEAN BIO-RAD SYSTEM

Reagents

1. Acrylamide/Bis-Acrylamide, 30% Solution 37.5:1 (BioShop 10.502)
    a. Store at 4°C
2. Under Tris Buffer
    a. 1M Tris-HCl, pH 8.8 (60.5g/500ml)
    b. Store at 4°C
3. Over Tris Buffer
    a. 1M Tris-HCl, pH 6.8 (12.1g/100ml)
    b. Bromophenol Blue (for colour)
    c. Store at 4°C
4. Ammonium Persulfate (APS)
    a. 10% (w/v) APS in ddH_20 (1g/10ml)
    b. Stored at 4°C
5. Sodium Dodecyl Sulfate (SDS)
    a. 10% (w/v) in ddH_20 (1g/10ml)
    b. Store at room temperature
6. TEMED (Sigma T-9281)
7. Electrophoresis Buffer, pH 8.3 (10L)
    a. 25mM Tris 30.34g, 192mM Glycine 144g, 0.1% SDS 10g
    b. Volume to 10L with ddH_20
    c. Store at room temperature
8. 6X SDS
    a. Warm 100% glycerol in water bath at 65°C for 30 minutes
    b. Combine 1.2g SDS, 0.06g Bromophenol Blue, 3mls of 1M Tris, pH 6.8 and 1ml of ddH_20 and stir at 4°C for 5 minutes
    c. Add 3mls of 100% glycerol, stir and aliquot mixture.
    d. Store at -20°C
    e. Add 5% (v/v) ß-mercaptoethanol (Sigma M6250) to 6X SDS <u>just prior</u> to use
9. *tert*-Amyl alcohol ReagentPLus, 99% (Sigma 152463)

Procedure

1. **Prepare electrophoresis rack:**
    a. Clean glass plates thoroughly with soap followed by 95% ethanol then ddH_20.
    b. Dry carefully with a kimwipe.
    c. Assemble glass plates as shown below:

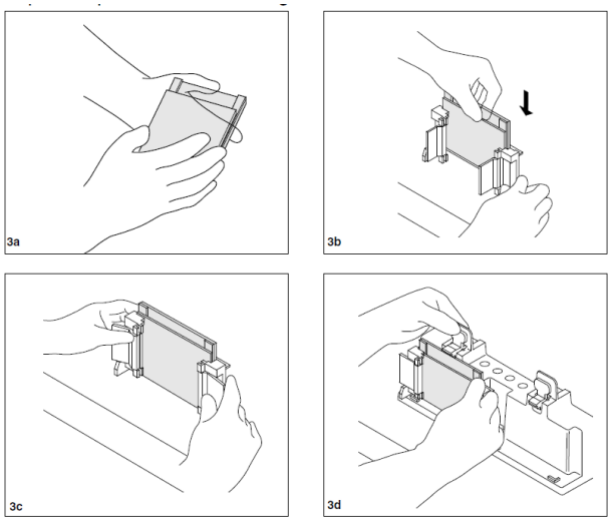

c. Check the seal y adding a small volume of ddH_20 then pour off and let dry.

2. Prepare separating gels:

a. Mini Protean 3 Bio-Rad System volumes:

	8%	**10%**	**12%**	**15%**	**18%**
Acrylamide	2.7 ml	3.3 ml	4.0 ml	5.0 ml	6.0 ml
ddH_20	4.1 ml	3.5 ml	2.8 ml	1.8 ml	0.8 ml
Under Tris	3.0 ml	3.0 ml	3.0 ml	3.0 ml	3.0 ml
SDS	100µl	100µl	100µl	100µl	100µl
APS	100µl	100µl	100µl	100µl	100µl
TEMED	10µl	10µl	10µl	10µl	10µl

b. Mix the contents of the separating gel without adding APS or TEMED. Stir.
c. Add APS and TEMED. Stir.
d. Slowly pour the entire volume of the solution into the space between the two plates while keeping plates tilted to prevent bubble formation.
e. Add *tert*-Amyl alcohol to coat top surface of gel solution.
f. Allow 30 minutes for gel polymerization.
g. Remove *tert*-Amyl alcohol by pouring it off and remove any remainder with a kimwipe. Rinse with ddH_20.

3. Prepare stacking gel:

a. For a single mini gel use the following volumes:

Acrylamide	500 µl
Over Tris	625 µl
ddH_20	3.75 ml
SDS	50 µl
APS	50 µl
TEMED	7.5 µl

b. Mix the contents of the stacking gel without adding APS or TEMED. Stir.
c. Add APS and TEMED. Stir.
d. Using a Pasteur pipette slowly add the entire volume from the beaker in between the plates.
e. Add comb for desired number of wells.
f. Allow 30 minutes for gel polymerization.

4. Prepare samples:

a. Turn of the block heater to 95ºC.
b. Pipette required volume of sample into new eppendorf with 6X SDS (1 volume of sample to 1/6 sample volume of 6X SDS). Keep samples on ice until all samples are prepared.
c. Briefly spin each sample to bring volume to the bottom of the eppendorf.
d. Incubate each sample at 95 ºC for 5 minutes in the heating block to denature the proteins.
e. Briefly spin again to return volume to the bottom of the eppendorf.

5. Assemble Mini-PROTEAN gel caster system:

a. See images below:

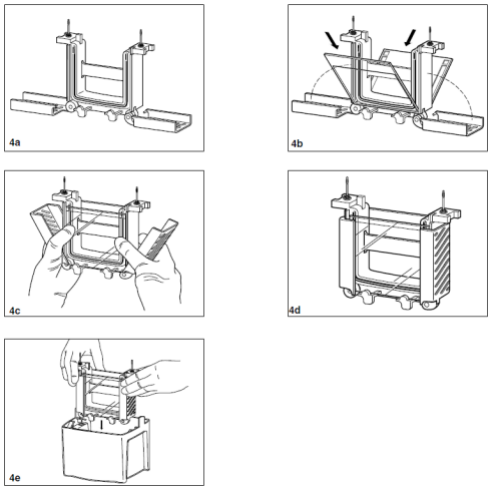

b. If you are only running one gel a plastic rectangular pseudo plate must be clamped on the other side of the caster.
c. Fill with electrophoresis buffer between the plates and outside of the plates in the chamber.
d. Slowly remove the comb using both hands (one on each side) by pulling the comb straight upwards.
e. Fix any wells that are deformed using a small spatula.
f. Clean out the wells using a syringe filled with electrophoresis buffer.
g. Withdraw the entire volume of the sample using a Hamilton syringe. Inject volume slowly into the bottom of the well.

6. Gel electrophoresis

a. Immediately after all samples are loaded place the lid on the gel chamber.

b. Place positive and negative plugs into the power supply and turn on power supply.
c. Set power supply to 120V. Gel will run for ~2 hours depending on percent gel made.
d. When the bromophenol blue has run off the bottom of the gel turn off the power supply. Remove plugs from power supply and remove lid.
e. Prepare for electrotransfer of proteins from the gel to nitrocellulose membrane.

WESTERN BLOTTING AND IMMUNODETECTION

Reagents

1. Transfer Buffer
    a. 0.025M Tris-HCl pH 8.3 12.14g
    b. 0.15M Glycine 45.05g
    c. 20% Methanol 800ml
    d. make up to 4L with ddH_20
    e. store at 4°C
2. Ponceau S stain
    a. 0.1% (w/v) Ponceau S
    b. 0.5% (v/v) Acetic Acid
    c. Store at room temperature
3. Wash Buffer
    a. Tris-HCl pH 7.5 12g
    b. NaCl 58.5g
    c. 0.1% Tween 10ml
    d. Store at room temperature
4. Blocking Solution
    a. 5% (w/v) skim milk power in wash buffer OR
    b. 5% (w/v) BSA in wash buffer
5. Enhanced Chemiluminescence Fluid (ECL; Santa Cruz sc-2048)
6. Film/Developer/Fixer

Procedure

1. Transfer Procedure

a. Remove electrophoresis plates from chamber and separate the plates.
b. Cut away unnecessary parts of the gel using a spatula and measure remaining gel size.
c. Using a paper cutter cut 6 pieces of Whatman paper per gel to the same size as the gel. Wearing gloves cut nitrocellulose membrane (GE Healthcare RPN303D) to the dimensions of the gel.
d. Assemble Whatman paper, nitrocellulose memebrane and gel as shown below:

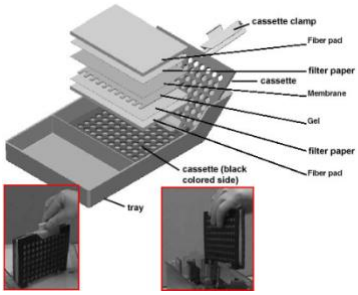

e. Close the cassette and place in the transfer chamber with the black side of the cassette facing the back side of the chamber.
f. Place ice pack in the chamber.
g. Place lid on the chamber and connect the leads to the power supply.
h. Turn on the power supply and run at 120V for 2 hours. This can vary depending on the size of the protein of interest.

2. Removal of transfer membrane:

a. Turn off the power supply and disconnect leads from the power supply then remove the lid from the chamber.
b. Remove the cassette from the chamber.
c. With gloves on, remove the Whatman paper and gel and place the nitrocellulose membrane in a plastic dish.
d. Add Ponceau S stain on the membrane and gently swirl.
e. Drain off the remaining Ponceau S and save for reuse.
f. Rinse the membrane with ddH_20 to reduce the red background. Wrap membrane in saran wrap and scan image.
g. Cut the membrane while protein bands are still visible at the desired molecular weight.
h. Rotate membrane at room temperature in wash buffer until remaining Ponceau S has been removed.
i. Incubate membrane for 1 hour with rotation in blocking solution.
j. Incubate membrane with desired antibody diluted in blocking solution overnight at 4ºC. Membrane is placed face down into the solution on a glass plate covered in parafilm. To maintain a moist environment overnight, wet a small kimwipe and form it into a ball and place in each corner of the dish. Cover the dish with saran wrap.

3. Immunodetection

a. Wash the blots in wash buffer with gentle rotation for 5 minutes 3X.
b. Incubate the blots for 1-2 hours with the appropriate secondary antibody diluted in blocking solution.
c. Membrane is placed face down in solution on a glass plate covered with parafilm. Place moist kimwipes in each corner of the dish and cover the dish with saran wrap.
d. Following the incubation, wash the membrane 3X for 5 minutes with wash buffer.

4. Enhanced Chemiluminescence Detection

a. Mix ECl fluids “A” and “B” in a 1:1 ratio in a disposable Rohr tube.
b. Place blots on saran wrap face up and apply ECL solution for 2 minutes.
c. Dab off excess ECL on a kimwipe and place blots face down on a fresh piece of saran wrap and wrap tightly.
d. Expose blot to film (time will vary depending on protein and antibody).

e. Place film into developer (time will vary).
f. Once image appears place film into fixer for 2 minutes. Wash with fresh water when complete.

RNA ISOLATION

PREPARATION:

1. The homogenizer must be sterilized in 0.1M NaOH for 1.5hrs and rinsed in sterile water prior to use with homogenizer turned on. Rinse in sterile water between samples. (Add 10ml St. H_2O to 1ml 1M NaOH to obtain desired concentration of 0.1M NaOH)
2. Label St. 1.5ml eppendorfs and 13ml test tubes accordingly.
3. Get ice.
4. Make sure to autoclave graduated cylinders (50ml-100ml), flasks(1L, 200ml) and distilled water before beginning the isolation.

IMPORTANT:

1. Dispose test tubes and pipette tips that have come into contact with the tri-reagent in the phenol waste bags under the fume hood.
2. Change gloves frequently and sterilize them with wash ethanol (located near sinks).
3. Use sterile pipette tips. (1ml = blue, 200µl = medium sized clear ones)
4. Make sure homogenizer and centrifuge are available for use.

PROCEDURE:

DAY 1:

1. Add **1 ml of Tri-reagent** (in fridge/green cap) to a 13ml Sarstedt tube.
2. Add **200mg** of tissue to the Tri-reagent. (Tap test tube to mix tissue with the tri-reagent.)
3. **Homogenize @ 30% power output** for **30sec**. (Always go for an extra 1-2sec because the homogenizer takes time to reach full power.)

NOTE

Rinse homogenizer before and after each use with St. H_2O. Homogenizer must turned on when rinsing. Wipe dry with Kimwipes.

When homogenizing move the test tube left and right quickly.

Observe colour change to light pink.

4. **Transfer** to a St. 1.5ml eppendorf.
5. Let stand for **5 min** at **room temperature**.
6. Add **0.2 ml chloroform** and shake vigorously for 15 sec; let stand for **2-3 min at room temperature.** (Colour will change to a milky-pink pepto-bismol colour)
7. Spin at **max speed (~16 000 rcf) for 15 min at 4°C**. (Located in the glass fridge)

8. Transfer upper aqueous phase to 1.5ml eppendorf. (Use a p1000 pipette)
9. Add **0.5 ml isopropanol** and gently tap to mix; precipitate RNA **overnight @ -20°C or -80°C for 1hr.**
10. Sterilize gel canister, 8-tooth comb (white), gel holder in 0.1% SDS.

    0.1%SDS = 10mg SDS (in chemical cabinet) + 1L St. H_2O
    Note Wear mask when handling SDS powder.

Day 2:

11. Let stand at room temperature for **10 min**.
12. Spin at **max speed (~16 000rcf) for 10 min at 4°C**.
13. Discard supernate and add **0.7 ml 70% ethanol**.

    Note Wash (do not resuspend) ie. Pellet should be floating in the ethanol not dissolved in the ethanol. Use the p1000.

14. Spin for **1 min** in eppendorf centrifuge at **4°C.**
15. Discard supernate. (Remove excess liquid with a 20 µl pipette – **DO NOT touch pellet**)
16. Air Dry.
17. Dissolve pellet in 30 µl sterile distilled water (by pipetting up and down) and measure absorbance at 260 nm.

Measuring Absorbance:

Use the KC4 program on the Jupiter computer.

Settings:

Go to Wizard → Reading Parameters

Under reader → click absorbance.
Under wavelenths → set it to 260nm

Check the following boxes: 1.) Pre read blank plate and 2.) pathlength correction wavelengths

Use the Costar 96 well blank plate. (Wash with ethanol **only** carefully/saran wrap and store on desk for future use)

Dilution: Fill desired number of wells with 95 µl sterile water and 5 µl of sample.

NOTE Always add the largest volume first.

After samples have been analyzed:

Click on report (found in the menu bar) and select M260 Corr and print!

Note 1.8 is the minimum value → generally.

RNA Concentration:

@260 reading x 40 µg/µl x dilution factor (20) = [RNA] µg/µl

Dilution factor = Total Volume / Volume of sample
= 100µl / 5µl
= 20

FIRST-STRAND cDNA SYNTHESIS (REVERSE TRANSCRIPTION)

First-strand cDNA synthesis is performed following the manufacturer's recommendations that are outlined below:

REAGENTS:

1. total RNA (isolated as described)
2. Oligo$(dT)_{12\text{-}18}$
3. 10 mM dNTPs (dATP, dTTP, dCTP, dGTP; 10 mM each)
4. Sterile ddH_20
5. RNAse OUT (40 units/ µl)
6. 0.1 M DTT
7. 5X First-strand Buffer
8. SuperScript II RT

*Note: All reagents except RNA are supplied with the SSII kit from Invitrogen.

PROCEDURE:

1. Add following components to a nuclease/ RNA-free 500 µl eppendorf:

Oligo$(dT)_{12\text{-}18}$	1µl
1 µg of RNA	x µl
dNTP mix	1 µl
Sterile ddH_20	to 20 µl

2. Heat mixture to 65°C for 5 minutes and quick chill on ice. Collect the contents with a quick spin in a tabletop microcentrifuge and then add:

5X First-strand buffer	4 µl
0.1 M DTT	2 µl
RNAse OUT	1 µl

3. Mix contents of tube gently and incubate at 42°C for 2 minutes.
4. Add 1 µl (200 units) of Superscript II RT and mix by pipetting gently up and down.
5. Incubate at 42°C for 50 minutes.
6. Inactivate the reaction by heating at 70°C for 15 minutes.
7. cDNA is ready for use in PCR amplification.

MITOCHONDRIA ISOLATIONS FROM SKELETAL MUSCLE

Reagents

All buffers are set to pH 7.4 and stored at 4 °C

- Buffer 1
  - 100 mM KCl
  - 5 mM MgSO4
  - 5 mM EDTA
  - 50 mM Tris base

- Buffer 1 + ATP
  - Add 1 mM ATP to Buffer 1

- Buffer 2
  - 100 mM KCl
  - 5 mM MgSO4
  - 5 mM EGTA
  - 50 mM Tris base
  - 1 mM ATP

- Resuspension medium
  - 100 mM KCl
  - 10 mM MOPS
  - 0.2% BSA

- Nagarse protease (Sigma, P-4789)
  - 10 mg/ml in Buffer 2
  - Make fresh for each isolation, keep on ice

Procedure

(Refer to Flow Chart below)

1. Remove the tibialis anterior (TA) muscle from the rat, and put it in a beaker containing 5 ml Buffer 1, on ice immediately.
2. Place TA on a watch glass that is also on ice and trim away fat and connective tissue. Proceed to thoroughly mince the muscle sample with forceps and scissors, until no large pieces are remaining.
3. Place the minced tissue in a plastic centrifuge tube and record the exact weight of tissue.
4. Add a 10-fold dilution of Buffer 1 + ATP to the tube.
5. Homogenize the samples using the Ultra-Turrax polytron with 40% power output and 10 s exposure time. Rinse the shaft with 0.5 ml of Buffer 1 + ATP to help minimize sample loss.
6. Using a Beckman JA 25.50 rotor, spin the homogenate at a centrifuge setting of 800 g for 10 min. This step divides the IMF and SS mitochondrial subfractions. The supernate will contain the SS mitochondria and the pellet will contain the IMF mitochondria.

SS mitochondrial isolation:

1. Filter the supernate through a single layer of cheesecloth into a second set of 50 ml plastic centrifuge tubes.
2. Spin tubes at 9000 g for 10 min. Upon completion of the spin discard the supernate and gently resuspend the pellet in 3.5 ml of Buffer 1 + ATP. Since the mitochondria are easily damaged, it is important that the resuspension of the pellet is done carefully.

3. Repeat the centifugation of the previous step (9000 g for 10 min) and discard the supernate.
4. Resuspend the pellet in 200 µl of Resuspension medium, being gentle so as to prevent damage to the SS mitochondria. Some extra time is needed during this final resuspension to ensure the SS pellet is completely resuspended.
5. Keep the SS samples on ice while proceeding to islolate the IMF subfraction.

IMF mitochondrial isolation:

1. Gently resuspend the pellet (from step 6) in a 10-fold dilution of Buffer 1 + ATP using a teflon pestle.
2. Using the Ultra-Turrax polytron set at 40% power output, polytron the resuspended pellet for 10 s. Rinse the shaft with 0.5 ml of Buffer 1 + ATP.
3. Spin at 800 g for 10 min and discard the resulting supernate.
4. Resuspend the pellet in a 10-fold dilution of Buffer 2 using a teflon pestle.
5. Add the appropriate amount of nagarse. The calculation for the appropriate volume is 0.025 ml/g of tissue. Mix gently and let stand exactly 5 min.
6. Dilute the nagarse by adding 20 ml of Buffer 2.
7. Spin the diluted samples at 5000 g for 5 min and discard the resulting supernate.
8. Resuspend the pellet in a 10-fold dilution of Buffer 2. Gentle resuspension is with a teflon pestle.
9. Spin the samples at 800 g for 10 min. Upon the completion of the spin, the supernate is poured into another set of 50 ml plastic tubes (on ice), and the pellet is discarded.
10. Spin the supernate at 9000 g for 10 min. The supernate is discarded and the pellet is resuspended in 3.5 ml of Buffer 2.
11. Spin samples at 9000 g for 10 min and discard the supernate.
12. Gently resuspend the pellet in 300 µl of Resuspension medium.

Mitochondrial Isolations - Flowchart

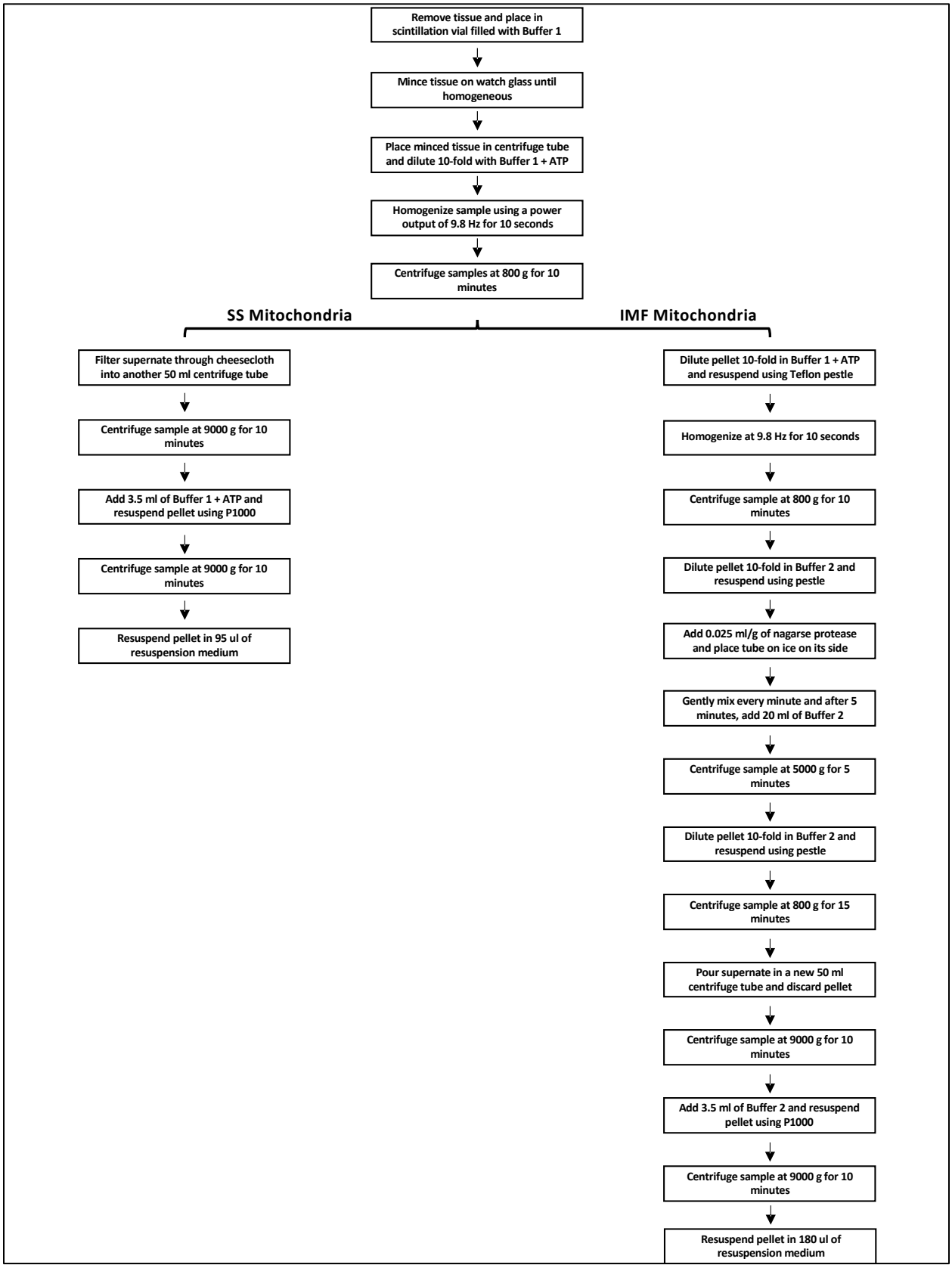

MITOCHONDRIAL RESPIRATION

Reference: Estabrook, R.W., Meth. Enzymol., **10**: 41-47 (1967)

The rate of mitochondrial respiration is an important consideration in the biochemical analysis of mitochondria. There are three phases of interest in analyzing the respiratory ability of mitochondria. Mitochondria produce ATP in the presence of oxygen. The respiratory ability of the freshly isolated IMF and SS mitochondrial fractions and the homogenates can be illustrated by measuring the rate of oxygen consumption using a Clark oxygen electrode in the presence of a) the substrate alone (e.g. glutamate for state 4 or resting respiration); b) ADP, (state 3 or active respiration); and c) $NADH^+$, which is used to measure the amount of damage that has occurred to the mitochondria, since the inner membrane is impermeable to $NADH^+$.

Reagents:

1. VO_2 Buffer for **muscle** mitochondria:

   250 mM **Sucrose** 42.8 g/500 ml
   50 mM **KCl** 1.86 g/500ml
   25 mM **Tris-HCl *** 1.97 g/500ml
   10 mM **K_2HPO_4** 0.871 g/500ml
   pH to 7.4

   * In place of 25mM Tris-HCl you can use 25 mM Tris (aka Tris (hydroxymethyl) methylamine). This works out to 1.5125 g/500ml (FW=121.4). Using Tris in place of Tris-HCl means that you will have to add more HCl to get the pH down to 7.4
2. **Glutamate** - final conc. of 11.1 mM.....**2.0 M initial conc**. (406.4 mg/ml)
3. **ADP** - Final conc of 0.44 mM ..... **20 mM initial conc.** (8.54 mg/ml)
4. **NADH** - Final conc.: 2.8 mM.....**0.5 M initial conc.** (354.7 mg/ml)

Procedure:

1. Set water bath at 30°C -- clean out chambers (Clark oxygen electrode; Yellow Springs Inst. Co., Yellow Springs, OH) and stir bars.

2. Add 250uL of VO_2 Buffer to each chamber.

3. Insert electrode # 2 into the chamber.

4. Remove all bubbles in the chamber and allow it to reach equilibrium temperature (30°C) while spinning.

5. Set recorder for chamber # 2 and paper speed for 3 cm/min.

6. Set monitor and recorder to 100 %.

7. Remove electrode. Add 50 µl of mitochondria into the chamber.

8. Allow a steady state to be reached.

9. Add 12.5 µl of pyruvate and 12.5 µl of malate (heart) or 12.5 µl glutamate (muscle).

10. Wait approximately 3 minutes then add ADP: 50 µl for muscle, 100 µl for heart.

11. Wait (about 2-3 minutes) for a steady rate of state 3 respiration before adding 12.5 µl of NADH. Prepare the next chamber while the respiration recordings are being made.

12. Clean out the chamber in the following manner : Remove the electrode and aspirate, remove the magnetic stir bar and aspirate, and finally, clean the electrode by rinsing with distilled water and pat dry.

13. Put electrode in the next chamber (which should already have the buffer and sample in it).

14. Prepare the next chamber while the measuring the respiration of the current chamber (ie. add 2 ml of VO_2 Buffer and allow to equilibrate).

15. Calculate the state 4, state 3 and $NADH^+$ rates for each sample. Remember that the chart speed is 3 cm/sec and full scale is 100 %. (slope=rate=blocks/min)

16. Calculate the rates of state 3 and state 4 respiration per mg of mitochondrial protein by dividing the state 3 and 4 rates by the amount of protein (mg) added to the VO_2 Buffer.

Calculate the Respiratory Control Ratio (RCR):

RCR = state 3 rate/ state 4 rate

For the above ratio you need only use slopes from the graph. However, for exact calculations of the state 3 and state 4 rates follow the method below:

References: Biological Oxygen Monitor Instruction Manual (table 1, p.13).
Chappel, J.B. Biochem. J. (1964) 90:225-237

- Assume a barometric pressure of 1 atm. (760 mmHg). At 1 atm. the amount of oxygen dissolved in medium equals 5.47 µl O_2/ml (value taken from Biological Oxygen Monitor Instruction Manual). Since 2 ml are being used in the chamber, total O_2 is equal to 2 x 5.47 = 10.94 µl. The rate of change from 100% O_2 can then be used to calculate the amount of O_2 consumed per unit time:

$$\frac{\text{State 3 or 4 /mg protein x 10.94 µl } O_2}{100\%}$$

- But the units of O_2 consumed are now typically expressed in units of natoms O_2. Thus,

$$\frac{\text{State 3 or 4 /mg prot. x 968 natoms } O_2}{100\%} = x \text{ natoms } O_2\text{/mg prot./min.}$$

ROS EMISSION

Background: Mitochondria are the primary source of reactive oxygen species (ROS) to the cell. It is estimated that about 2% of total cellular oxygen is converted ROS by the inappropriate reduction of molecular oxygen by intermediate members of the electron transport chain (ETC). ROS are damaging molecules that are capable of compromising the integrity of macromolecules within the mitochondria and may lead to overall organelle dysfunction. In particular, mtDNA may be prone to attack by ROS because 1) mtDNA is located in close proximity to the ETC, 2) mtDNA lacks the protective sheath of histones compared to nuclear DNA and, 3) mitochondria have an insufficient repair system for mtDNA mutations. ROS can exist in a variety of molecular permutations such as superoxide (O_2^-), hydroxyl radical (OH^-) and hydrogen peroxide (H_2O_2).

DCF (2,7,-dichloro-fluorescein; Fig.1) is a reagent that is non-fluorescent until the acetate groups are removed by intracellular esterases and oxidation occurs within the mitochondria (Fig.1). DCF is oxidized by all of the different forms of ROS and this can be detected by monitoring the increase in fluorescence with a fluorometric plate reader. The appropriate plate

reader filter settings for fluorescein are the following: **Excitation 485/20 and Emission 528/20** (Fig.2).

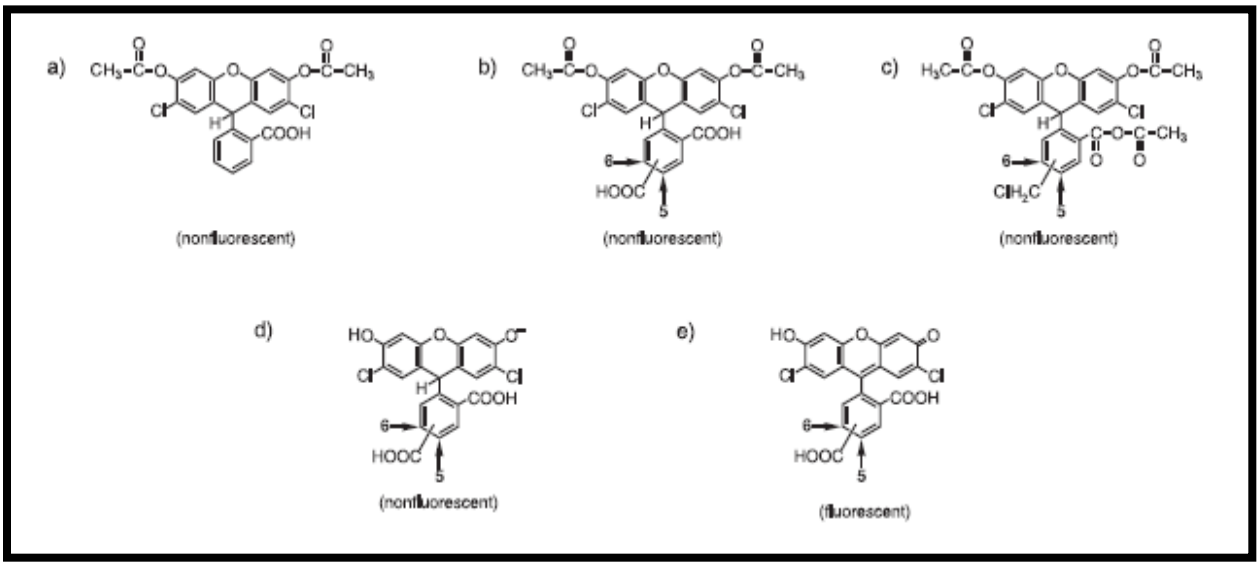

Fig.1-DCF molecule and oxidation of DCF resulting in fluorescence

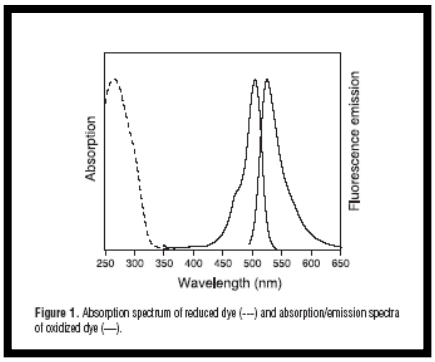

Fig.2-Absorption and Emission Spectra of oxidized dye

KC4 Software Settings: The Settings icon in the upper left corner allows the alteration of various parameters. Once clicked, another window appears, click on the Wizard Icon. In this window there will be a variety of components that can be altered. The following are the parameters that need to be changed in order to utilize the DCF and measure time-dependent ROS production from isolated mitochondria:

1) Top Middle Panel- Absorbance, Fluorescence, Luminescence- choose **Fluorescence**
2) Top Left Panel- End Point, Kinetic, Spectrum- choose **Kinetic**
3) Top Middle Panel- Click on larger box labeled Kinetic to set parameters- **Run Time 1:20:00, Interval 5:00 (takes a measure every 5 minutes),** click on box labeled **Allow Well Zoom during Read,** and also click on box labeled **Individual Well Auto Scaling**- The Well Zoom and Auto scaling allows for monitoring each individual well during the experiment and scales it appropriately.
4) Middle Panel-***Filter Set***- Choose #1, then set the **excitation to 485/20**, and **emission to 528/20** as described above. The optics position should be set to the **TOP** (i.e. readings are taken from the

top of the well) and the sensitivity is set at **50** (depending upon the amount and/or nature of the sample).
5) Plate-Type-choose **96-well plate**, choose which wells are to be read i.e. **A1-C12.**
6) Shaking-**Intensity** set at **1, Duration** set at **15s** and then click the box that is labeled **before every reading** (it shakes the samples for 15 s before every reading).
7) Temperature Control- Click on the box indicating **YES,** also click on box labeled pre-heating, and put 37°C into the temperature box.

Reagents:
DCF (2,7,-dichlorodihydrofluorescein diacetate) reagent MW=487.29 (Molecular Probes D-399/ 100mg)
1° STOCK- Make up **50mM** Stock Solution in EtOH- 24 mg/ml- only make about 500ul i.e. 14 mg per 500ul EtOH. Wrap stock solution in aluminum foil and limit exposure to light since DCF is light-sensitive.
Working Stock Solution-2° STOCK- Dilute 50mM by 100-fold by taking 10ul and adding 990 ul of EtOH to attain a **500uM DCF Stock Solution**. This will be the DCF concentration used to add to the reaction mixture.

VO_2 Buffer- refer to mitochondrial respiration protocol

Procedure:

1. SS and IMF mitochondria are isolated as described in the mitochondrial isolation protocol. Alternatively, frozen mitochondrial extracts can also be used.
2. Determine the volume necessary for 50ug of mitochondria. Typical volumes should range between 5-40ul depending upon concentration of mitochondrial extracts.
3. Final concentration of DCF is 50uM. The total volume of the reaction mixture is 250ul. Thus, 25ul of DCF is used in the reaction mixture since this represents a 10-fold dilution. Determine the amount of VO_2 buffer necessary to make each of the reaction mixtures equal to 250 ul. (Remember to include a ***control*** with only VO2 buffer and DCF reagent)
4. Once table is complete and volumes for all samples have been determined, place the frozen (already thawed) or fresh mitochondria, VO_2 buffer and DCF (500uM) into a 37°C circulating water bath for 5-10 min.
5. Pipette the volume of VO_2 buffer required for each of the samples followed by the mitochondrial samples into the appropriate wells of a 96-well plate. In addition, include a well (usually in the corner well) with only 250 ul of VO_2 buffer to monitor temperature (see below). Place the 96-well plate with the VO_2 buffer and mitochondria into a 37°C incubator. Using the YSI temperature probe, place the recording electrode into the well with buffer only and monitor the temperature until 37°C is reached. During this time, be sure that the KC4 software is set up and that the Biotek plate reader is pre-heating to 37°C.
6. Once mitochondria and buffer have reached temperature (37°C), take the DCF out of the circulating water bath (37°C) and quickly add the DCF to each of the reaction mixtures. Following addition of DCF, promptly place the plate into the Biotek plate reader for fluorescence measurement and start the KC4 program by pressing **READ** plate on the upper left portion of the computer screen. Kinetic program will operate for 1 h and 20 min.

OTHER CONTRIBUTIONS TO LITERATURE

PEER-REVIEWED PUBLICATIONS

1. **Slavin M.**, Memme J.M., Oliveira A.N., Moradi N., Hood D.A. Regulatory networks controlling mitochondrial quality control in skeletal muscle. *American Journal of Physiology-Cell Physiology.* (In preparation).
2. Triolo M., **Slavin M.,** Moradi N., Hood D.A. (2021). Time-dependent changes in autophagy, mitophagy and lysosomes in skeletal muscle during denervation-induced disuse. *The Journal of Physiology.* (Submitted - JP-RP-2021-282173).
3. Richards B.J., **Slavin M.,** Oliveira A.N., Sanfrancesco V.C., Hood D.A. (2021). Mitochondrial protein import and UPR^{mt} in skeletal muscle remodeling and adaptation. *Seminars in Cell and Developmental Biology.* (Submitted - YSCDB-D-21-00185).
4. Memme J.M., **Slavin M.,** Moradi N., Hood D.A. (2021). Mitochondrial bioenergetics and turnover during chronic muscle disuse. *International Journal of Molecular Sciences. 22*(10), 5179.
5. Oliveira A.N., Richards B.J., **Slavin M.**, Hood D.A. (2021). Exercise is muscle mitochondrial medicine. *Exercise and Sport Sciences Reviews. 49*(2), 67-76.

PUBLISHED ABSTRACTS AND CONFERENCE PROCEEDINGS

1. **Slavin M.** and Hood D.A. (2021) PGC-1α controls the basal expression of UPR^{mt} genes. CSEP. *Applied Physiology, Nutrition and Metabolism.* Online, October 2021.
2. **Slavin M.**, Memme J, Hood DA. (2020) One bout of aerobic exercise elicits alterations in the expression of mitochondrial unfolded protein response (UPR^{mt}) markers in skeletal muscle. *FASEB Journal*. Experimental Biology. Online, May 2021.
3. **Slavin M.**, Memme J, Hood DA. (2020) Changes in UPR^{mt} gene expression after one bout of acute aerobic exercise. CSEP. *Applied Physiology, Nutrition and Metabolism.* (Vol. 45, p. S319), 2020.
4. **Slavin M.**, Hood DA. (2020) The role of ATF5 in UPR^{mt} regulation following endurance exercise. *Proceedings of Muscle Health Awareness Day*, 11th edition. (p. 36): Toronto, ON, Canada. May 22, 2020.
5. Triolo M., **Slavin M**, Hood DA. (2020) Regulation of the autophagy-lysosome system in response to hindlimb denervation. *Proceedings of Muscle Health Awareness Day*, 11th edition. (p. 40): Toronto, ON, Canada. May 2020.
6. Triolo M, **Slavin M**, Kim Y, Hood DA. (2020) Lysosomal alterations in muscle plasticity with age, exercise, and disuse. *FASEB Journal.* Experimental Biology: Online, April 2020.
7. **Slavin M,** Triolo M, Hood DA. (2019) Progressive decline in autophagy with denervation. *Proceedings of Muscle Health Awareness Day*, 10th edition. Toronto, ON, Canada: May 2019.
8. Triolo M, **Slavin M**, Hood DA. (2019) Autophagy in hindlimb denervated rats. *Proceedings of Muscle Health Awareness Day*, 10th edition. Toronto, ON, Canada: May 2019.
9. Triolo M, Cheema N, **Slavin M**, Moradi N, Hood DA (2019) Skeletal muscle autophagy and mitophagy are altered in the time course of hindlimb denervation. *Proceedings of MitoNET Conference*. Toronto, ON, Canada: November 2019.

10. Triolo M, **Slavin M**, Hood DA. (2019) Hindlimb denervation alters the regulation of autophagy and mitophagy. *FASEB Journal.* Experimental Biology: Orlando, Florida, United States. April 2019.
11. Triolo M, **Slavin M**, Hood DA. (2019) The effects of hindlimb denervation on the regulation of autophagy and mitophagy. National Heart, Lung, and Blood Institute. *Proceedings of the Mitochondrial Biology Symposium:* Bethesda, Maryland, United States. September 2019.

ORAL PRESENTATIONS

1. ATF5 and the UPR^{mt} with exercise in skeletal muscle. *KAHS Graduate Seminar 2020.* York University, Toronto, ON., Canada. October 2020.
2. The effects of aerobic exercise on ATF5-mediated regulation of the mitochondrial unfolded protein response in skeletal muscle. *Kinesiology and Health Science Graduate Student Association Research Day 2020*: York University, Toronto, ON, Canada. July 2020. **(Oral Presentation Award)**